2018

Engineering of Two-Color ATP-Binding Cassette Biosensor Proteins for Discovery of Novel Substrates and Modulators

Bremansu Osa-Andrews
South Dakota State University

ENGINEERING OF TWO-COLOR ATP-BINDING CASSETTE BIOSENSOR PROTEINS FOR DISCOVERY OF NOVEL SUBSTRATES AND MODULATORS

BY

BREMANSU OSA-ANDREWS

A dissertation submitted in partial fulfillment of the requirements for the

Doctor of Philosophy

Major Biochemistry

South Dakota State University

2018

ENGINEERING OF TWO-COLOR ATP-BINDING CASSETTE BIOSENSOR PROTEINS FOR DISCOVERY OF NOVEL SUBSTRATES AND MODULATORS

BREMANSU OSA-ANDREWS

This dissertation is approved as a creditable and independent investigation by a candidate for the Doctor of Philosophy in Biochemistry degree and is acceptable for meeting the dissertation requirements for this degree. Acceptance of this does not imply that the conclusions reached by the candidate are necessarily the conclusions of the major department.

Surtáj H. Iram, Ph.D.

Dissertation Advisor Date

Douglas Raynie, Ph.D.

Head, Chemistry and Biochemistry Date

Kimchel Doerner, Ph.D.

Dean, Graduate School Date

I dedicate this dissertation to my dear wife Mrs. Lydia Osa-Andrews without whose unflinching support I wouldn’t achieve this document.

ACKNOWLEDGEMENTS

I am first and foremost grateful to my Lord and Savior Jesus Christ for being the sole source of my motivation for this accomplishment. I am forever grateful to Mrs. Lydia Osa-Andrews for enduring aloneness sometimes to spare me time to achieve this goal. I am thankful to my dear mother, Agnes Torgbor for her constant encouragement to strife for excellence. I appreciate the regular words of motivation of my stepdad, Rev. Emmanuel Bossman. I thank my dissertation/academic advisor, Dr. Surtaj Iram for his training, tutelage, advising, guidance and mentorship throughout the course of my studies. I thank my advisory committee members, Prof. Fathi Halaweish, Prof. Christian Steward, Dr. Suvobrata Chakravarty, and Prof. James Rice (Retired) for their useful reviews, feedback, and overall assistance during my studies. I am thankful to Dr. Kee Tan (former postdoctoral fellow in Iram Lab) for training me in membrane vesicle preparation, vesicular transport assay and other techniques. I am thankful to all Iram lab mates for their various support during my research work in the lab. I am thankful for faithful friends who were there for me when the going got tough, Dr. and Dr./Mrs. Essel, Prof. Michael Hildreth, Eric Nana Osei-Akoto, Dr. Duke Appiah, Dr. Chris Opoku-Agyeman, Dr. Paul Atta-Boakye, the African community here in Brookings, SD, members of Grace Victors Ministry, Ghana, Veritas Church and Holy Life Tabernacle, Brookings, SD and many others not mentioned for want of space.

CONTENTS

ABBREVIATIONS

ABC	ATP-binding cassette
ADME	absorption, distribution, metabolism and excretion
ADP	adenosine diphosphate
ATP	adenosine triphosphate
BCRP	breast cancer resistance protein
Caco-2	colorectal adenocarcinoma
CFTR	cystic fibrosis transmembrane conductance regulator
CNS	central nervous system
CSF	cerebrospinal fluid
E_2SO_4	estrone sulfate,
E_217Bg	17β-estradiol-17-β-(D-glucuronide)
EGFR	endothelial growth factor receptor.
FRET	fluorescence resonance energy transfer
GFP	green fluorescent protein
GSH	reduced glutathione
GSSG	oxidized glutathione
HEK293	human embryonic kidney 293

HPLC	High pressure liquid chromatography
LC-MS/MS	Liquid chromatography mass spectrometry
LTC4	cysteinyl leukotriene
MDCK	Madin-Darby Canine Kidney
MDR	multidrug resistance
MRP1	multidrug resistance protein 1
MSD	membrane spanning domain
NBD	nucleotide binding domain
P-gp	permeability glycoprotein
Pi	phosphate
qPCR	quantitative polymerase chain reaction
RFP	red fluorescent protein
RT-PCR	reverse-transcriptase polymerase chain reaction
SUR	sulfonylurea receptor
TMD	transmembrane domain

LIST OF FIGURES

LIST OF TABLES

ABSTRACT

ENGINEERING OF TWO-COLOR ATP-BINDING CASSETTE BIOSENSOR PROTEINS FOR DISCOVERY OF NOVEL SUBSTRATES AND MODULATORS

BREMANSU OSA-ANDDREWS

2018

ATP-binding cassette (ABC) transporter proteins are a vast, ubiquitous superfamily of proteins most of which unlock the energy from ATP-binding and hydrolysis to influx or efflux a wide spectrum of structurally dissimilar substrates across cell membranes. All eukaryotic ABC transporters including P-gp and MRP1 only exist as efflux pumps whose prominent expression in cells is associated with multidrug resistance of antiretrovirals, antiepileptics, antimalarials and anticancer agents. P-gp and MRP1 reduce the bioavailability and efficacy of chemotherapeutic drugs by actively pumping out these drugs, thereby, leading to poor clinical outcomes during chemotherapy. Due to their clinical importance, profiling of the interaction of MRP1 and P-gp with therapeutic drugs is pertinent. Here, we developed an innovative two-colorMRP1 and P-gp biosensors by fusing the transporter with green fluorescent (GFP) and red fluorescent (RFP) proteins. These biosensors exhibit large dynamic FRET changes in response to movements of the transporter upon substrate-binding and is useful for high throughput screening for potential modulators. Following a steady-state FRET screening, the two-colorMRP1 biosensor identified 10-anticancer drug-hits of 40, and the two-color P-gp detected 6 hits of 50 antitumor drugs, which are ligands and potential substrates of their respective transporters. In the absence of a single known high throughput screening for detection of

drug-ABC transporter interaction, our coupled ensemble FRET model is transformative as it holds promise for fluorescent plate reader-based high throughput screening for substrates and ligands of these transporters. Future projects will focus on vesicular transport-coupled LC-MS/MS assay to verify the ABC transporter-substrate status of the anticancer drug-hits discovered in the present study.

CHAPTER 1

INTRODUCTION

Scope

The general goal and significance of the present study is to develop an ATP-binding cassette (ABC) transporter protein biosensor, suitable for the profiling of substrates and ligands using fluorescence spectroscopy. This section opens by exploring the literature regarding membrane proteins and transport proteins in general and their significant role in the movement of solutes in and out of cells. The mode of transport by the proteins as well as the source of energy utilized, if needed for the transport process. Of interest in this segment of the present treatise is the ubiquity of ABC transporter proteins in all phyla; bacteria, archaea bacteria and eukaryotes. The section then looks at the types of ABC transporters in prokaryotes and eukaryotes. The general structural organization of ABC transporter proteins are described in detail as it is core to the methodological strategy for the current project. The distribution, physiological functions and implications of the transport activity of ABC transporter proteins are expounded next. The significance of ABC transporter proteins regulating multidrug resistance (MDR) and the clinical correlation this has on health and diseases are delved into as it relates to the current project. The section then makes an argument for the significance of the current project by explaining the need for profiling of drug-ABC protein interactions. Next, the methodological tools which have been employed for the identification of substrates of key ABC transporter proteins, P-glycoprotein and Multidrug resistance protein-1 (MRP1) are described. The section then describes the literature regarding fluorescence spectroscopy, the key tool for Fluorescence based procedures in the present

project. This chapter concludes by providing a relevant rationale for carrying out the present work and the potential adaptation of the methods and our work and utilization of our findings of by members within the ABC transporter field and beyond.

Membrane transport proteins

Membrane transport proteins are primarily responsible for translocating materials across cell membranes down or against an electrochemical gradient. Three major membrane transport proteins exist in nature including channel proteins, secondary active transporters and primary active transporters which includes ATP-binding cassette (ABC) transporter proteins. Channel proteins are involved in an energy-independent facilitated diffusion down a concentration gradient, of solutes across cell membranes, while secondary active transporters mediate the uniport, symport and antiport of substances, harnessing stored ion-gradient energy [1, 2]. The source of energy, if used by transport proteins is the key feature which dichotomizes the kind of transport proteins they are. Primary active transporters, like ABC transporter proteins couple transport to ATP hydrolysis by unlocking the energy from the hydrolytic reaction to power transport of solutes across the phospholipid bilayer. On the other hand, two types of membrane proteins are attached to the lipid bilayer with varying degrees of strength; Peripheral membrane proteins attach loosely to the bilayer and integral membrane proteins are permanently associated with the cell membrane (Figure 1.1). ABC transporter proteins are a classical integral, transmembrane protein core [3].

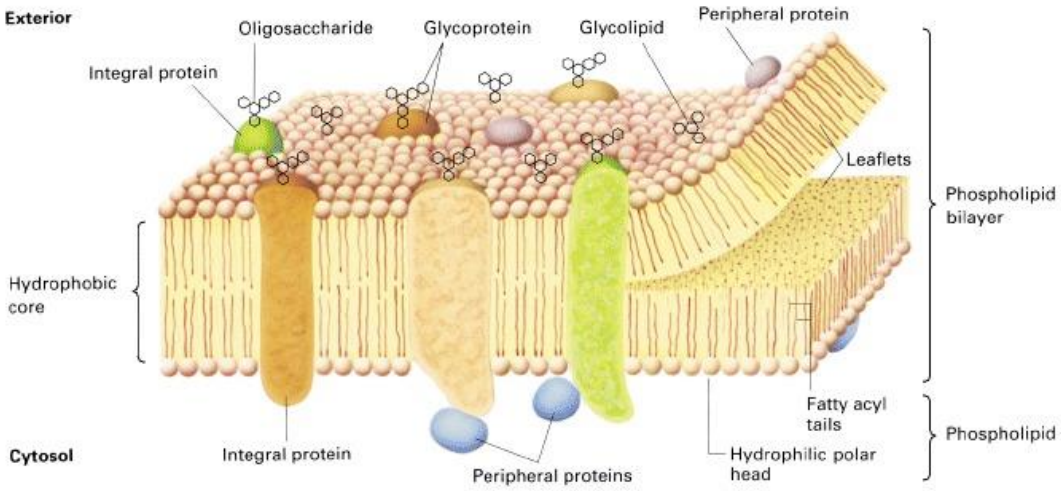

Figure 1.1 Schematic presentation of biological membranes.

Phospholipid bilayer creates a hydrophobic transmembrane core and hydrophilic extracellular portions and intracellular divisions. Peripheral membrane proteins are loosely attached, and integral membrane proteins are tightly connected and spans the hydrophobic core [3].

ATP-binding cassette transporter proteins

Adenosine triphosphate (ATP) -binding cassette (ABC) transporter proteins are a ubiquitous superfamily of integral membrane proteins characterized by multimembrane spanning domains and cytoplasmic subtended ATP-binding [4]. Majority of the members of the ABC transporter proteins actively utilize the energy from an of ATP-dependent hydrolysis to shuttle a broad spectrum of molecules across biological membranes [5]. The diversity of substrates translocated by ABC transporters span solutes, anions, amino acids, sugars, vitamins and many other structurally unrelated molecules. ABC transporters are evolutionarily conserved proteins which are found in all phyla, spanning

prokaryotes, archaea-bacteria and eukaryotes. In prokaryotes, some ABC proteins are known as importers where they function to uptake nutrients into the cell, while others, exporters, efflux molecules out of cells [6]. Eukaryotic ABC transporters are exclusively exporters.

Bacterial ABC transporters

ABC importers are one of the two types of bacteria ABC transporters. They mainly regulated the influx of a wide variety of essential nutrients needed for bacterial survival. The nutrient needs of prokaryotes are diverse and quantitively disparate and require efficient supervision [7]. Carbon and nitrogen sources are required in large amounts whereas only trace quantities of transition metals can be accommodated by bacterial cells. Efficient regulation of the uptake of these nutrients which widely includes peptides, amino acids, saccharides, vitamins, ions, organic and inorganic substances, in just the right amounts are essential to the functions of ABC importers [2]. The uptake-role played by ABC importers is classically vital for the survival of pathogenic bacteria in the nutrient-scarce environment of host mammalian organism. Animal infection models have been used to show that mutations in zinc, iron, magnesium-uptaking ABC importers impacts negatively on the virulence of the bacteria. This has been shown particularly in pathogens such as *vibrio cholerae* and *salmonella enterica* strains. In addition, bacterial ABC importers are involved in cell to cell communication, osmoregulation and internalization of signaling molecules [8, 9].

Bacterial ABC exporters are similar systems as found in eukaryotes. They mediate efflux transport of a host of structurally dissimilar drugs and toxins from the bacterial cell. ABC exporters in bacteria confer multidrug resistance (MDR) to several antibiotics by pumping these drugs out of cells. The LmrA transporter found in *Lactobacillus lactis* is a classic example of MDR conferring efflux pump in prokaryotes [10]. ABC exporters also participate in the secretion of certain proteins particularly the sec independent type I protein secretion system [11]. Bacterial ATP-dependent exporters are also involved in lipid translocation, biosynthesis of lipopolysaccharides and delivery of precursors for protein glycosylation as shown in *Campylobacter jejenum* (Pg1K) and *Escherichia coli* (MsbA) [12, 13].

Eukaryotic ABC transporters

Eukaryotic ABC transporters lack the importing and cellular-uptake activity of bacterial transporters, with only efflux function. ABC transporters in eukaryotes mediate the efflux of solutes and ligands from the interior to the exterior of the cell or to the interior of organelles. Some ABC transporters such as multidrug resistance protein 1 (MRP1) are exclusively eukaryotic without any discovery yet made in prokaryotes. Not all eukaryotic ABC transporters are classical efflux pumps. The cystic fibrosis transmembrane conductance regulator (CFTR, ABCC7) and sulfonyl urea receptor (SUR or ABCC8) which are associated with cystic fibrosis and diabetes, are ATP-reactive protein channels but do not directly transport drugs [14-16]. At least three clinical MDR-mediating human ABC transporters have been characterized; P-glycoprotein, MRP1 and Breast cancer resistance protein (BCRP) [17, 18]. These human transporters have been

found to be are prominently expressed in tumor cells have been found to extrude a broad spectrum of hydrophobic substrates including anticancer agents. The scope of the current work remains within exploring the development of methods for identification of substrates of human ABC transporters.

Structural organization of ABC transporter proteins

ATP-binding cassette transporter proteins belong to the largest superfamily of all transporter proteins. All ABC transporter proteins share a similar architecture. They consist of four domains, two membrane-spanning domains (MSD1 and MSD2) and two nucleotide binding domains (NBD1 and NBD2) [2, 14]. Some ABC proteins have an extra N-terminal membrane spanning domain (MSD0) but the utility of this domain is yet unclear. In most eukaryotes, all four domains are in a single polypeptide chain. Each MSD consists of α-helices which span the lipid bilayer membrane multiple times. The two MSDs combine to form the substrate translocation pathway. The NBDs extend into the cytoplasm where they bind and hydrolyze ATP during catalytic activity. In eukaryotes, the MSDs and the NBDs are connected by cytoplasmic loops unlike in bacterial ABC importers where they are separate polypeptides [19]. The MSDs and the NBDs in eukaryotes fuse together at the core creating the substrate binding pocket which consists of amino acids that recognize a great diversity of structurally unrelated compounds and ligands. In prokaryotic exporters, one MSD and one NBD fuse to form a half-transporter which needs to dimerize with the other half prior to functional catalytic activity by the transporter.

The NBDs are the most evolutionarily conserved region in the ABC superfamily as they all bind to a common nucleotide. This is pertinently due to the presence of three short motifs in the primary sequence of the NBDs; Walker A motif consisting of GXXGXGKS/T, X may be variable and walker B motif, hhhhD, where h represents hydrophobic amino acid and motif C (signature C) which is the most conserved sequence of all ABC transporters (Figure 1.2) [6]. Walker A is involved with binding of the β-γ phosphates of ATP to the Gly loop o γ-phosphate linker. The highly hydrophobic walker B is responsible for Mg^{2+}, a needed metal ion for ATP hydrolysis. Motif C is called the signature sequence since it is useful in putative discovery of new ABC proteins [20]. These walker A and B motifs of the primary sequence of the NBDs is generally what the 'AB' of ABC proteins refers to. In contrast, primary sequence and structural composition of the MSDs are uniquely varied and this reflects the broad substrate diversity of ABC transporters [21, 22].

Studies conducted on mouse P-gp and bovine MRP1 reveal two conformations the NBDs of ABC transporters prior to and during a catalytic activity; the substrate-deficient open and substrate-bound closed conformations [23, 24]. It is thought that the binding of the substrate brings the NBDs, whose affinity for ATP increases come into proximity. Functional characterization of bovine MRP1 shows that substrate binding pulls the NBDs to 0.2 Å closer (Figure 1.3) to each other prior to nucleotide binding [23]. This process elicits conformational changes in the MSDs which create space for the substrate to be pumped out through the substrate translocation pathway. This alternating switch in conformations between the open and close, reflects the rationale for the cloning strategy employed in the present study.

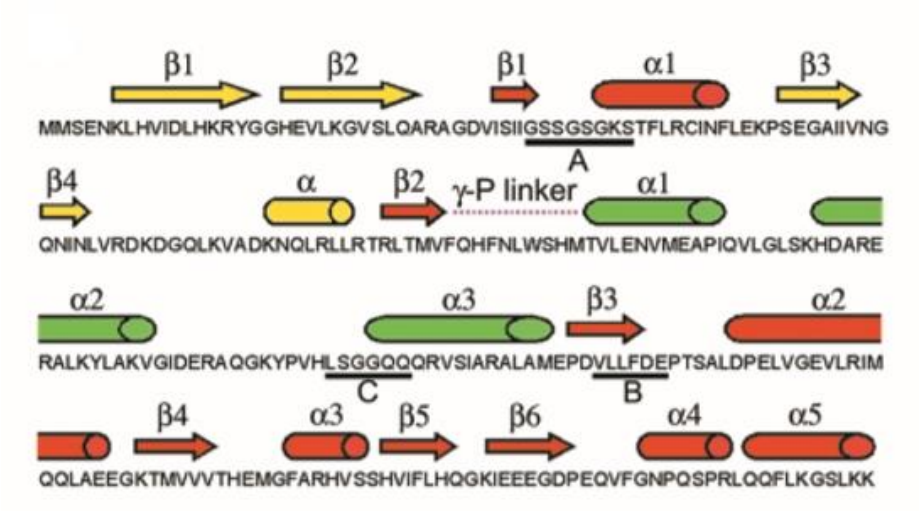

Figure 1.2 Structure of the NBD of a typical ABC transporter.

Primary and secondary structure of HisP. α-helices are represented as rod-shapes and the arrows stand for β-sheets. The conserved motifs Walker A, B and motif C (the signature sequence) are underlined. The γ-phosphate linker is shown as purple dotted lines *[20]*.

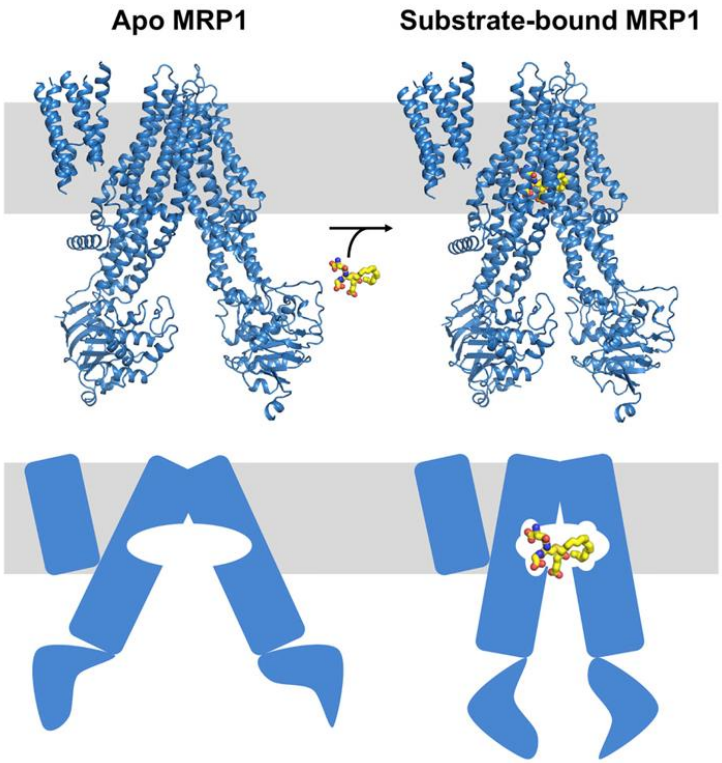

Figure 1.3 Structure of bovine MRP1

The structure shows LCT_4- recognition and binding in the binding pocket of the transporter. On the left are the ligand-free tertiary structures (top is PDB tertiary structure, bottom is a schematic structure) in the open conformation of the NBDs. On the right are the LTC_4-bound closed conformation in both PDB structure (top) and schematic (bottom) *[23]*. The predominantly yellow molecule in the binding pocket is the LTC4. The NBDs shift 0.02 nm closer to each other following substrate binding.

Catalytic mechanism of ABC proteins

Following extensive studies of the structure of P-gp, the ATP-switch model has been postulated [4]. The ATP-switch model employs the possible substrate-loving ‘open’ state, the low substrate affinity-closed conformations of the NBDs and ATP hydrolysis to interpret the catalytic mechanism of transport [25]. In the absence of a substrate, the NBDs are thought to distant from each other, but they come into proximity once a substrate binds to the active site. This open and closed conformations of the NBDs have been corroborated from recent studies on cryoelectron-microscopic structure and substrate affinity of the bovine MRP1. In the bovine MRP1 study, they found that the NBD-pair moves 0.02 nm closer in the presence of leukotriene C4 (LTC4) [23]. ABC proteins enact their function essentially by switching between the two conformational NBD-states.

The detailed steps which describe the transport mechanism of ABC proteins are expounded as follows, starting from the substrate-loving ‘open’ stance; substrate binding, closure of NBDs, ATP binding, substrate evacuation, ATP hydrolysis open conformation regained. Substrate-binding at the active site orchestrates conformational changes in association with cytoplasmic loops to gives rise to increased affinity of the NBD1 for the ATP-molecule. Of note in the mechanism is that in the open NBD conformation, the MSDs are also in a cytosolic-facing open conformation which makes the substrate-binding site accessible by molecules. Binding of ATP elicits a closing-movement of the NBDs toward each other, a pull strong enough to rearrange the MSDs to outward-facing stance. This open stance of the NBDs in conjunction with proximal NBDs forms the substrate-translocation pathway through which the substrate is eventually pumped out.

The substrate-dependent closed-proximity of the NBDs is thought to be a reversible transient state which reduces the affinity of the transporter for the substrate and hence, substrate evacuation. One key element in the mechanism is the inevitable ATP hydrolysis which destabilizes the closed conformation of the NBDs provides the energy required from release of adenosine diphosphate (ADP) and phosphate (Pi) to actively pump out the substrate.

The occurrence of hydrophilic amino acid sequence in the upper half of the binding pocket and hydrophobic groups in the lower half is responsible for the substrate promiscuity [26]. Consequently, several chemically dissimilar ligands have been discovered as substrates of important ABC proteins (figure 5). In the present study, the ATP-switch movement of the NBDs was harnessed to design and attach fluorophores to them for FRET-based analysis to identify potential substrates of ABC transporters.

Physiological functions of ABC transporter proteins

Generally, there are three classes of ABC proteins and which class a protein belongs to, defines their functionality. Class-2 ABC proteins, which do not mediate ATP-hydrolytic transport of solutes contain nucleotide binding domains but lack the membrane spanning domains and are associated with biological processes such as DNA repair instead of transport [27]. However, class-1 and class-3 ABC proteins are usually transporters involved in transport of ligands across plasma membranes through ATP-dependent hydrolysis [20]. A few ABC transporters are not transporters in particular, even though they stimulate ATP hydrolytic process to allow the passage of ions. CFTR, a

Cl^- channel is the one of the commonest ion channels which regulates movement of chloride ions. Sulfonylurea receptors (SUR) are ABC proteins which regulate potassium channels in an ATP-dependent process [28]. Some classic ABC transporters such as P-gp, in addition to mediating translocation of solutes, also regulate chloride channels [29].

Most ABC transporters mediate the evacuation of endogenous molecules and xenobiotics from the inside to extracellular spaces across plasma membranes. ABC transporter proteins demonstrate a high degree of substrate diversity, being responsible for the efflux of a wide variety of structurally unrelated compounds as shown in figure 5. These ABC transporters are involved in several physiological functions such as tissue defense against exogenous insults and maintenance of balance between antioxidant and free radical concentrations (the MRPs) detoxification (P-gp), absorptive and secretory activities (ABCBs and MRPs), antigen presentations (ABCB2 and ABCB3) and lipid metabolism (ABCA1 and ABCGs) [26, 30, 31]. Substances transported by ABC proteins include amino acids, lipids, hydrophobic compounds, metals ions, saccharides, and a host of others. The mode of transport of many solutes is through conjugation with glutathione (GSH) such as estradiol glucuronide or to sulphate such as estrone sulfate, E_2SO_4 [24]. GSH is the most abundant non-protein thiol in the cell, mediating the thiol-redox status of cellular processes. Therefore, efflux of glucuronide conjugates in both the oxidized and reduced forms of glutathione (Gamma-Glu-Cys-Gly), indicates ABC transporters are involved in the regulation of other physiological and pathophysiological processes glutathione is associated with [32]. Figure 1.4 shows a schematic diagram of the singular export of LTC4 as well as the co-export of vincristine from cells.

ABC proteins are vital in several biological process so mutations in their genes lead to genetic diseases such as cystic fibrosis, bile defects, cholesterol transport disorders and neuro-degenerative diseases [33]. These modes of transport are particularly characteristic of multidrug resistance associated protein-1. The tissue distribution of many ABC transporters depicts their role in tissue defense and protection. There are fifty known human ABC transporters out of which fourteen are known to be associated with diseases [4]. The ABC transporters P-gp, MRP1 and BCRP play a key role in the efficacy, disposition and toxicity of therapeutic agents[32, 34-37]. Figure 1.5 displays the vast spectrum of substrates exported by ABC transporters.

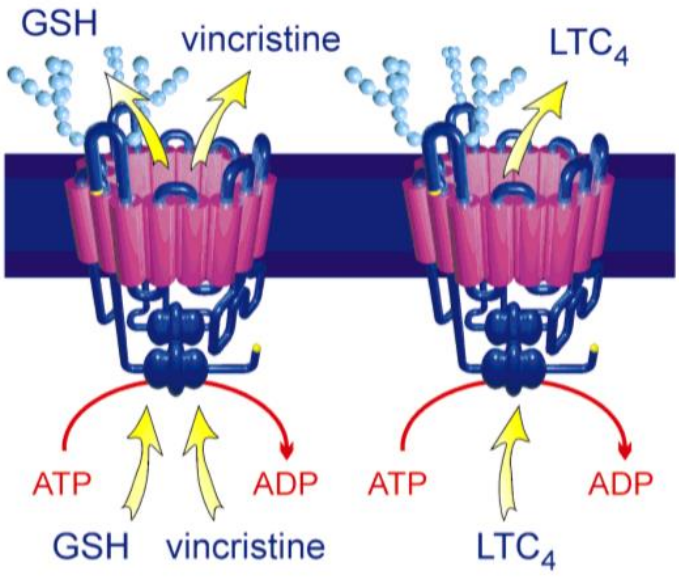

Figure 1.4 ATP-dependent ABCC/MRP transport model depiction.

The ABC transporter effluxes LTC4 out of the cell (right). The co-transport of vincristine and GSH by the transporter is being depicted on the left.

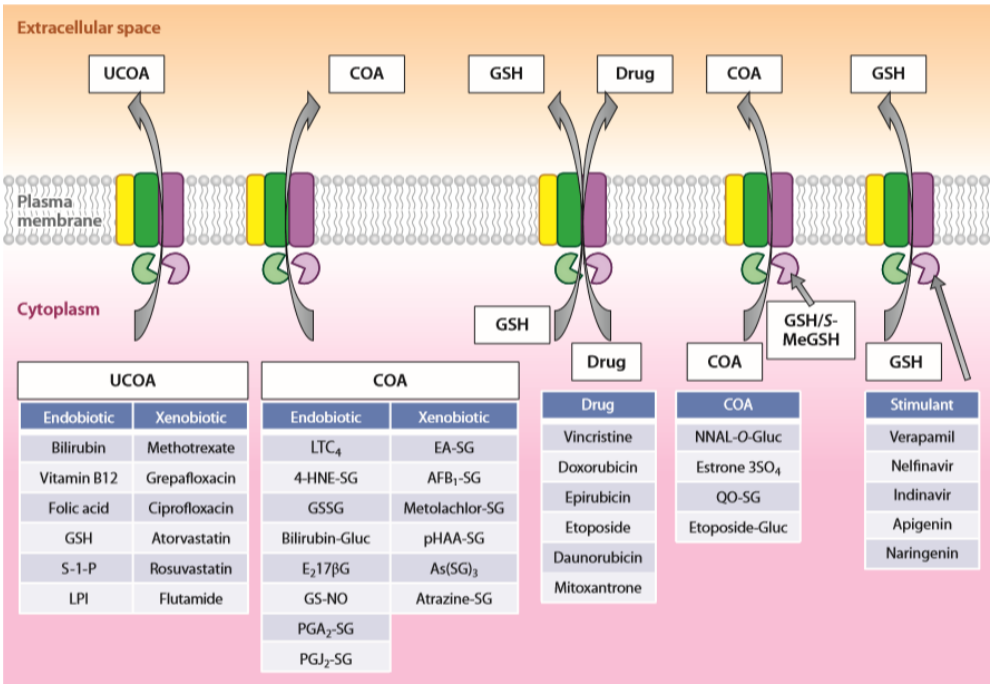

Figure 1.5 Substrate diversity of ABC transporters.

The transporters pump out a vast number of structurally unrelated endogenous and exogenous compounds.

Absorption, Distribution, Metabolism and Excretion (ADME)

Absorption of ingested drugs is a key pharmacokinetic index of cells lining the small intestines. In the apical and the basolateral sides of the lumen of the small intestines are lined both influx transporters and efflux pumps, notably MRP1, P-gp and BCRP. Digested food from the gut is absorbed from the lumen of the small intestines through tight junctions into the blood to be carried through-out the body [31, 38-40]. Animal studies have shown the importance of ABC transporters in the absorption of nutrients from food and administered drugs. The prominent expression of these ABC transporters at this brush border membrane suggest they can pump out drugs back out into the lumen

of the small intestines, affecting the bioavailability of these drugs. This underscores the pharmacokinetic significance of ABC transporters in restricting the extent of absorption of drugs. Of the three aforementioned ABC transporters which govern absorption, MRP1 is the most well studied for that specific physiological function [4, 25, 41].

Drug distribution is critical for their effectiveness as they need to be shuttled precisely from the location of administration to target tissues. The prime target tissue for many therapeutic drugs is the brain and this makes the blood brain barrier (BBB) An important site. Contrary to earlier notion that lipophilicity is all that was required for drugs to traverse the BBB, many hydrophobic drugs have been found to display impaired BBB penetration [4, 42]. It is now thought that ABC transporters and their export activities could be blamed for poor BBB permeability of drugs. These findings underscore the importance of ABC proteins, particularly MRP1, MRP2, BCRP and P-gp in protecting delicate tissues such as those of the central nervous system (CNS).

Drug metabolism is generally impacted by drug absorption and distribution. The less the amount of drugs accumulated in cells, the less will be metabolized. *Drug excretion* occurs in the kidneys and liver which are notable for detoxification [43, 44]. Hepatocytes for instance are lined in the sinusoidal (basolateral) and the canaliculi (apical) side with influx and efflux transporters [45]. Hepatocytes containing canalicular lined efflux pumps such as P-gp abstract and transport drugs from circulation and channel them into the bile to be excreted. The integrity of these ABC transporter and the efficiency of this process influences the extent of drug excretion. These can significantly impact on drug toxicity as well. P-gp is noted for transport of cationic drugs and drug

metabolites while MRP2 and BCRP transport conjugate anionic drugs such as conjugate glutathione [4].

The multidrug resistance phenotype

The extreme substrate variety of ABC transporter also inadvertently renders them susceptible to a phenomenon known as multidrug resistance. Multidrug resistance is generally characterized by over expression of ABC proteins, excessive pumping out of therapeutic drugs and desensitization of pharmacological products in their target cells. The primary etiology of ABC transporters-mediated is prominently expressed transporters constantly pumping out therapeutic drugs, reducing accumulation and efficacy of such drugs. Three ABC transporters highly expressed in the liver, the gut and kidneys are major players in the multidrug resistance phenotypes since they govern the bioavailability of administered therapeutic agents [4]; P-gp, MRP1 and BCRP. These ABC proteins are structurally suited to interact with and pump out a host of structurally diverse drugs including antimalarials, antiretrovirals and anticancer agents. The substrate diversity of these ABC transporters is the lead cause of the multidrug resistance phenotype in which cells overexpressing these proteins become desensitized to the effect of many drugs simultaneously. The first multidrug resistant implicated ABC transporter is P-glycoprotein (P-gp) [46]. P-gp is widely distributed in the apical surfaces of the epithelial cells including the epithelial lining of the colon, pancreatic ducts, small intestines, adrenal glands, proximal tubules the kidneys, where excretory roles are heavily demanding. The scope of this project focuses mainly on P-gp and MRP1. Multidrug resistance mediated by these ABC transporters are a major set-back in chemotherapy and

this underscores the significance of discovering substrates of these ABC transporters. Screening of anticancer agents for their interaction with ABC transporters in a timely manner could inform withdrawal of such drugs before they reach the clinical trials stages. The present project seeks to provide methodological alternatives to identification of substrates of ABC transporters MRP1 and P-gp through high throughput FRET screening.

Methodologies for evaluation of drug-ABC transporters interactions

Electron pragmatic resonance, X-Ray crystallography, cryogenic electron microscopy, double electron-electron resonance spectroscopy, and fluorescence lifetime imaging microscopy (FLIM) have been used to elucidate the structural dynamics and functional significance of MRP1 and P-gp [47-51]. The limitations and inaccessibility of most of these sophisticated techniques, for structure-function investigation cannot be overlooked. The need for more readily available, accessible and less-expensive tools to characterize ABC transporter proteins is crucial. Fluorescence resonance energy transfer (FRET) is rising in prominence and fluorometer-based steady state fluorescence spectroscopy is not only economical but also holds promise for investigation of MRP1.

Fluorescence resonance energy transfer

Fluorescence spectroscopy is a fast increasing technology which has been harnessed for the understanding of the structure-function relationship of ABC transporters [52]. When molecules absorb photons, they become excited and upon

deexcitation, they release the photon of a specific wavelength. In the presence of a stable molecule in the ground state within 100 nm of the excited molecule, the deexcitation energy is not emitted but rather transferred to the second molecule which becomes excited. The molecule which becomes excited first is known as the fluorescent donor while the second molecule which absorbs the released photon is known as the fluorescent acceptor. The inter-fluorophore distance is the distance between the fluorescent donor-acceptor pair where the transfer efficiency is 0.5. It has been shown that the inter-fluorophore distance has a sigmoidal relationship with the transfer efficiency achieved. It is estimated that the shorter the inter-fluorophore distance, the closer the proximity between the fluorescent couple and concomitantly, the higher the transfer efficiency of the donor fluorophore. The mechanism of excitation, transfer and emission of energy can be harnessed to study the movement of proteins with in the presence of ligands. These can shed light on the mechanism, structure and function of specific proteins such as ABC transporters. FRET has been used to show dynamic structural changes of ABC transporters (P-glycoprotein) using recombinant mutants and labelled fluorophores [52]. Engineering a molecular ligation of fluorescent proteins with MRP1 and coupling it with FRET spectroscopy has also recently emerged from our group.

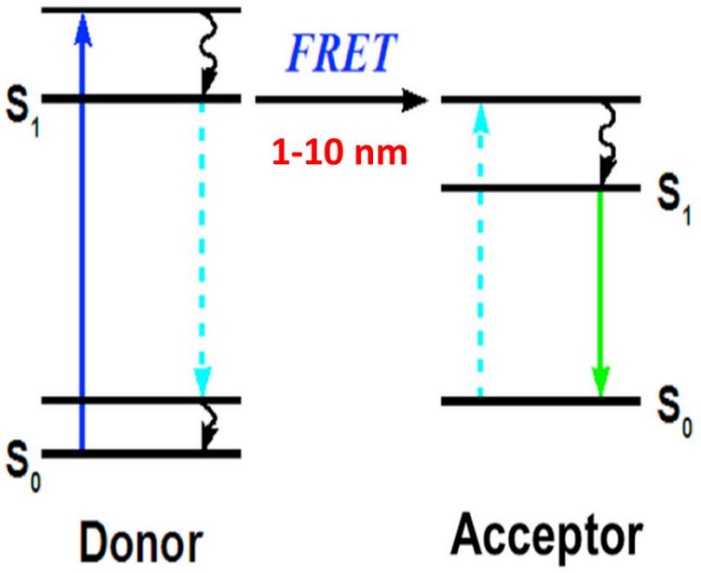

Figure 1.6 Schematic diagram showing the basic principle of fluorescence resonance energy transfer (FRET). If an acceptor molecule in the ground state is within less than 10 nm distance from the donor molecule, the acceptor can be excited by the energy transferred from the donor upon de-excitation.

The rationale for the present study

A few years ago, our laboratory group produced a recombinant MRP1 biosensor which consisted of intra-sequence cloned green and C-terminal red protein fluorophores (green and red fluorescent proteins). This two-colorMRP1 biosensor reports dynamic ligand-induced FRET changes as a measure of structural movements of the NBDs. Additionally, the biosensor was a reporter of eight drug-hits which interact with MRP1, following a screening of pool of NIH drug-like compounds [24]. In the dynamic FRET change experiments, epifluorescence microscopy was used to image the activities and the recombinant protein within a cell-based matrix. Fluorescence lifetime plate reader

technology was employed for the screening protocols to evaluate the interaction of the MRP1 biosensor with several compounds in a cell-based assay. Despite the reasonable data generated from epifluorescence microscopy and Fluorescence lifetime projects, the notion that the use of cells as matrix for both experiments may have slightly compromised the purity and integrity of the fluorescence activities. Moreover, the epifluorescence and Fluorescence lifetime technologies are sophisticated and usually require special expertise to operate.

In the present study, our primary goals were to expand the two-color biosensor FRET-coupled model by further seeking a FRET biosensor which is more FRET sensitive than the precious two-colorMRP1. We engineered six MRP1 biosensors and evaluated their FRET sensitivity in the presence of known ligands of MRP1 with the anticipation of finding a more potent FRET biosensor. In the framework that movement of the NBDs is related to substrate binding and catalytic activities of most ABC transporters, we fused green fluorescence proteins and red fluorescence proteins to the NBD-1 and NBD-2 of the transporter. The six constructs differ in the position where the GFP protein was inserted on the NBD of the transporter. In the presence of a known substrate at the binding pocket of the transporter, it is expected that the NBDs will draw closer together which could elicit changes trackable by fluorescent energy transfer technology. During the primer design and the cloning process, extreme care was taken evade the highly conserved sequences of the NBDs.

Given that P-gp is a more important and well-characterized ABC transporter than MRP1, we developed a FRET sensitive P-gp biosensor, useful for profiling drug interaction with the lipid bilayer embedded protein. The mandate by the Food and Drug

Administration of the United States of America to evaluate all drugs for their interaction with P-gp provides rational for developing a potent P-gp biosensor which could hold promise for high throughput screening of drugs. Using a similar cloning strategy as with MRP1, six clones were engineered by altering the positions of the NBD-located GFP insertion sites.

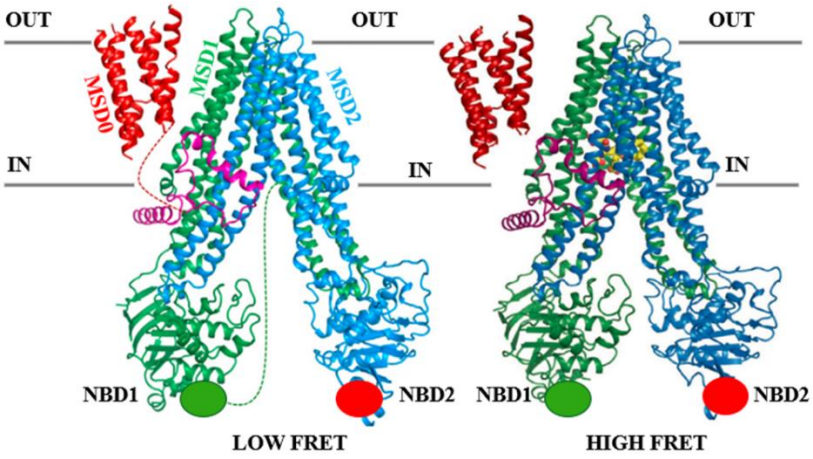

Figure 1.7 Tertiary structure of ABCC1 transporter. Showing where the green and red fluorescent proteins were attached on the NBDs which indicate low and high FRET signal structures. The left structure is the substrate-free open conformation and the right one is the LTC4-bound structure. The proximal movement of the NBDs when the substrate binds, is captured by the movement of the fluorescent pair attached to them which then translates into a FRET signal.

References

1. Saier, M.H., Jr., *A functional-phylogenetic classification system for transmembrane solute transporters.* Microbiol Mol Biol Rev, 2000. **64**(2): p. 354-411.
2. Davidson, A.L., et al., *Structure, function, and evolution of bacterial ATP-binding cassette systems.* Microbiol Mol Biol Rev, 2008. **72**(2): p. 317-64, table of contents.
3. Harvey Lodish, A.B., S Lawrence Zipursky, Paul Matsudaira, David Baltimore, and James Darnell., *Molecular Cell Biology*. 4th ed. 2000, New York: W. H. Freeman.
4. Mamo, G. and A. Pandi, *A Review on ATP Binding Cassette (ABC) Transporters.* Int J Pharma Res Health Sci, 2017. **5**(2): p. 1607-1615.
5. Langmann, T., et al., *Molecular cloning of the human ATP-binding cassette transporter 1 (hABC1): evidence for sterol-dependent regulation in macrophages.* Biochemical and biophysical research communications, 1999. **257**(1): p. 29-33.
6. Schneider, E. and S. Hunke, *ATP-binding-cassette (ABC) transport systems: functional and structural aspects of the ATP-hydrolyzing subunits/domains.* FEMS microbiology reviews, 1998. **22**(1): p. 1-20.
7. Eitinger, T., et al., *Canonical and ECF-type ATP-binding cassette importers in prokaryotes: diversity in modular organization and cellular functions.* FEMS Microbiol Rev, 2011. **35**(1): p. 3-67.
8. Garmory, H.S. and R.W. Titball, *ATP-binding cassette transporters are targets for the development of antibacterial vaccines and therapies.* Infect Immun, 2004. **72**(12): p. 6757-63.
9. Fetherston, J.D., V.J. Bertolino, and R.D. Perry, *YbtP and YbtQ: two ABC transporters required for iron uptake in Yersinia pestis.* Mol Microbiol, 1999. **32**(2): p. 289-99.
10. Piddock, L.J.V., *Clinically relevant chromosomally encoded multidrug resistance efflux pumps in bacteria.* Clinical Microbiology Reviews, 2006. **19**(2): p. 382-+.
11. Delepelaire, P., *Type I secretion in gram-negative bacteria.* Biochimica Et Biophysica Acta-Molecular Cell Research, 2004. **1694**(1-3): p. 149-161.
12. Alaimo, C., et al., *Two distinct but interchangeable mechanisms for flipping of lipid-linked oligosaccharides.* EMBO J, 2006. **25**(5): p. 967-76.
13. Doerrler, W.T., H.S. Gibbons, and C.R.H. Raetz, *MsbA-dependent translocation of lipids across the inner membrane of Escherichia coli.* Journal of Biological Chemistry, 2004. **279**(43): p. 45102-45109.
14. Rees, D.C., E. Johnson, and O. Lewinson, *ABC transporters: the power to change.* Nat Rev Mol Cell Biol, 2009. **10**(3): p. 218-27.
15. Higgins, C.F. and K.J. Linton, *The ATP switch model for ABC transporters.* Nature Structural & Molecular Biology, 2004. **11**(10): p. 918-926.
16. Licht, A. and E. Schneider, *ATP binding cassette systems: structures, mechanisms, and functions.* Central European Journal of Biology, 2011. **6**(5): p. 785-801.
17. Kerr, I.D., P.M. Jones, and A.M. George, *Multidrug efflux pumps: the structures of prokaryotic ATP-binding cassette transporter efflux pumps and implications*

for our understanding of eukaryotic P-glycoproteins and homologues. FEBS J, 2010. **277**(3): p. 550-63.
18. Higgins, C.F., *Multiple molecular mechanisms for multidrug resistance transporters.* Nature, 2007. **446**(7137): p. 749-757.
19. Locher, K.P., *Review. Structure and mechanism of ATP-binding cassette transporters.* Philos Trans R Soc Lond B Biol Sci, 2009. **364**(1514): p. 239-45.
20. Altenberg, G.A., *The engine of ABC proteins.* News Physiol Sci, 2003. **18**: p. 191-5.
21. Biemans-Oldehinkel, E., M.K. Doeven, and B. Poolman, *ABC transporter architecture and regulatory roles of accessory domains.* FEBS Lett, 2006. **580**(4): p. 1023-35.
22. Dawson, R.J., K. Hollenstein, and K.P. Locher, *Uptake or extrusion: crystal structures of full ABC transporters suggest a common mechanism.* Mol Microbiol, 2007. **65**(2): p. 250-7.
23. Johnson, Z.L. and J. Chen, *Structural Basis of Substrate Recognition by the Multidrug Resistance Protein MRP1.* Cell, 2017. **168**(6): p. 1075-1085 e9.
24. Iram, S.H., et al., *ATP-Binding Cassette Transporter Structure Changes Detected by Intramolecular Fluorescence Energy Transfer for High-Throughput Screening.* Mol Pharmacol, 2015. **88**(1): p. 84-94.
25. Holland, I.B. and M.A. Blight, *ABC-ATPases, adaptable energy generators fuelling transmembrane movement of a variety of molecules organisms from bacteria to humans.* Journal of Molecular Biology, 1999. **293**(2): p. 381-399.
26. Pedersen, P.L., *Transport ATPases into the year 2008: a brief overview related to types, structures, functions and roles in health and disease.* Journal of Bioenergetics and Biomembranes, 2007. **39**(5-6): p. 349-355.
27. Bouige, P., et al., *Phylogenetic and functional classification of ATP-binding cassette (ABC) systems.* Curr Protein Pept Sci, 2002. **3**(5): p. 541-59.
28. Bryan, J. and L. Aguilar-Bryan, *Sulfonylurea receptors: ABC transporters that regulate ATP-sensitive K(+) channels.* Biochim Biophys Acta, 1999. **1461**(2): p. 285-303.
29. Senior, A.E. and D.C. Gadsby, *ATP hydrolysis cycles and mechanism in P-glycoprotein and CFTR.* Semin Cancer Biol, 1997. **8**(3): p. 143-50.
30. Dassa, E. and P. Bouige, *The ABC of ABCs: a phylogenetic and functional classification of ABC systems in living organisms.* Research in Microbiology, 2001. **152**(3-4): p. 211-229.
31. Saier, M.H., Jr., et al., *The transporter classification database.* Nucleic Acids Res, 2014. **42**(Database issue): p. D251-8.
32. Cole, S.P., *Targeting multidrug resistance protein 1 (MRP1, ABCC1): past, present, and future.* Annu Rev Pharmacol Toxicol, 2014. **54**: p. 95-117.
33. Dean, M., Y. Hamon, and G. Chimini, *The human ATP-binding cassette (ABC) transporter superfamily.* Journal of lipid research, 2001. **42**(7): p. 1007-1017.
34. Leslie, E.M., R.G. Deeley, and S.P.C. Cole, *Multidrug resistance proteins: role of P-glycoprotein, MRP1, MRP2, and BCRP (ABCG2) in tissue defense.* Toxicology and Applied Pharmacology, 2005. **204**(3): p. 216-237.
35. Su, W. and G.W. Pasternak, *The role of multidrug resistance-associated protein in the blood-brain barrier and opioid analgesia.* Synapse, 2013. **67**(9): p. 609-19.

36. Knauer, M.J., et al., *Human skeletal muscle drug transporters determine local exposure and toxicity of statins.* Circ Res, 2010. **106**(2): p. 297-306.
37. Lee, S.H., et al., *MRP1 polymorphisms associated with citalopram response in patients with major depression.* J Clin Psychopharmacol, 2010. **30**(2): p. 116-25.
38. Dean, M., Y. Hamon, and G. Chimini, *The human ATP-binding cassette (ABC) transporter superfamily.* J Lipid Res, 2001. **42**(7): p. 1007-17.
39. Vasiliou, V., K. Vasiliou, and D.W. Nebert, *Human ATP-binding cassette (ABC) transporter family.* Hum Genomics, 2009. **3**(3): p. 281-90.
40. Borst, P. and R.O. Elferink, *Mammalian ABC transporters in health and disease.* Annual Review of Biochemistry, 2002. **71**: p. 537-592.
41. Dean, M. and R. Allikmets, *Complete characterization of the human ABC gene family.* J Bioenerg Biomembr, 2001. **33**(6): p. 475-9.
42. Blight, M.A. and I.B. Holland, *Structure and function of haemolysin B,P-glycoprotein and other members of a novel family of membrane translocators.* Mol Microbiol, 1990. **4**(6): p. 873-80.
43. Oldham, M.L., A.L. Davidson, and J. Chen, *Structural insights into ABC transporter mechanism.* Current Opinion in Structural Biology, 2008. **18**(6): p. 726-733.
44. Procko, E., et al., *The mechanism of ABC transporters: general lessons from structural and functional studies of an antigenic peptide transporter.* Faseb Journal, 2009. **23**(5): p. 1287-1302.
45. Piehler, A.P., et al., *The human ABC transporter pseudogene family: Evidence for transcription and gene-pseudogene interference.* Bmc Genomics, 2008. **9**.
46. Cole, S.P. and R.G. Deeley, *Multidrug resistance mediated by the ATP-binding cassette transporter protein MRP.* Bioessays, 1998. **20**(11): p. 931-40.
47. Jin, M.S., et al., *Crystal structure of the multidrug transporter P-glycoprotein from Caenorhabditis elegans.* Nature, 2012. **490**(7421): p. 566-9.
48. Srinivasan, V., A.J. Pierik, and R. Lill, *Crystal structures of nucleotide-free and glutathione-bound mitochondrial ABC transporter Atm1.* Science, 2014. **343**(6175): p. 1137-40.
49. Korkhov, V.M., S.A. Mireku, and K.P. Locher, *Structure of AMP-PNP-bound vitamin B12 transporter BtuCD-F.* Nature, 2012. **490**(7420): p. 367-72.
50. Du, D., et al., *Structure of the AcrAB-TolC multidrug efflux pump.* Nature, 2014. **509**(7501): p. 512-5.
51. Choudhury, H.G., et al., *Structure of an antibacterial peptide ATP-binding cassette transporter in a novel outward occluded state.* Proc Natl Acad Sci U S A, 2014. **111**(25): p. 9145-50.
52. Verhalen, B., et al., *Dynamic ligand-induced conformational rearrangements in P-glycoprotein as probed by fluorescence resonance energy transfer spectroscopy.* J Biol Chem, 2012. **287**(2): p. 1112-27.

CHAPTER 2

DEVELOPMENT OF NOVEL INTRAMOLECULAR FRET-BASED MRP1 BIOSENSORS TO IDENTIFY NEW SUBSTRATES AND MODULATORS.

Abstract

Multidrug resistance protein 1 (MRP1) can efflux a wide variety of molecules including toxic chemicals, drugs and their derivatives out of cells. Substrates of MRP1 include anti-cancer agents, antibiotics, anti-virals, anti-HIV and many other drugs. To identify novel substrates and modulators of MRP1 by exploiting intramolecular FRET, we genetically engineered 6 different two-color MRP1 proteins by changing GFP insertion sites while keeping the RFP at the C-terminal of MRP1. Four of six recombinant proteins showed normal expression, localization and transport activity. We quantified intramolecular FRET using ensemble fluorescence spectroscopy in response to binding of known substrate or ATP alone, substrate/ATP and trapping of the transporter in closed conformation by vanadate. Recombinant MRP1 proteins GR-881, GR-888 and GR-905 exhibited reproducible and higher FRET changes under all tested conditions and are very promising to be used as MRP1 biosensor. Furthermore, we used GR-881 to screen 40 novel anticancer drugs and identified 10 hits that potentially directly interact with MRP1 and could be substrates or modulators. Profiling of drug libraries for interaction with MRP1 can provide very useful information to improve the efficacy and reduce the toxicity of various therapies.

Keywords: ATP-binding cassette proteins, Multidrug resistance, Fluorescence resonance energy transfer, Two-color MRP1, Biosensors.

Introduction

ATP-binding cassette (ABC) membrane proteins are a large superfamily of proteins consisting of seven subfamilies (A to G), which mediate the ATP-dependent transport of diverse solutes including lipids, peptides, heavy metals, ions, and a wide variety of endogenous and exogenous compounds and their metabolites across biological membranes [1–7]. Ubiquitously found in all phyla, ABC transporters are unidirectional importers or exporters in bacteria, but only exporters in eukaryotes [8, 9]. When overexpressed in tumors, ABC proteins such as P-glycoprotein (P-gp/ABCB1), multidrug drug resistance protein 1 (MRP1/ABCC1), and breast cancer resistance protein (BCRP/ABCG2) are implicated in poor patient response to chemotherapy. These ABC transporters function in an ATP-dependent manner and efflux their substrate drugs out of cells, negatively impacting the efficacy of those drugs. MRP1 can also efflux a remarkable variety of xenobiotics and organic anions from endogenous sources, which are mostly conjugated to glutathione, glucuronide, or sulfate [10, 11].

The prototypical functional ABC transporter is composed of four domains, two membrane spanning domains (MSDs), each containing six transmembrane (TM) α-helices, and two nucleotide-binding domains (NBDs) that are cytosolic [12–14]. The structure of MRP1 and several “C” subfamily members contains five domains. The two membrane-spanning domains (MSD1 and MSD2) [15, 16] are intertwined to form the substrate-binding site/s and the substrate translocation pathway, and an additional MSD (MSD0) at the amino-terminus of the protein, whose specific biological function is poorly understood [9, 17, 18]. When bound with ATP and substrate, the two cytosolic

NBDs dimerize in a head-to-tail orientation. The energy required to translocate the substrates is generated by the binding and hydrolysis of ATP [20–22].

Overexpression of MRP1 was reported to confer multidrug resistance in acute leukemia, prostate cancer, breast cancer, and neuroblastoma by actively pumping out anti-cancer agents, thereby preventing the accumulation of anti-cancer drugs, eventually causing poor chemotherapeutic outcomes [10, 23–25]. In addition to anti-cancer agents, MRP1 can reduce the efficacy of a wide variety of drugs commonly used for various metabolic diseases and neurological disorders, as well as antivirals, antimalarials, antibiotics, antidepressants, and anti-human immunodeficiency virus (HIV) drugs [1, 26, 27]. The strategic distribution of human MRP1 at “pharmacological sanctuary sites” such as the blood–brain and blood–testis barriers, indicates the chemoprotective and tissue-defensive roles of the protein [10]. Consequently, MRP1 plays an important role in the absorption and disposition of a remarkably diverse set of substrates across different organs and physiological barriers [28]. The critical role MRP1 plays in health and disease is further corroborated by its involvement in biochemical processes such as redox homeostasis, cellular processes such as hormone secretion, and the etiology of neurodegenerative, immunological, and cardiovascular pathologies [29–36].

Generally, drug development involves painstaking steps which include basic research, in vitro drug screening, in vivo experimentation, preclinical stage, stage 1 to stage 4 clinical trials, expending billions of dollars before the drug can be accessible to the population [37]. However, a significant percentage of drugs fail in the clinical trials due to a lack of efficacy and toxicity issues, costing billions of dollars. Profiling drug–transporter interactions may allow discarding undesirable compounds at the very early

stage to reduce economic burden and may avoid potential drug–drug or food–drug interactions. Furthermore, profiling drug interactions with MRP1 can identify drugs that are at high or low risk of developing multidrug resistance, as well as discovery of novel inhibitors useful for clinical chemotherapy, especially in cancers where MRP1 is overexpressed and contributes to multidrug resistance.

To investigate the structural changes of MRP1 during transport activity in live cells, we previously engineered a two-color MRP1 construct by inserting green fluorescent protein (GFP) and red fluorescent protein (TagRFP) at the C-terminus of NBD1 and NBD2, respectively (Figure 1A), and quantified intramolecular fluorescence resonance energy transfer (FRET) changes as an index of NBD conformational changes [27]. We also used the two-color MRP1 to detect substrate/inhibitor/activator candidates and identified eight compounds that directly interact and induce a conformational change in the structure of MRP1 after screening of the National Institutes of Health (NIH) Clinical Collection (NCC; a library of 446 drug-like compounds) [27]. Six of the eight hits were later found to directly interact with MRP1 [38], while further work is needed to verify the interaction of the remaining two hits. These findings validated the utility of the intramolecular FRET-based approach using two-color MRP1 to identify compounds that directly interact with MRP1. Our claim that substrate binding results in conformational changes in the NBDs and brings them closer was further supported by recent high-resolution structures of bovine MRP1 in apo and substrate-bound states (Figure 2C).

However, based on our ongoing work and our expert knowledge of MRP1 substrate specificity, we expected many more hits from screening 446 NIH drug-like compounds. We strongly felt that many potential compounds that directly interact with

MRP1 were missed out in this screening due to high noise-to-signal ratio. In our proof-of-concept study, we used a highly specialized fluorescence lifetime microplate reader for high-throughput drug screening, which is not yet commercially available through an established manufacturer. In addition, the FRET change signal upon ligand interaction was not sufficiently high to perform screening with a more commonly used fluorescence intensity microplate reader or a fluorometer. In order to make this innovative and potentially transformative technology more readily accessible, economical, and commercially more attractive, we decided to create a more efficient two-color MRP1 construct, which can produce a bigger FRET change signal upon interaction with the substrate. Therefore, our objective in this study was to engineer several new two-color MRP1 recombinant proteins by altering the GFP insertion site and to identify the most efficient FRET reporter of NBD conformational changes in MRP1.

Materials and methods

Chemicals

Nucleotides, doxorubicin, anti-GFP antibody, benzamidine, poly-D-lysine, saponin, and 2-mercaptoethanol were purchased from Sigma Aldrich (St. Louis, MO, USA). Estradiol glucuronide (E217βG) and sodium orthovanadate were obtained from Santa Cruz (Dallas, TX, USA). MK571 was received from Cayman Chemicals (Ann Arbor, MI, USA). Restriction enzymes were purchased from New England Biolabs (New England, MA, USA) and phosphate-buffered saline (PBS) was purchased from Thermo Scientific (Sunnyvale, CA, USA).

Engineering two-colorMRP1 constructs

All the genetically engineered two-color MRP1 proteins have a pTagRFP-N vector as a backbone. To engineer the GR-638 construct, firstly, a C-terminal 2.6-kb insert fragment of MRP1 which encodes amino acids 639–1531 (stop codon removed) was generated by polymerase chain reaction (PCR) using the following primers: forward, 5' GTA CCG CGG GGG GGC ACG AAC AGC ATC ACC G 3'**;** reverse, 5' GTA ACC GGT CT CAC CAA GCC GGC GTC TTT GGC CAT G 3'. It was cloned in frame with TagRFP (underlined sequence is the designed restriction site). Secondly, a 0.7-kb insert fragment which codes for GFP was amplified using the following primers: forward, 5' GTA GTC GAC ATG GTG AGCAAG GGC GAG GAG 3'; reverse, 5' GTA CCG CGG CTT GTA CAG CTC GTC CAT GCC 3'. It was fused to the construct. In the third step, an N-terminal 2-kb fragment of MRP1, which codes for amino acids 1–638, was

amplified with the following primers: forward, 5’ GTA GAG CTC ATG GCG CTC CGG GGC TTC TGC AG 3’; reverse, 5’ CTA GTC GAC GCC GTC TTT GAC AGG CCG TCG CTC 3’. It was inserted in frame with GFP to generate the final construct. The GFP sequence in the final two-color recombinant protein construct was separated from the N-terminus and C-terminus of MRP1 via amino-acid linkers, valine–aspartate and proline–arginine, respectively. With the stop codon of MRP1 eliminated, the C-terminal end of the protein was ligated to TagRFP, separated by a linker made of five amino acids—threonine, glycine, leucine, alanine, and threonine.

The schematic diagram of the six engineered two-color MRP1s is shown in Figure 2.1A. A similar cloning strategy was employed to engineer five other constructs distinguishable by the variants of GFP insertion sites. Accordingly, constructs GR-648, GR-859, GR-881, GR-888, and GR-905 were cloned by inserting GFP after amino-acid residues 648, 859, 881, 888, and 905, respectively, in the MRP1 protein. The primer sequences of GFP, as well as those of N-terminal and C-terminal MRP1 fragments, are shown in table 2.1. A schematic diagram of two-color MRP1, showing the distinctive GFP insertion sites, is shown in Figure 2.1B. A tertiary structure representation of bovine MRP1 in open (substrate-free) and closed (substrate-bound) conformations is shown in Figure 2.1C.

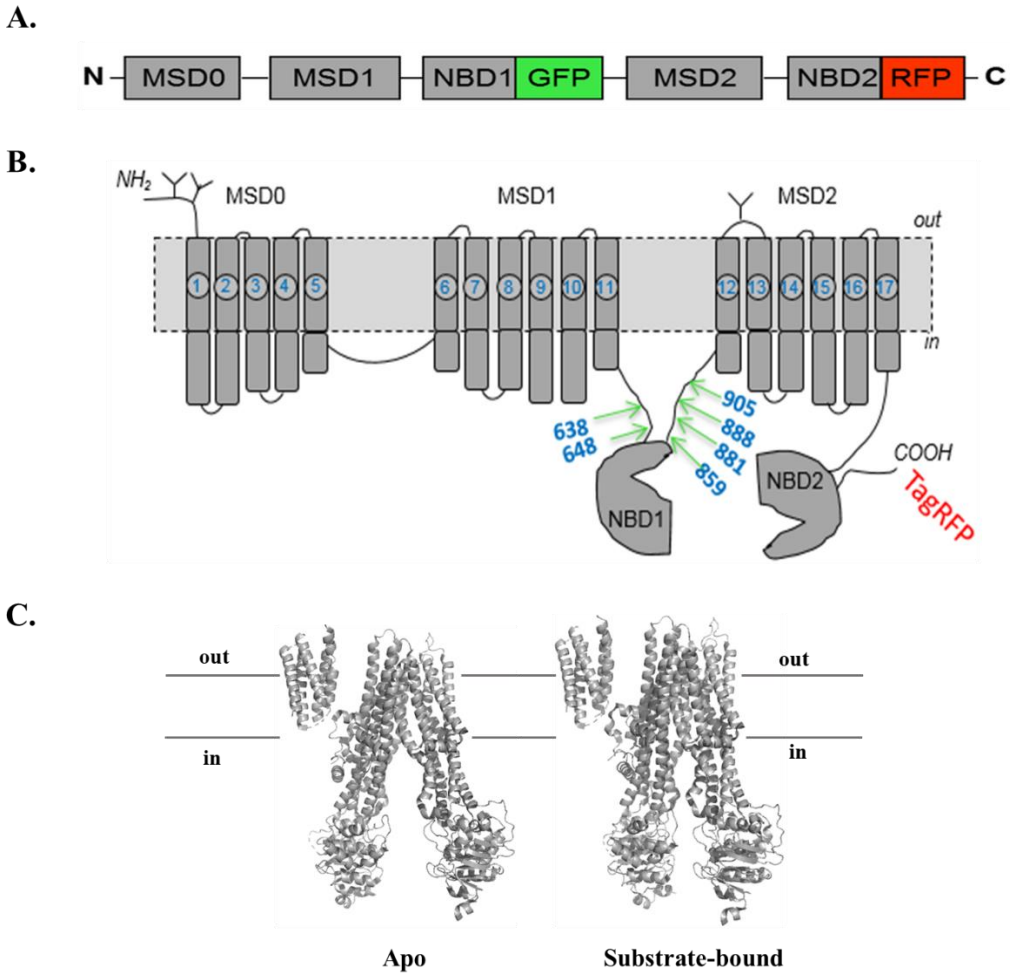

Figure 2.1. Schematic of two-color MRP1 structures. A- Schematic diagram of two-color MRP1 construct showing C-terminal TagRFP and an intra-sequence GFP. B- Predicted secondary structure of two-color MRP1 showing the three membrane spanning domains (MSD0, MSD1 and MSD2), the two cytoplasmic nucleotide binding domains (NBD1, NBD2) and the GFP insertion sites for engineering the constructs. The numbers 638, 648, 860, 881, 888 and 905 represent the amino acid residue number of the wild-type MRP1 after which GFP is inserted. TagRFP is fused

to the C-terminal of MRP1. C- Structure of bovine MRP1 in the apo (left, PDB code: 5UJ9) and substrate bound (right, PDB code: 5UJA) condition.

Table 2.1 Primer used to clone two-color MRP1 constructs

Primer Names	Sequences (5'⟶3')
$MRP1_{1–638}$ forward	GTA GAG CTC ATG GCG CTC CGG GGC TTC TGC AG
$MRP1_{1–638}$ reverse	CTA GTC GAC ATT CCT CAC GGT GAT GCT GTT CGT GCC C
$MRP1_{639–1531}$ forward	GTA CCG CGG GCC ACA TTC ACC TGG GCC AGG AGC
$MRP1_{639–1531}$ reverse	GTA ACC GGT CT CAC CAA GCC GGC GTC TTT GGC CAT G
$MRP1_{1–648}$ forward	GTA GAG CTC ATG GCG CTC CGG GGC TTC TGC AG
$MRP1_{1–648}$ reverse	CTA GTC GAC ATT CCT CAC GGT GAT GCT GTT CGT GCC C
$MRP1_{649–1531}$ forward	GTA CCG CGG GCC ACA TTC ACC TGG GCC AGG AGC
$MRP1_{649–1531}$ reverse	GTA ACC GGT CT CAC CAA GCC GGC GTC TTT GGC CAT G
$MRP1_{1–859}$ forward	GTA GAG CTC ATG GCG CTC CGG GGC TTC TGC AG
$MRP1_{1–859}$ reverse	CTA GTC GAC GTC TCG AGC CAG CAG CTC CTG GTA GG
$MRP1_{860–1531}$ forward	GTA CCG CGG GGC GCC TTC GCT GAG TTC CTG
$MRP1_{860–1531}$ reverse	GTA ACC GGT CT CAC CAA GCC GGC GTC TTT GGC CAT G
$MRP1_{1–881}$ forward	GTA GAG CTC ATG GCG CTC CGG GGC TTC TGC AG
$MRP1_{1–881}$ reverse	CTA GTC GAC GTT CTC CTC TGC ATC CTG CTC CTG C
$MRP1_{882–1531}$ forward	GTA CCG CGG GGG GTC ACG GGC GTC AGC GGT
$MRP1_{882–1531}$ reverse	GTA ACC GGT CT CAC CAA GCC GGC GTC TTT GGC CAT G
$MRP1_{1–888}$ forward	GTA GAG CTC ATG GCG CTC CGG GGC TTC TGC AG
$MRP1_{1–888}$ reverse	CTA GTC GAC ACC GCT GAC GCC CGT GAC CCC GT
$MRP1_{889–1531}$ forward	GTA CCG CGG CCA GGG AAG GAA GCA AAG CAA ATG GAG

$MRP1_{889–1531}$ reverse	GTA ACC GGT CT CAC CAA GCC GGC GTC TTT GGC CAT G
$MRP1_{1–905}$ forward	GTA GAG CTC ATG GCG CTC CGG GGC TTC TGC AG
$MRP1_{1–905}$ reverse	CTA GTC GAC ACT GTC CGT CAC CAG CAT GCC ATT CTC C
$MRP1_{906–1531}$ forward	GTA CCG CGG GCA GGG AAG CAA CTG CAG AGA CAG C
$MRP1_{906–1531}$ reverse	GTA ACC GGT CT CAC CAA GCC GGC GTC TTT GGC CAT G
GFP-forward	GTA GTC GAC ATG GTG AGC AAG GGC GAG GAG CTG
GFP-reverse	CTA CCG CGG CTT GTA CAG CTC GTC CAT GCC GAG AG

Cell lines and cell culture

The HEK293T (human embryonic kidney) cell line was generously donated by Dr. Adam Hoppe (South Dakota State University, Brookings, SD, USA). Dulbecco's modified Eagle medium (DMEM) (GE Healthcare, Marlborough, MA, USA) enriched with 10% fetal bovine serum (FBS) was used to grow the HEK293 cell lines. Cell lines were grown in a humidified incubator maintained at 5% CO_2 and 37 °C. This incubation condition was retained in all subsequent cell culture procedures.

Preparation of MRP1-enriched membrane vesicles

Membrane vesicles were prepared based on the method described by Leo et al. (1996) with minor alterations. Thawed frozen cell pellets from −80 °C were resuspended in homogenization buffer (250 mM sucrose, 50 mM Tris-HCl, and 0.25 mM $CaCl_2$) supplemented with 1× protease inhibitor cocktail (enriched with 1mM ethylenediaminetetraacetic acid (EDTA)). Cell suspension was pressurized to 450 psi in a pre-cooled nitrogen bomb chamber for 5 min to disrupt the plasma membrane. Exploded

cell lysates were then centrifuged at 500× *g* at 4 °C for 10 min. The supernatant was collected into clean pre-cooled high-speed ultracentrifuge tubes, while the cell pellets were re-suspended in homogenization buffer and re-centrifuged to pool the second supernatant. The entire supernatant retrieved was layered over 35% (*w*/*w*) sucrose complemented with 10 mM Tris-HCl and 1 mM EDTA (pH 7.4) and centrifuged at 25,000 rpm at 4 °C using a Beckman SW28 swinging bucket rotor in the Beckman Optima LE-80K ultracentrifuge (Beckman Coulter, Brea, CA, USA) for 1 h 10 min. About 8 mL of the opaque interface was recovered in low-sucrose buffer (25 mM sucrose and 10 mM Tris-HCl; pH 7.4) and centrifuged again for 35 min at 25,000 rpm at 4 °C. The supernatant was discarded, while the pellets were resuspended and washed in 1 mL of transport buffer (50 mM Tris-HCl and 250 mM sucrose; pH 7.4) by ultracentrifugation at 55,000 rpm for 20 min using the mini-ultra rotor in the Beckman TL-100 ultracentrifuge. The plasma membrane pellets were resuspended in transport buffer and passed through a 27-gauge needle 20 times for vesicle formation. All centrifuges and rotors were pre-cooled to 4 °C at least 1 h prior to respective centrifugations. The quick-start Bradford Protein Assay kit (BioRad, Hercules, CA, USA) was used to measure protein concentration.

Two-color MRP1 expressing stable cell lines

Stable cell lines expressing two-color MRP1 constructs were prepared by transfecting the two-color MRP1 expression plasmids into HEK293T cells using jetPRIME mammalian transfection reagent (Polyplus-transfection SA, Illkrich, France) following the manufacturer's guidelines. Cultures were incubated for 24 h before

replacing the complete DMEM with medium containing 400 µg/mL Geneticin (G418). After two weeks of maintaining cells, the G418 concertation was doubled to 800 µg/mL. Using flow cytometry, cells expressing both GFP and RFP were sorted from non-expressing cells, and consequently maintained under a lower G418 selection concentration of 200 µg/mL.

Immunoblot analysis

Lysates of HEK293 cells transfected with two-color and wild-type MRP1 expression vectors were prepared in Halt Protease Inhibitor Cocktail (ThermoFisher Scientific, Waltham, MA, USA) supplemented with radioimmunoprecipitation assay (RIPA) buffer. Pierce bicinchoninic acid (BCA) Protein Assay was the method of choice for protein concentration determination. Prior to an hour-long room-temperature membrane blocking, protein electrophoresis (20 µg of protein) was performed on 7.5% Mini-PROTEAN® TGX™ gels and placed onto an Immobilon® polyvinylidene fluoride (PVDF) membrane (EMD Millipore). After blocking, membranes were incubated at 4 °C overnight using monoclonal anti-MRP1 antibody (IU5C1), or anti-α-tubulin antibody or anti-GFP at 1:250 and 1:5000 dilutions, respectively. Incubation with a secondary antibody was done for an hour at room temperature with horseradish peroxidase-conjugated goat anti-mouse immunoglobulin G (IgG; H+L) and target proteins were detected using enhanced chemiluminescence substrate (PerkinElmer) and the OMEGA LUM G imaging system (Aplegen, Pleasanton, CA, USA).

Detection of MRP1 localization

HEK293T cells were plated and incubated in a humidified 5% CO_2-supplemented incubator at 37 °C for 24 h before being transfected with the six two-color MRP1 plasmids using jetPRIME transfection reagent (Polyplus-transfection SA, Illkrich, France), following the manufacturer's protocol. After 48 h of incubation, cells were imaged with a 63× oil objective confocal microscope (TILL Photonics GmbH, Gräfelfing, Germany). GFP and RFP were excited at 470 nm and 561 nm, respectively. Emissions of GFP and RFP were correspondingly achieved at 496–530 nm and 573–637. All images were processed with the ImageJ software (NIH).

Doxorubicin accumulation assay

HEK293T cells were plated at 3×10^5 cells/well in 2 mL of complete medium on a coverslip coated with poly-D-lysine in a six-well plate and incubated in a humidified incubator (5% CO_2, 37 °C). After 24 h, the HEK293T cells were transiently transfected with the six different two-color MRP1 constructs in separate wells using jetPRIME mammalian transfection reagent and incubated as previously for 48 h prior to doxorubicin treatment for 1 h. Images were taken using a confocal microscope equipped with a 63× oil immersion objective and a 1.35 numeral aperture capacity (TILL Photonics GmbH, Gräfelfing, Germany). GFP and Doxorubicin were excited at 470 nm wavelength using Ar laser illumination, with emission bands of 480–530 nm for GFP and 570–605nm for doxorubicin. RFP was excited at 561 nm with an emission band of 573–637 nm. All images were processed with ImageJ (NIH).

Ensemble fluorescence spectroscopy

HEK-293 cells stably expressing GFP–MRP1 or two-color MRP1 were used to prepare membrane vesicles. Steady-state ensemble fluorimetry was used to determine apo and ligand-induced FRET efficiency with minor modifications in the experimental conditions described previously [39]. Briefly, 10 µg of MRP1-enriched membrane vesicles in Tris sucrose buffer (250 mM Tris and 50 mM sucrose; pH 7.4) were kept for 2 min at 37 °C. Membrane vesicles were then incubated with 10 µM of test compounds for 10 min at 37 °C in a water bath prior to FRET measurements. Fluorescence spectroscopy was carried out in a 50-uL quartz glass cuvette with the Fluorimeter model FL3-11. GFP was excited at 465 nm. Emission for GFP was recorded at 480–650 nm with 3 s of integration time. Excitation and emission slit widths of 5 nm were used in all measurements. Firstly, an emission scan of the GFP–MRP1 sample (donor only) was collected while monitoring average donor emission peak. Emission scans were collected for various two-color MRP1 constructs under different experimental conditions (apo or in the presence of a ligand or test compound) while monitoring donor quenching, and the average donor emission peaks were recorded. The emission scan was collected every 3 s with an interval of 5 nm for a total of 10 min.

To calculate FRET efficiency, the relative fluorescence intensity of the donor in the presence and absence of the acceptor was measured. The ratio of the average donor emission peak intensity in the two-color MRP1 sample to the average donor emission peak intensity in the GFP-MRP1 sample was subtracted from 1 to obtain the transfer efficiency of apo and compound-induced conditions, as shown in Equation (1) [40].

Transfer efficiencies of compound-induced samples were normalized with that of the apo condition to obtain the percent change in FRET.

$$(1 - I_{DA}/I_D) \times 100, \quad (1)$$

where I_D and I_{DA} represent the intensities (counts per second, cps) of the donor and acceptor fluorophores, respectively.

Table 2.2 Parameters for steady state fluorometry

Construct	Donor	Acceptor	Excitation slit nm	Emission slit nm	Excitation wavelength nm	Emission wavelength nm
GFP-MRP1	GFP	-	5	5	465	480-650
GR-638	GFP	RFP	5	5	465	480-650
GR-881	GFP	RFP	5	5	465	480-650
GR-888	GFP	RFP	5	5	465	480-650
GR-905	GFP	RFP	5	5	465	480-650

Anticancer drug-screening using fluorescence spectroscopy-based FRET approach

To validate the two-color MRP1/FRET model as a viable tool for the discovery of potential modulators of the transporter, 40 anti-cancer drugs were screened using the

most sensitive biosensor. Two-color GR-881 was selected as the lead biosensor based on pre-screening results and was, therefore, used for the screening of the 40 clinically tested anti-cancer agents (Appendix A). Firstly, 10 µg of membrane vesicles purified from HEK293/GR-881 were preincubated for 2 min and combined with 10 µM of each of the 40 anti-cancer agents in separate reactions using Tris–sucrose buffer (TSB) as the buffer medium. Prior to FRET measurements with Fluorimeter model FL3-11, the reaction was incubated for 10 min at 37 °C. JNJ-38877605 was used as a negative control for the experiments. Experiments were repeated three times independently, and the percent FRET change was measured and reported as previously described.

Results and discussion

Genetic engineering and expression of two-color MRP1 recombinant proteins

We previously engineered a two-color MRP1 recombinant protein that could be utilized for high-throughput screening of drug libraries to discover unknown activators, inhibitors, or transportable substrates of MRP1 [27]. In order to make this innovative approach more robust and readily accessible, we decided to create new two-color MRP1 constructs, which are more sensitive to substrate interaction. To test if altering the position of the GFP insertion resulted in enhanced FRET sensitivity, we generated six additional two-color MRP1 constructs by inserting the GFP tag at different sites within the MRP1 coding sequence, while keeping the RFP at the end of MRP1 (Figure 2B). Different GFP insertion sites were chosen using our knowledge of ABC transporter structure–function relationships, guided by the homology models of MRP1 and sequence alignments with related transporters. The other major consideration in the design was to avoid regions critical for the expression and function of MRP1. We chose two sites in the loop region preceding NBD1 and four sites for GFP insertion in the loop region connecting NBD1 to TM12. These regions are predicted to be very flexible and dynamic. Based on available structural information for MRP1 and related ABC drug transporters, the fused GFP and RFP tags are expected not to disrupt the binding of various substrates to the binding site/s formed by the MSDs.

MRP1 expression was checked by immunoblot analysis using cell lysates of HEK293 cells transfected with complementary DNA (cDNA) expression vectors encoding wild-type or two-color MRP1, loading 10 μg of whole-cell lysate per lane. The six newly created two-color MRP1 recombinant proteins were GR-638, GR-648, GR-

859, GR-881, GR-888, and GR-905. GR-873 two-color MRP1 was the construct made in our previous proof-of-concept study. Tagging MRP1 with GFP and RFP is reflected by GR, and numbers in the name indicate the GFP insertion site. For instance, in GR-638, GFP is inserted after residue 638 of the wild-type MRP1 sequence. Two-color MRP1 proteins were detected using anti-GFP antibody, and the immunoblot results indicated the expected molecular mass of ~250 kDa for all new two-color MRP1 recombinant proteins, similar to the previously characterized protein GR-873, an indication of the collective sizes of the GFP (27 kDa), TagRFP (27 kDa), and the 190-kDa wild-type MRP1 (Figure 2.2). We demonstrated earlier that the GR-873 expression level and activity are same as wild-type MRP1 (WT-MRP1) protein. Based on immunoblot analysis, expression levels of GR-638, GR-881, GR-888, and GR-905 were normal and similar to GR-873, and, as expected, WT-MRP1 was not detected with anti-GFP antibody. However, the expression levels were moderately reduced for GR-859 and dramatically reduced for GR-648. The insertion of GFP after residue 859 or 648 of MRP1 likely interfered with the proper folding of MRP1 because both insertion sites were closest to NBD1, which is a highly conserved domain in the ABC family of transporters.

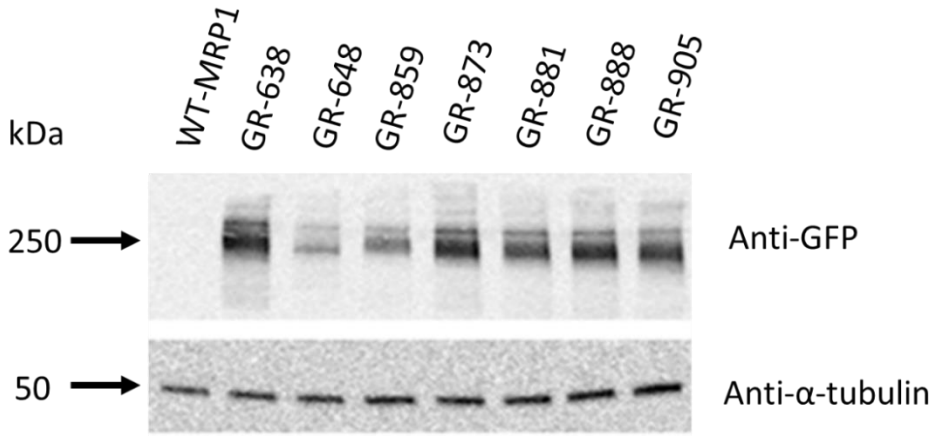

Figure 2.2 Two-color MRP1 immunoblots. Immunoblots of whole-cell lysates (10 μg) containing wild type (WT-MRP1) and 6 two-color MRP1 constructs. Detection was by rabbit polyclonal anti-GFP antibody (1:5000 dilution, overnight at 4 °C) and mouse monoclonal Anti-α-tubulin (1:8000 dilution, overnight at 4 °C).

Localization and transport activity of two-color MRP1 proteins in live cells

Fluorescent protein tags like GFP or RFP are usually fused at the amino-terminal or carboxyl-terminal, and do not often cause protein folding and trafficking issues. However, insertion of GFP within the coding sequence of MRP1 could potentially cause problems with the correct folding and trafficking of MRP1. Although all the two-color MRP1 recombinant proteins showed the expected size, we wanted to make sure that both fluorophores (GFP and RFP) matured properly and that the recombinant MRP1 proteins were folded, trafficked, and localized properly at the plasma membrane of cells. HEK293 cells were transfected with cDNA expression vectors encoding different two-color MRP1 proteins, and confocal microscopy was used to visualize the localization and expression

levels of recombinant MRP1 proteins. Confocal images in Figure 2.3 showed that all two-color MRP1 recombinant proteins except GR-648 localized properly at the plasma membrane. In addition, upon acquiring images using the GFP and RFP channel, and analyzing the merged images, it was obvious that both fluorophores matured properly. However, insertion of GFP in the GR-648 recombinant protein was not tolerated and induced misfolding and processing defects, leading to reduced levels of the recombinant protein, as well as intracellular retention; therefore, this construct was not included in further investigation. The GR-859 recombinant protein showed partial mislocalization and intracellular retention that can be attributed to the moderately reduced levels observed in the Western blots, but the recombinant protein was predominantly localized at the plasma membrane.

To determine if the engineered two-color MRP1 recombinant proteins were functional, their transport activities were evaluated in live cells by measuring accumulation of the fluorescent anti-cancer drug, doxorubicin, a well-known substrate of MRP1 [41,42]. HEK293 cells were transfected with cDNA expression vectors encoding different two-color MRP1 proteins, and confocal microscopy was used to visualize the accumulation of doxorubicin (Dox) inside the cells. Images were captured for GFP, RFP, and Dox, and images were merged for analysis. Transiently transfected cells are expected to have a mixed population of cells, whereby some cells that pick up the vector DNA will express two-color MRP1 while untransfected cells will not at the plasma membrane. HEK293 cells are known to express extremely low or negligible levels of endogenous MRP1. Confocal microscopy of transiently transfected HEK293 cells showed high doxorubicin accumulation in the nucleus of untransfected cells, but doxorubicin

fluorescence was very low or negligible in cells expressing either GR-638, GR-881, GR-888, or GR-905 (Figure 2.4). These results demonstrate that recombinant MRP1 proteins GR-638, GR-881, GR-888, and GR-905 were functionally active. In contrast, HEK293 cells transfected with GR-859 showed high doxorubicin accumulation in the nucleus, indicating that this recombinant protein was not functional, despite having the expected size and proper localization at the plasma membrane. Consequently, GR-859 was not included in further studies.

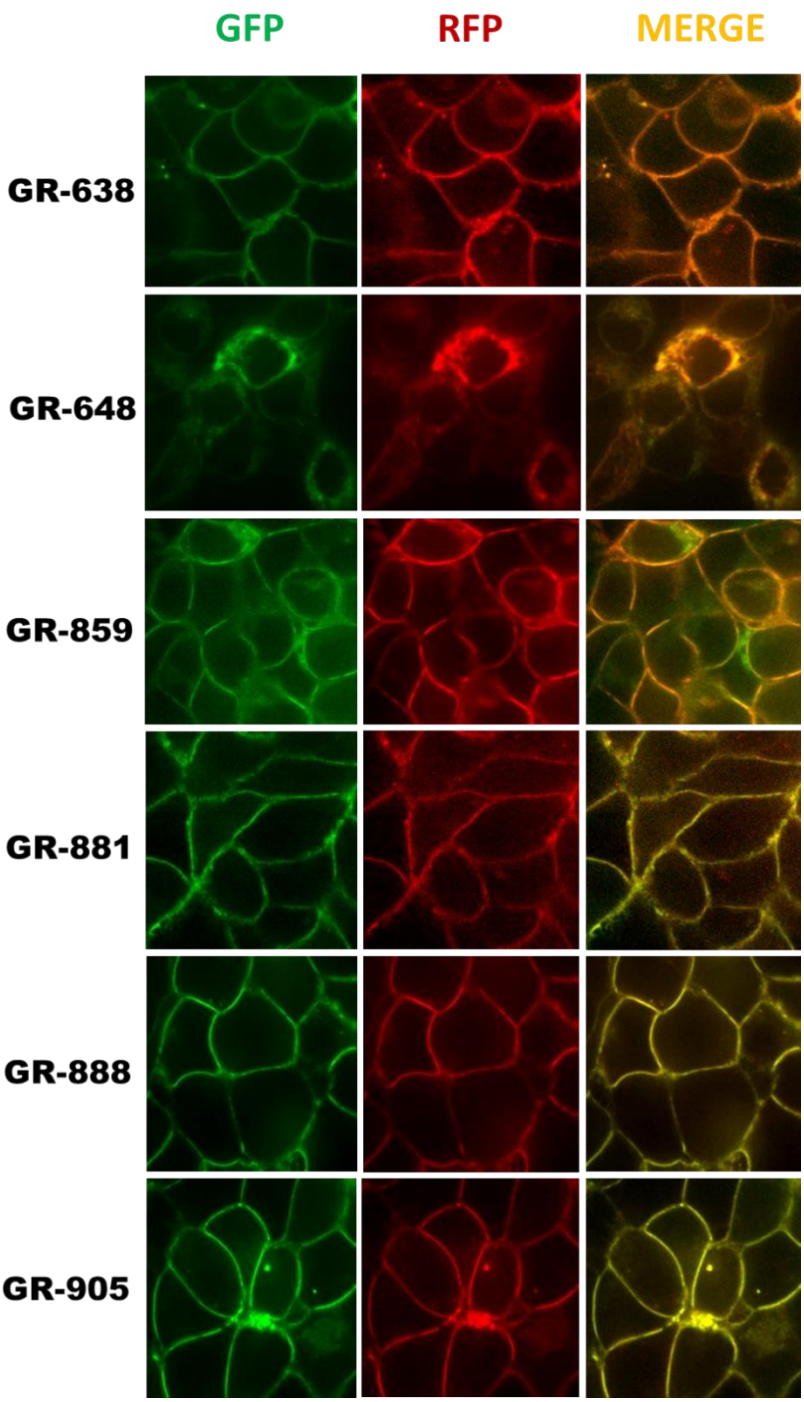

Figure 2.3. Localization and expression of two-color MRP1. HEK-293 cells were plated on glass-bottom chambered coverslips as described in Materials and Methods. Fluorescent images were taken using a confocal microscope equipped with a 63× oil-immersion objective. GFP and

TagRFP were excited at 470 nm and 561 nm respectively. Emission was accomplished at 480-530 nm for GFP and 580-669 nm for RFP respectively.

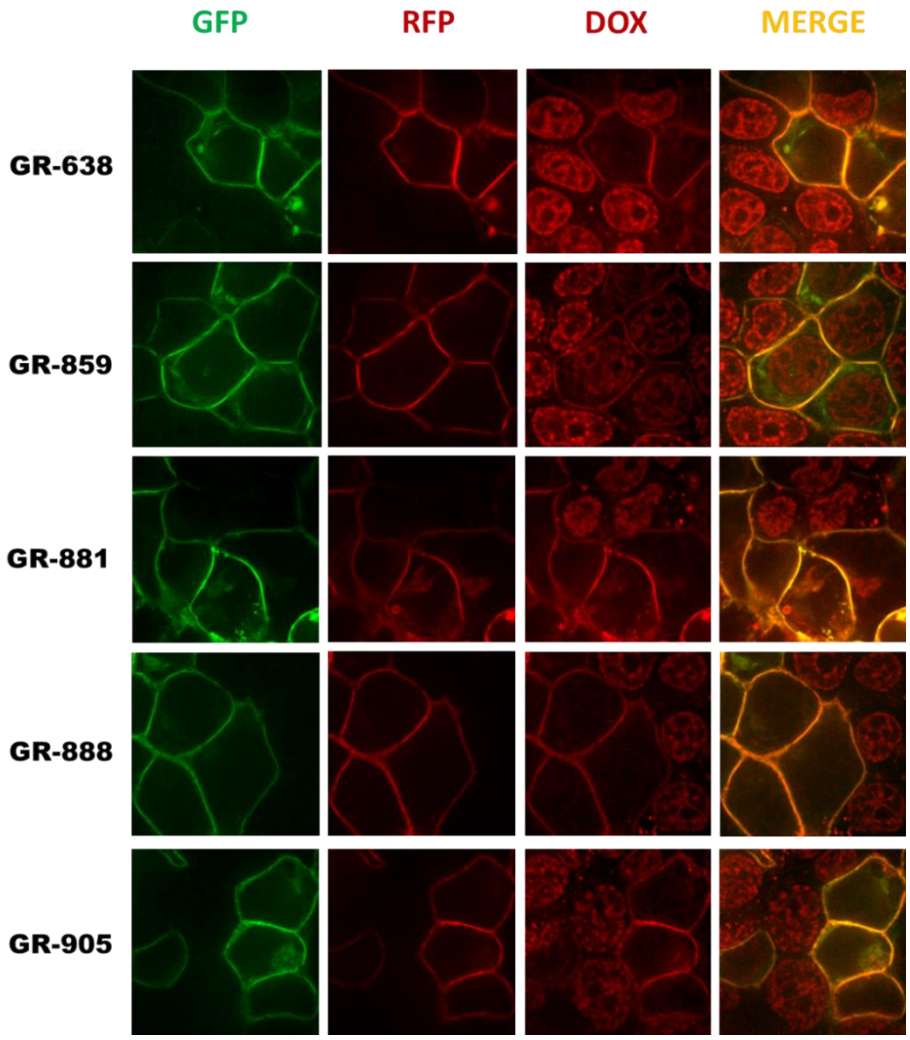

Figure 2.4. Doxorubicin (Dox) accumulation assay. HEK293T cells were transiently transfected with 6 different two-color MRP1 constructs and incubated for 48 hours after which doxorubicin treatment was done. Images were taken using a confocal microscope equipped with 63× objective. GFP and Dox were excited at 470 nm wavelength using Ar laser, with emission bands of 480-530 nm for GFP and 573-637 nm for Dox. RFP was excited at 561 nm and its

emission was collected at 580-669 nm. Data was collected from all three different channels, GFP, RFP and Dox.

Substrate-free FRET efficiencies of the two-color MRP1 proteins

FRET is a very useful tool to detect biochemical interactions, such as protein–protein interactions and protein–DNA interactions, and to study protein structural dynamics [27,43–49]. The efficiency of this nonradiative energy transfer is inversely proportional to the sixth power of the distance between donor and acceptor fluorophores, which makes the FRET approach extremely powerful for detecting conformational changes within a protein. Figure 2.5A shows a graphical representation of the relationship between FRET efficiency and the distance between the donor and acceptor fluorophores. Our goal was to create a two-color MRP1 biosensor that produces a high FRET efficiency change upon substrate interaction. If the intramolecular FRET efficiency of the apo (FRET in the absence of substrate) two-color MRP1 is too low, then the FRET biosensor protein would not be very sensitive reporter to small distance changes in the structure of the protein (representing the bottom part of the curve in Figure 2.5A). Similarly, if the intramolecular FRET efficiency of the apo two-color MRP1 is too high, then the FRET biosensor protein would also not be very sensitive to small distance changes in the structure of the protein (representing the top part of the curve in Figure 2.5A). A two-color MRP1 protein that exhibits an intramolecular FRET efficiency in the range of approximately 30–70% is desirable, because the curve is the steepest in that region; correspondingly, a small structural change upon substrate binding can result in a higher FRET change from the basal level [50].

Previously, we engineered a two-color MRP1 protein (GR-873) that reported substrate-induced intramolecular FRET change as a function of structural changes in the nucleotide domains of MRP1 [27]. To determine the basal intramolecular FRET efficiencies of the new two-color MRP1 proteins, we employed steady-state fluorescence spectroscopy using a fluorometer. To keep the protein in its native environment, membrane vesicles isolated from HEK293 cells stably expressing different two-color MRP1 proteins were used for the FRET experiments. As shown in Figure 2.5B, fluorescence intensity of the donor (GFP) was highest for the GFP-MRP1 construct (donor-only construct with no RFP). The fluorescence intensity of GFP decreased to varying degrees in the different two-color MRP1 recombinant proteins due to donor quenching in the presence of the acceptor, RFP. The shorter the inter-fluorophore distance between the inserted GFP and the terminal RFP, the higher the apo FRET efficiency of the construct. The calculated intramolecular FRET efficiency (%) for GR-638, GR-881, GR-888, and GR-905 was 10.5 ± 1.5%, 66.0 ± 1.0%, 72 ± 1.0%, and 83.5 ± 1.5%, respectively (Figure 2.5C). This indicates that the distance between GFP and RFP is shortest in GR-905 and longest in GR-638. The intramolecular FRET efficiency (%) for apo GR-873 was previously reported to be ~16%. Based on these data, GR-881, GR-888, and GR-905 appear very promising in terms of reporting higher FRET efficiency changes upon interaction with substrate.

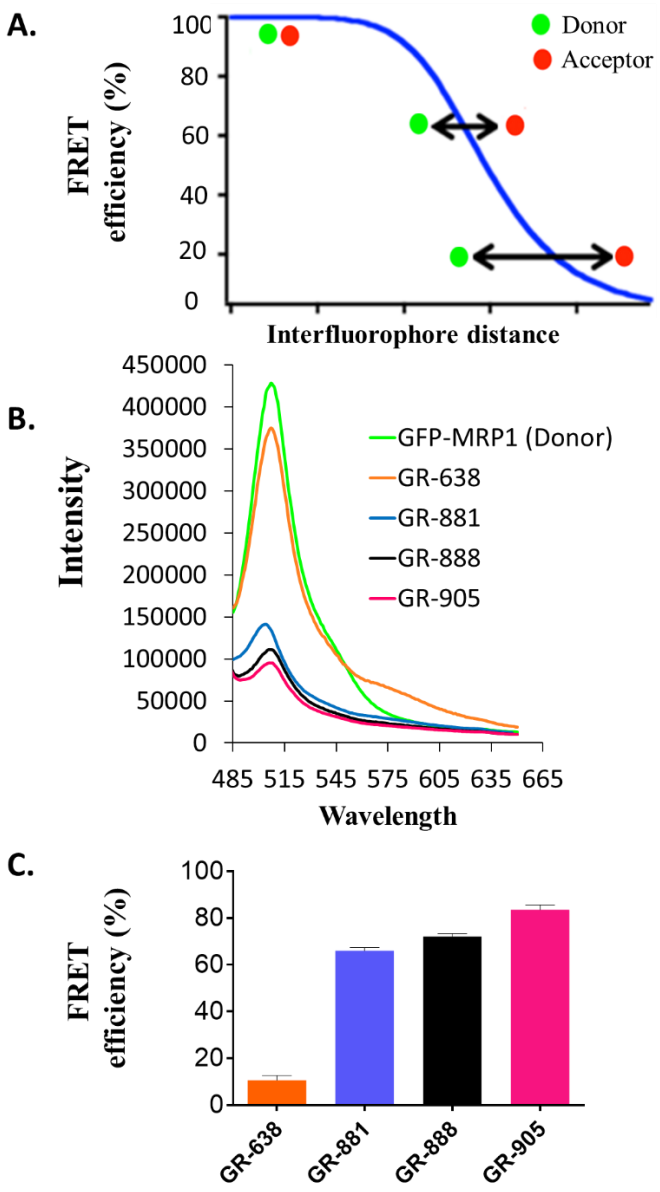

Figure 2.5. Variable ligand-free (Apo) FRET efficiencies of the two-color MRP1 constructs.

A- Graphical representation of the influence of inter-fluorophore distance on transfer efficiency. The more proximal the fluorophores, the higher the FRET efficiency. The higher the apo FRET, the higher the change in transfer efficiency until a certain threshold is reached. B- Fluorescence

spectra of different two-color MRP1 proteins (GFP-MRP1 used as donor control). C-Ligand-free FRET efficiency of different two-color MRP1 proteins. Membrane vesicles were prepared from HEK-293 cells stably expressing different two-color MRP1 proteins (GR-638, GR-881, GR-888, GR-905). 20 µg of each two-color protein in Tris sucrose buffer was prepared and measured for ligand-free FRET with Fluorimeter model FL3-11 using 465 nm excitation wavelength for GFP and 480-650 nm emission wavelength range for both GFP and RFP. Experiments were done in duplicates and in some cases between different membrane vesicle preparation batches. Intensities of the two-color MRP1 constructs were normalized to the donor GFP-MRP1. FRET efficiency was calculated using the equation 1.0.

Evaluation of two-color MRP1 proteins as FRET-based biosensors

To determine the capacity of the engineered two-color MRP1 proteins as biosensors and reporters of conformational changes in the NBDs upon substrate binding, we measured ligand-dependent structural changes of the MRP1 protein through steady-state FRET spectroscopy using the fluorometer. Membrane vesicles isolated from HEK293 cells stably expressing different two-color MRP1 proteins were used for the FRET experiments. In the presence of E217βG (a well-known physiological substrate of MRP1) [51–53], the average FRET efficiency changes observed for GR-638, GR-881, GR-888, and GR-905 were 0.5, 3.35, 2.25, and 2.5%, respectively (Figure 2.6). These results are in agreement with earlier findings that reported conformational changes in the NBDs upon interaction with substrate alone [30,39]. Different two-color MRP1 proteins also showed a range of FRET efficiency changes in the presence of ATP alone or E217βG + ATP. With the exception of GR-638, all the two-color MRP1 proteins produced higher FRET

efficiency changes in the presence of E217βG + ATP compared with either E217βG or ATP alone. This is expected because the presence of both E217βG and ATP should shift the equilibrium toward the closed conformation of the transporter. In addition, all two-color MRP1 proteins produced the highest FRET efficiency change when the transporter was trapped in the closed conformation (E217βG + ATP + vanadate) and this is consistent with the vanadate-locking phenomenon reported for other ABC transporters [54,39]. It is important to note that our previously engineered GR-873 was not able to show detectable FRET change in the presence of E217βG alone, whereas GR-881, GR-888, and GR-905 exhibited significant FRET efficiency changes in the presence of E217βG alone. As shown in Figure 2.6, the three two-color MRP1 proteins (GR-881, GR-888, and GR-905) consistently produced higher FRET efficiency changes in various tested conditions, while the highest FRET efficiency change was observed with GR-881 upon interaction with the substrate alone.

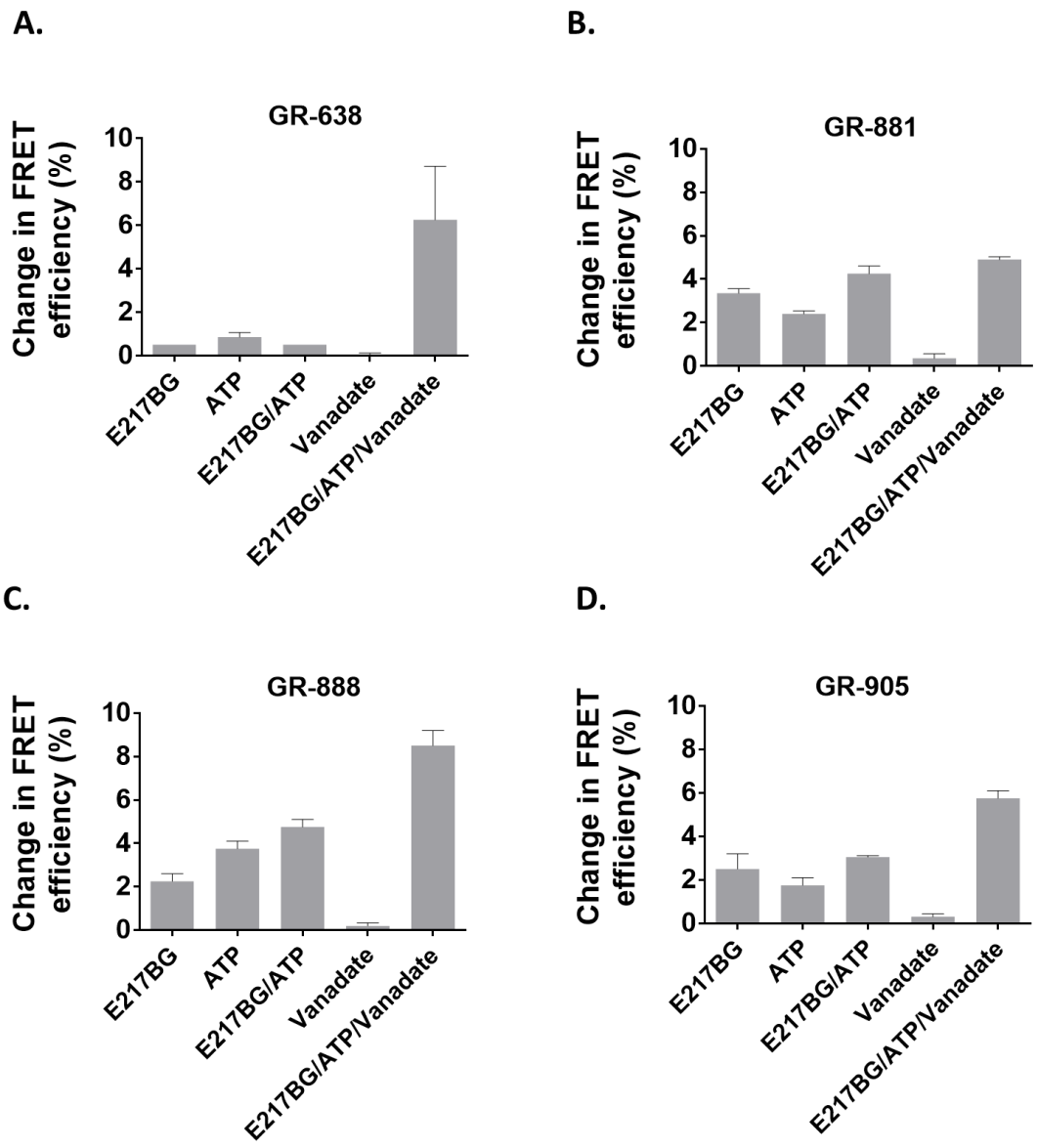

Figure 2.6. Ligand-dependent intramolecular FRET measurements. A- Ligand-dependent FRET changes of GR-638 protein. B- Ligand-dependent FRET changes of GR-881 protein. C- Ligand-dependent FRET changes of GR-888 protein. D- Ligand-dependent FRET changes of GR-905 protein. 20 µg of protein in tris sucrose buffer was prepared and incubated with 5 µM of E217βG and/or 4mM/5 mM ATP/MgCl2 and 1 mM sodium vanadate for 10 minutes prior to FRET Measurements using Fluorimeter model FL3-11. GFP excitation was done at 465 nm and

RFP at 530 nm. Emissions for GFP and RFP were collected at 480-650 nm. Experiments were done in duplicates and in some cases between different membrane vesicle preparation batches.

Identification of Anti-cancer drugs that interact with MRP1

To further validate the two-color MRP1 protein model as a potent biosensor system, and two-color MRP1-coupled steady-state fluorescence spectroscopy as a viable tool for the drug screening to identify novel substrates, inhibitors, or activators of MRP1, we screened 40-novel clinically tested anti-cancer drugs. GR-881 was chosen for this screening because it was found to be most sensitive to substrate binding. Membrane vesicles isolated from HEK293 cells stably expressing the GR-881 MRP1 biosensor were used in the fluorescence spectroscopy-based FRET experiments. We screened the 40-drug library at least two independent times for their interaction with the GR-881 MRP1 biosensor. Results from a single screening are presented in Figure 2.7A. Ten drugs, whose chemical structures are shown in figure 2.8, were identified which increased FRET and produced high and consistent FRET changes in three independent experiments (Figure 2.7B). Means of the FRET efficiency changes observed for the identified hits were as follows: PF-04217903 (1.75%), GDC-0879 (3%), BI-2536 (2.75%), triciribine (2.85%), TW-37 (3.5%), axitinib (3.8%), MK-2206 (5.1%), linsitinib (9.25%), lapatinib ditosylate (9%), and cediranib (11.75%) (Figure 2.7B). Epigallocatechin gallate (EGCG), a known substrate of MRP1 and one of eight compounds previously identified in the FRET-based screening, was used as a positive control and produced a mean value of 3.5% FRET efficiency change. JNJ-38877605, an anti-cancer drug which does not

interact with MRP1, was used as a negative control, and no detectable FRET efficiency change was observed in this case.

In the present study, using our newly engineered GR-881 MRP1 biosensor, we identified 10 compounds that are suggested to directly interact with and induce a conformational change in the structure of MRP1 after screening only 40 anti-cancer drugs. The identified compounds from this screen could be substrates, inhibitors, activators, or molecules that simply interact with MRP1 to stimulate transport of a substrate or bind with the transporter for unknown reasons or could be a false hit due to non-specific interaction with MRP1. Preliminary data in a related ongoing project suggest that three of these 10 hits (triciribine, MK-2206, and cediranib) interact with MRP1, and we plan on conducting a detailed investigation for all 10 hits to understand and confirm the biochemical nature of their interaction with MRP1. Our results indicate that the GR-881 MRP1 biosensor is a very powerful tool for identifying drugs and compounds that interact with MRP1.

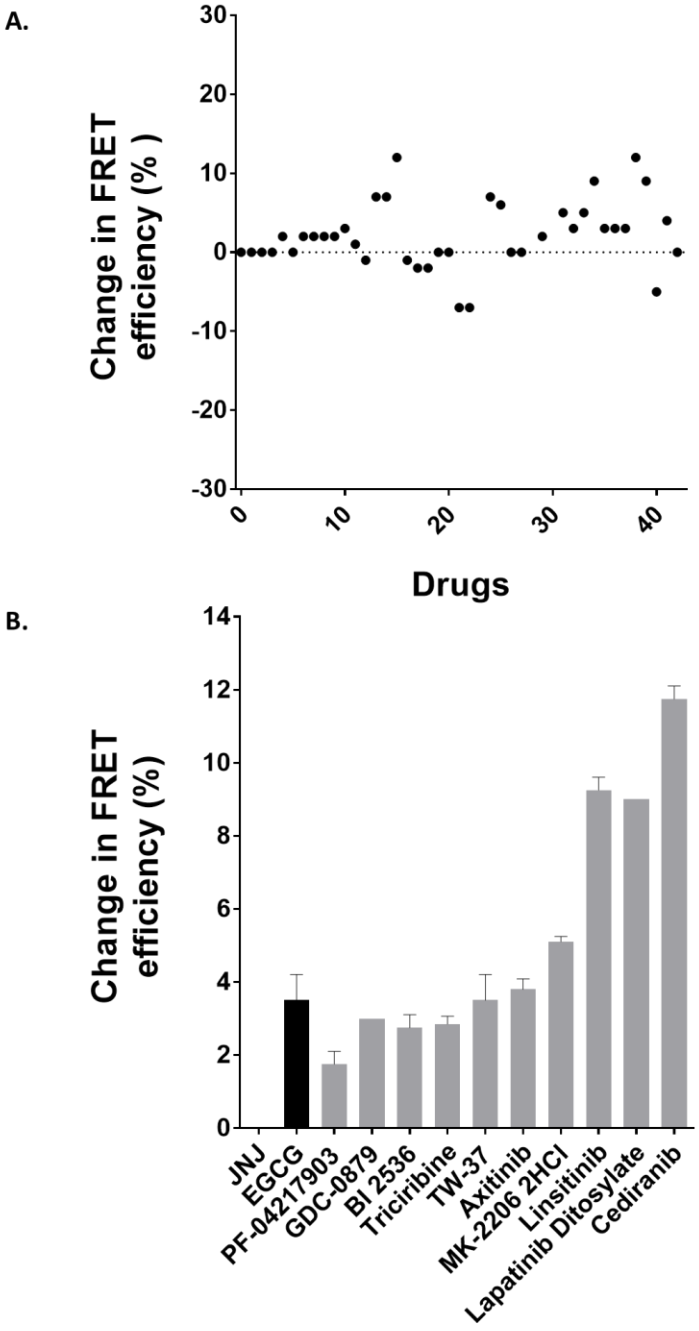

Figure 2.7 Anticancer drug screening with two-color GR-881. A- Change in FRET efficiency (%) for the 40 anticancer drugs from one trial. B- Ten anticancer compound-hits showed consistently reproducible FRET changes with GR-881. FRET measurements were performed using Fluorimeter model FL3-11. Donor excitation occurred at 465 nm and emission was

collected within the 480-650 nm range. GFP quenching observed. The criteria for selecting the ten hits was drugs which recorded reproducible FRET changes in independent screens. The data is represented as mean ± SEM from three independent experiments.

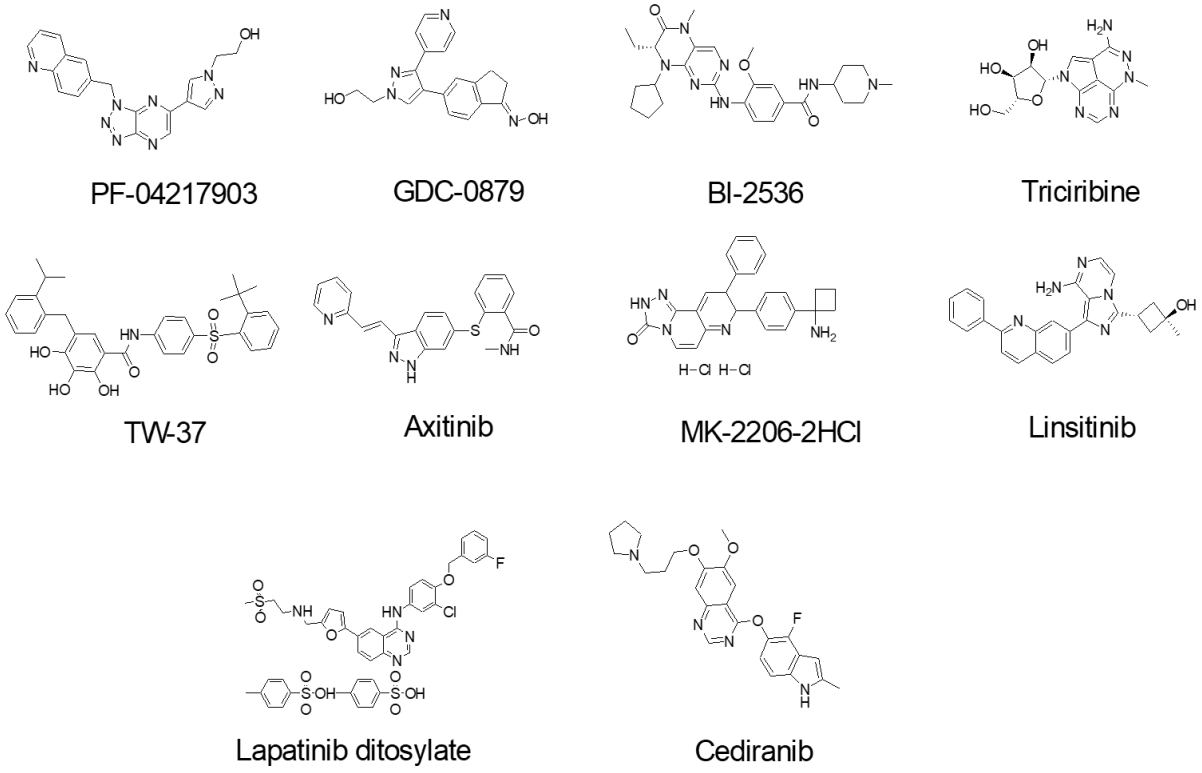

Figure 2.8 Chemical structures of the ten-drug hits.

Conclusion

We previously engineered a two-color MRP1 protein and demonstrated the proof of concept of measuring intramolecular FRET efficiency as an index of protein conformational changes upon ligand binding. When this recombinant protein was used in screening a library of 446 drug-like compounds, we identified eight hit compounds (~2% of total compounds screened). In the present study, we engineered six additional two-color MRP1 recombinant proteins and, after detailed characterization, identified three two-color MRP1 proteins (GR-881, GR-888, and GR-905), which report improved substrate-induced intermolecular FRET changes as a function of structural changes of the protein. The two-color MRP1 biosensor GR-881 was used to screen 40 anti-cancer drugs and was able to identify 10 drugs as hits (25% of total compounds screened). The newly engineered GR-881 has an apo FRET of 66% as compared to 16% apo FRET for the previous construct. Based on Figure 2.5A, GR-881 falls in the middle region of the sigmoidal curve and is expected to produce a higher FRET signal upon a certain structural change. In addition, we think the use of MRP1-enriched membrane vesicles as an experimental matrix instead of cells reduces the complexity of reaction matrices and avoids nonspecific noise, thereby enhancing the overall intramolecular FRET sensitivity in the steady-state fluorescence spectroscopy-based approach.

Traditionally, researchers focused on functional-based approaches to identify modulators of ABC transporter proteins. For MRP1, the membrane-vesicle-based in vitro radiolabeled $E_2$17βG uptake assay is commonly used to identify modulators [55,19]. However, MRP1 and other drug transporters are expected to have multiple distinct substrate-binding sites. A functional assay based on quantifying transport is unable to

detect substrates that bind to a different site and fail to compete with the test substrate. Currently, there is no established high-throughput assay available to identify substrates of MRP1. The idea of the intramolecular FRET-based MRP1 biosensor approach to identifying substrates and modulators is highly innovative and transformative. This approach could potentially be applied to other efflux transporters, and especially to ABC proteins with no known substrate or functional assay. In addition to the discovery of novel substrates and modulators, the two-color MRP1 biosensor protein could be used for single-molecule FRET-based studies to understand the structural dynamics of MRP1 in the native membrane environment. Future projects will focus on the development of a vesicular transport coupled LC–MS/MS assay to verify the MRP1 substrate status of the hits. We also plan on developing a two-color MRP1 fluorescent plate-reader-based high-throughput screening assay to identify more novel substrates of MRP1.

References

1. Cole, S.P. Multidrug resistance protein 1 (MRP1, ABCC1), a 'multitasking' ATP-binding cassette (ABC) transporter. *J. Biol. Chem.* **2014**, *289*, 30880–30888.
2. Dean, M.; Annilo, T. Evolution of the ATP-binding cassette (ABC) transporter superfamily in vertebrates. *Annu. Rev. Genomics Hum. Genet.* **2005**, *6*, 123–142.
3. Annilo, T.; Tammur, J.; Hutchinson, A.; Rzhetsky, A.; Dean, M.; Allikmets, R.Human and mouse orthologs of a new ATP-binding cassette gene, ABCG4. *Cytogenet. Cell Genet*. **2001**, *94*, 196–201.
4. Li, Y.; Revalde, J.; Paxton, J.W. The effects of dietary and herbal phytochemicals on drug transporters. *Adv. Drug Deliv. Rev.* **2017**, 116, 45–62.
5. Dean, M.; Allikmets, R. Evolution of ATP-binding cassette transporter genes. *Curr. Opin. Genet. Dev.* **1995**. 5, 779–785.
6. Mamo, G.; Pandi, A. A Review on ATP Binding Cassette (ABC) Transporters. *Int. J. Pharma. Res. Health Sci.* **2017**, *5*, 1607–1615.
7. Langmann, T.; Klucken, J.: Reil, M.: Liebisch, G.: Luciani, M. F.; Chimini, G.; Kaminski, W. E.; Schmitz, G. Molecular cloning of the human ATP-binding cassette transporter 1 (hABC1): Evidence for sterol-dependent regulation in macrophages. *Biochem. Biophys. Res. Commun.* **1999**, *257*, 29–33.
8. Schneider, E.; Hunke, S. ATP-binding-cassette (ABC) transport systems: Functional and structural aspects of the ATP-hydrolyzing subunits/domains. *FEMS Microbiol. Rev.* **1998**, *22*, 1–20.
9. Dean, M.; Rzhetsky,A.; Allikmets, R. The human ATP-binding cassette (ABC) transporter superfamily. *Genome. Res.* **2001**, *11*, 1156–1166.
10. Deeley, R.G.; Westlake, C.; Cole, S.P. Transmembrane transport of endo- and xenobiotics by mammalian ATP-binding cassette multidrug resistance proteins. *Physiol. Rev.* **2006**, *86*, 849–899.
11. Conseil, G.; Deeley, R.G.; Cole, S.P. Functional importance of three basic residues clustered at the cytosolic interface of transmembrane helix 15 in the multidrug and organic anion transporter MRP1 (ABCC1). *J. Biol. Chem.* **2006**, *281*, 43–50.
12. Rees, D.C.; Johnson, E.; Lewinson, O. ABC transporters: The power to change. *Nat. Rev. Mol. Cell Biol.* **2009**, *10*, 218–227.
13. Davidson, A.L.; Dassa, E.; Orelle, C.; Chen, J. Structure, function, and evolution of bacterial ATP-binding cassette systems. *Microbiol. Mol. Biol. Rev.* **2008**, *72*, 317–364.
14. Dean, M.; Allikmets, R. Complete characterization of the human ABC gene family. *J. Bioenerg. Biomembr.* **2001**, *33*, 475–479.
15. Iram, S.H.; Cole, S.P. Expression and function of human MRP1 (ABCC1) is dependent on amino acids in cytoplasmic loop 5 and its interface with nucleotide binding domain 2. *J. Biol. Chem.* **2011**, *286*, 7202–7213.
16. Locher, K.P. Review. Structure and mechanism of ATP-binding cassette transporters. *Philos. Trans. R. Soc. Lond.* B. *Biol. Sci.* **2009**, *364*, 239–245.
17. Aittoniemi, J.; Fotinou, C.; Craig, T. J.; de Wet, H.; Proks, P.; Ashcroft, F. M. Review. SUR1: A unique ATP-binding cassette protein that functions as an ion channel regulator. *Philos. Trans. R. Soc. Lond.* B. *Biol. Sci.* **2009**, *364*, 257–267.
18. Iram, S.H.; Cole, S.P. Differential functional rescue of Lys(513) and Lys(516) processing mutants of MRP1 (ABCC1) by chemical chaperones reveals different

domain-domain interactions of the transporter. *Biochim. Biophys. Acta* **2014**, *1838*, 756–765.

19. Slot, A.J.; Wise, D. D.; Deeley, R. G.; Monks, T. J.; Cole, S. P. Modulation of human multidrug resistance protein (MRP) 1 (ABCC1) and MRP2 (ABCC2) transport activities by endogenous and exogenous glutathione-conjugated catechol metabolites. *Drug Metab. Dispos.* **2008**, *36*, 552–560.
20. Biemans-Oldehinkel, E.; Doeven, M.K.; Poolman, B. ABC transporter architecture and regulatory roles of accessory domains. *FEBS Lett.* **2006**, *580*, 1023–1035.
21. Dawson, R.J.; Hollenstein, K.; Locher, K.P. Uptake or extrusion: Crystal structures of full ABC transporters suggest a common mechanism. *Mol. Microbiol.* **2007**, *65*, 250–257.
22. Iram, S.H.; Cole, S.P. Mutation of Glu521 or Glu535 in cytoplasmic loop 5 causes differential misfolding in multiple domains of multidrug and organic anion transporter MRP1 (ABCC1). *J. Biol. Chem.* **2012**, *287*, 7543–7555.
23. Li, J.; Li, Z. N.; Yu, L. C.; Bao, Q. L.; Wu, J. R.; Shi, S. B.; Li, X. Q. Association of expression of MRP1, BCRP, LRP and ERCC1 with outcome of patients with locally advanced non-small cell lung cancer who received neoadjuvant chemotherapy. *Lung Cancer* **2010**, *69*, 116–122.
24. Bagnoli, M.; Beretta, G. L.; Gatti, L.; Pilotti, S.; Alberti, P.; Tarantino, E.; Barbareschi, M.; Canevari, S.; Mezzanzanica, D.; Perego, P. Clinicopathological impact of ABCC1/MRP1 and ABCC4/MRP4 in epithelial ovarian carcinoma. *Biomed. Res. Int.* **2013**, *2013*, 143202.
25. Hlavac, V.; Brynychova, V.; Vaclavikova, R.; Ehrlichova, M.; Vrana, D.; Pecha, V.; Kozevnikovova, R.; Trnkova, M.; Gatek, J.; Kopperova, D.; Gut, I.; Soucek, P. The expression profile of ATP-binding cassette transporter genes in breast carcinoma. *Pharmacogenomics* **2013**, *14*, 515–529.
26. Peterson, B.G.; Tan, K. W.; Osa-Andrews, B.; Iram, S. H. High-content screening of clinically tested anticancer drugs identifies novel inhibitors of human MRP1 (ABCC1). *Pharmacol. Res.* **2017**, *119*, 313–326.
27. Iram, S.H.; Gruber, S. J.; Raguimova, O. N.; Thomas, D. D.; Robia, S. L. ATP-Binding Cassette Transporter Structure Changes Detected by Intramolecular Fluorescence Energy Transfer for High-Throughput Screening. *Mol. Pharmacol.* **2015**, *88*, 84–94.
28. Schinkel, A.H.; Jonker, J.W. Mammalian drug efflux transporters of the ATP binding cassette (ABC) family: An overview. *Adv. Drug Deliv. Rev.* **2012**, *64*, 138–153.
29. Cole, S.P. Targeting multidrug resistance protein 1 (MRP1, ABCC1): Past, present, and future. *Annu. Rev. Pharmacol. Toxicol.* **2014**, *54*, 95–117.
30. Johnson, Z.L.; Chen, J. Structural Basis of Substrate Recognition by the Multidrug Resistance Protein MRP1. *Cell* **2017**, *168*, 1075–1085.
31. Lee, S.H.; Lee, M. S.; Lee, J. H.; Kim, S. W.; Kang, R. H.; Choi, M. J.; Park, S. J.; Kim, S. J.; Lee, J. M.; Cole, S. P.; Lee, M. G. MRP1 polymorphisms associated with citalopram response in patients with major depression. *J. Clin. Psychopharmacol.* **2010**, *30*, 116–125.
32. Knauer, M.J.; Urquhart, B. L.; Meyer zu Schwabedissen, H. E.; Schwarz, U. I.; Lemke, C. J.; Leake, B. F.; Kim, R. B.; Tirona, R. G. Human skeletal muscle drug transporters determine local exposure and toxicity of statins. *Circ. Res.* **2010**, *106*, 297–306.

33. Su, W.; Pasternak, G.W. The role of multidrug resistance-associated protein in the blood-brain barrier and opioid analgesia. *Synapse* **2013**, *67*, 609–619.
34. Leslie, E.M.; Deeley, R.G.; Cole, S.P. Multidrug resistance proteins: Role of P-glycoprotein, MRP1, MRP2, and BCRP (ABCG2) in tissue defense. *Toxicol. Appl. Pharmacol.* **2005**, *204*, 216–237.
35. Wijnholds, J.; Evers, R.; van Leusden, M. R.; Mol, C. A.; Zaman, G. J.; Mayer, U.; Beijnen, J. H.; van der Valk, M.; Krimpenfort, P.; Borst, P. Increased sensitivity to anticancer drugs and decreased inflammatory response in mice lacking the multidrug resistance-associated protein. *Nat. Med.* **1997**, *3*, 1275–1279.
36. Wijnholds, J.; deLange, E. C.; Scheffer, G. L.; van den Berg, D. J.; Mol, C. A.; van der Valk, M.; Schinkel, A. H.; Scheper, R. J.; Breimer, D. D.; Borst, P. Multidrug resistance protein 1 protects the choroid plexus epithelium and contributes to the blood-cerebrospinal fluid barrier. *J. Clin. Invest.* **2000**, *105*, 279–285.
37. Umscheid, C.A.; Margolis, D.J.; Grossman,C.E. Key concepts of clinical trials: A narrative review. *Postgrad. Med.* **2011**, *123*, 194–204.
38. Tan, K. W.; Sampson, A.; Osa-Andrews, B.; Iram, S. H. Calcitriol and Calcipotriol Modulate Transport Activity of ABC Transporters and Exhibit Selective Cytotoxicity in MRP1 overexpressing Cells. *Drug Metab. Dispos.* **2018**, doi:10.1124/dmd.118.081612.
39. Verhalen, B.; Ernst, S.; Borsch, M.; Wilkens, S. Dynamic ligand-induced conformational rearrangements in P-glycoprotein as probed by fluorescence resonance energy transfer spectroscopy. *J. Biol. Chem.* **2012**, *287*, 1112–1127.
40. Remedios, C.G.D., Fluorescence Resonance Energy. In *Encyclopedia of Life Sciences*. Nature Publishing Group: London, UK, 2001.
41. Carvalho, C.; Santos, R. X.; Cardoso, S.; Correia, S.; Oliveira, P. J.; Santos, M. S.; Moreira, P. I. Doxorubicin: The good, the bad and the ugly effect. *Curr. Med. Chem.* **2009**, *16*, 3267-85.
42. Szebeni, J.; Fulop, T.; Dezsi, L.; Metselaar, B.; Storm, G. Liposomal doxorubicin: The good, the bad and the not-so-ugly. *J. Drug Target* **2016**, *24*, 765–767.
43. Jin, M.S.; Oldham, M. L.; Zhang, Q.; Chen, J. Crystal structure of the multidrug transporter P-glycoprotein from Caenorhabditis elegans. *Nature* **2012**, *490*, 566–569.
44. Srinivasan, V.; Pierik, A.J.; Lill, R. Crystal structures of nucleotide-free and glutathione-bound mitochondrial ABC transporter Atm1. *Science* **2014**, *343*, 1137–1140.
45. Korkhov, V.M.; Mireku, S.A.; Locher, K.P. Structure of AMP-PNP-bound vitamin B12 transporter BtuCD-F. *Nature* **2012**, *490*, 367–372.
46. Du, D.; Wang, Z.; James, N. R.; Voss, J. E.; Klimont, E.; Ohene-Agyei, T.; Venter, H.; Chiu, W.; Luisi, B. F. Structure of the AcrAB-TolC multidrug efflux pump. *Nature* **2014**, *509*, 512-515.
47. Choudhury, H.G.; Tong, Z.; Mathavan, I.; Li, Y.; Iwata, S.; Zirah, S.; Rebuffat, S.; van Veen, H. W.; Beis, K. Structure of an antibacterial peptide ATP-binding cassette transporter in a novel outward occluded state. *Proc. Natl. Acad. Sci. USA* **2014**, *111*, 9145–9150.
48. Hou, Z.J.; Hu, Z.; Blackwell, D. J.; Miller, T. D.; Thomas, D. D.; Robia, S. L. 2-Color Calcium Pump Reveals Closure of the Cytoplasmic Headpiece with Calcium Binding. *PLoS ONE* **2012,** *7*, e40369.

49. Pallikkuth, S.; Blackwell, D. J.; Hu, Z.; Hou, Z.; Zieman, D. T.; Svensson, B.; Thomas, D. D.; Robia, S. L. Phosphorylated phospholamban stabilizes a compact conformation of the cardiac calcium-ATPase. *Biophys. J.* **2013**, *105*, 1812–1821.
50. Lam, A.J.; St-Pierre, F.; Gong, Y.; Marshall, J. D.; Cranfill, P. J.; Baird, M. A.; McKeown, M. R.; Wiedenmann, J.; Davidson, M. W.; Schnitzer, M. J.; Tsien, R. Y.; Lin, M. Z. Improving FRET Dynamic Range with Bright Green and Red Fluorescent Proteins. *Biophys J.* **2013**, *104*, 683a.
51. Beedholm-Ebsen, R.; van de Wetering, K.; Hardlei, T.; Nexo, E.; Borst, P.; Moestrup, S. K. Identification of multidrug resistance protein 1 (MRP1/ABCC1) as a molecular gate for cellular export of cobalamin. *Blood* **2010**, *115*, 1632–1639.
52. Leier, I.; Jedlitschky, G.; Buchholz, U.; Center, M.; Cole, S. P.; Deeley, R. G.; Keppler, D. ATP-dependent glutathione disulphide transport mediated by the MRP gene-encoded conjugate export pump. *Biochem. J.* **1996**, *314*, 433–437.
53. Jedlitschky, G.; Leier, I.; Buchholz, U.; Barnouin, K.; Kurz, G.; Keppler, D. Transport of glutathione, glucuronate, and sulfate conjugates by the MRP gene-encoded conjugate export pump. *Cancer Res.* **1996**, *56*, 988–994.
54. Senior, A.E.; Al-Shawi, M.K.; Urbatsch, I.L. The catalytic cycle of P-glycoprotein. *FEBS Lett.* **1995**, *377*, 285–289.
55. Myette, R.L.; Conseil, G.; Ebert, S. P.; Wetzel, B.; Detty, M. R.; Cole, S. P. Chalcogenopyrylium dyes as differential modulators of organic anion transport by multidrug resistance protein 1 (MRP1), MRP2, and MRP4. *Drug Metab. Dispos.* **2013**, *41*, 1231–1239.

CHAPTER 3

ENGINEERING OF TWO-COLOR P-GLYCOPROTEIN BIOSENSOR FOR FLUORESCENCE-BASED PROFILING OF DRUG INTERACTION.

Abstract

P-glycoprotein, a member of the ABC transporter proteins, mediates the efflux-translocation a diverse array of dissimilar solutes across plasma membranes and by an ATP-dependent hydrolysis. The involvement of the lipid bilayer-located P-gp in tissue defense, efficacy/toxicity of drugs and clinical MDR of antiretrovirals, anti-malignancies and antiparasitic provides a rationale for investigating structure, function and ligands of the transporter. Our group previously developed a two-color MRP1 biosensor by fusing Green fluorescence protein and red fluorescent proteins with the transporter. The MRP1 biosensor detects FRET changes as an index of small movements in the domains of the protein including the NBDs using epifluorescence microscopy. Here, we expanded the two-color FRET model by engineering a set of six P-gp biosensors to determine which one responds most sensitively to dynamic FRET changes. We observed that two-color P-gp, GR-678, localizes precisely in the plasma membrane, extracellularly exports doxorubicin and is inhibited by verapamil. Consequently GR-678 was selected as the lead biosensor for steady state FRET measurements using fluorometer model H-11, an affordable and readily accessible instrument. Our results show that GR-678 displays etoposide-induced percent FRET change which increases upon inclusion of ATP, suggesting normal FRET response. In addition, we observed the highest percent FRET change in the presence of etoposide/ATP/sodium orthovanadate. This result suggests that

GR-678 reports vanadate trapping of hydrolytic reactions in the ADP-bound condition which is consistent with earlier reports. GR-678 also identified six hits drugs following a 50-drug screening of NIH anticancer library. Overall, we have developed for the first time, a FRET sensitive two-color P-gp biosensor which is useful for discovery of novel ligands of P-gp and holds promise for high throughput profiling of direct drug-P-gp interactions using a more economical ensemble FRET approach.

Key words: Two-color P-gp, ATP-binding cassette proteins, Multidrug resistance, Fluorescence resonance energy transfer, Two-color MRP1, Biosensor, membrane vesicles.

Introduction

Adenosine triphosphate (ATP) binding cassette transporters (ABC) are a large superfamily of proteins, many of which harness energy from ATP hydrolysis to overcome a concentration gradient and translocate a variety of structurally unrelated exogenous compounds from the cell [1-3]. ABC transporter genes are found in all life forms; eukaryotes, prokaryotes, and algae encoding channel proteins, importers or exporters [4, 5]. ABC transporters are generally composed of transmembrane domains and intracellularly located nucleotide binding domains which are responsible for the ATP-dependent extrusion of solutes from cells [6, 7]. One of the most important and well-studied ABC transporters is ABCB1, also known as permeability or phosphoglycoprotein (P-gp or P-glycoprotein).

The secondary structure of the P-gp is characterized by a pair of homologues divides, each consisting of six-transmembrane helical-domain and a cytoplasmic subtended nucleotide binding domain. These 12 helixes combine to form the pore which contains an array of evolutionarily conserved sequences responsible for substrate recognition of a diverse range of ligands [2, 8]. The extracellular side of the pore is prominently hydrophobic while polar and charged amino acids characterize the cytosolically-facing portion [2, 9]. The P-gp structure is conformationally malleability which allows for multiple structural movements of its domains. This aids P-gp to discern stereoisomeric compounds while concurrently providing multiple binding sites for many substrates with extensive diversity. Studies of the crystal structure of mouse P-gp reveal two conformational states of the protein; the high-substrate affinity open conformation in which the NBSs are apart and the substrate-bound closed conformation [10, 11].

P-glycoprotein is pertinently expressed by immunologically active tissues and organs because of the extreme diversity of their substrate recognition and translocation activity [4] of the transporter. P-gp is remarkably distributed in the canaliculi of the liver and the lumen of the small intestines where they avert the cytotoxicity of orally ingested drugs by extracellularly pumping out these drugs. Physiologically, the 1280 amino acid-long P-gp is involved with immune responses at crucial sanctuary sites such as the blood-placenta, blood-cerebrospinal fluid and blood-testis barriers and this underscores the importance of the protein in tissue defense [12]. Permeability glycoprotein also plays a key role in physiological processes required for normal brain and spinal functions such as lipid homeostasis within the central nervous system [13, 14]. Furthermore, fetal drug toxicity, neurological damage and several fold increase in drug influx have been reported in animals naturally deficient in the abcb1 gene or which lack the gene by genetic modification [15, 16].

Multidrug resistance (MDR) is responsible for over 90% of poor patient outcomes during chemotherapy of metastatic tumors and is a key drawback in cancer healthcare [17-19]. The170 kD P-gp is a major player in the clinical MDR phenotype. Overexpression of P-gp in tumor and brain cells, causes significant impairment in therapies targeting the brain, including antiepileptics, antiretrovirals and chemotherapeutics because the protein actively excludes these drugs from the cells [20, 21]. P-gp-mediated MDR is reported to be responsible for non-responsiveness of drugs targeting sarcoma, acute myeloid leukemia, neuroblastoma in children, and its prominent expression is prognostic of approximately 40% failure in epilepsy treatment [22-24].

Given that P-gp governs pharmacokinetic indices such as absorption, distribution, metabolism, excretion (ADME) [4], mediates drug efficacy/toxicity, and is implicated in clinical and anticancer MDR, profiling of the interaction of drugs with P-gp is imperative. Besides, some known ligands and high-affinity substrates (cysteinyl leukotriene and doxorubicin) of P-gp overlap with those of other ABC transporters and this could pose hindrances to P-gp investigation. This further justifies the development of methodological approaches and strategies to detect direct interaction of the transporter with P-gp-exclusive ligands. A few years ago, the Food and Drugs Administration (FDA) authorized the profiling of all drugs in clinical trials for their interaction with P-gp. This mandate warrants the exploration of more tools and experimental approaches to characterize ligands and modulators of P-gp.

Recently, our group engineered a two-color multidrug resistance protein 1 (MRP1) by fusing green and red fluorescence proteins (GFP and RFP) to the protein [11]. The recombinant transporter reported dynamic fluorescence resonance energy transfer changes (FRET) changes as an index of structural movements of MRP1 using live-cell based epifluorescence microscopy. The two-color clone further identified 8 hits following high throughput screening of an NIH library of clinically tested drugs using Fluorescence lifetime technology (FLIM). This two-color FRET model unlocked opportunities for high throughput screening of ligands of not only MRP1 but also other ABC transporters. Unfortunately, epifluorescence microscopy and FLIM technologies are advanced, uncommon and sophisticated and require highly-skilled expertise to operate.

Here, we present a more economical and applicable two-color based-steady state FRET approach to expand the two-color FRET model to P-gp, a more clinically

important ABC transporter than MRP1. The goal of the present study was to engineer six two-color P-gp biosensors by altering the position of GFP on the transporter to determine which clone is the most FRET-sensitive biosensor using membrane vesicle-based steady state FRET approach. The lead two-color P-gp biosensor, responded normally to dynamic FRET changes and detected 6-hits from a 50-compound screening of anticancer library of drugs. We anticipate that this lead FRET biosensor of the six will be a useful reporter in high throughput profiling of P-gp-substrate interactions.

Methods and materials

Chemicals

Nucleotides, doxorubicin, anti-GFP antibody, benzamidine, poly-D-lysine, saponin and 2-mercaptoethanol were purchased from Sigma Aldrich (St. Louis, MO). E217βG and sodium orthovanadate were from Santa Cruz (Dallas, Texas).

Primer design and molecular cloning

The interest of our group in the two-color ATP-binding cassette transporter proteins (ABC) model began with the engineering of a two-color multidrug resistance associated protein-1 (MRP1) by ligating a green fluorescence protein (GFP) and red fluorescence protein with MRP1. Essentially, the two-color MRP1 is composed of a GFP protein sandwiched between two fragments of the MRP1 protein, upstream at N-terminal and downstream, at C-terminal to which TagRFP is fused. Following the success of this two-color MRP1, here, we expand the two-color biosensor innovation to include the most important ABC transporter, P-glycoprotein, by cloning six two-color ABCB1 (1280 amino acids) vectors. The first clone to be engineered was two-color GR-642. The cloning process was initiated by using the original two-color MRP1 clone from our previous study [11] as the backbone vector. The N-terminal 2 kb fragment of GR-873 which codes for amino acids 1-873 was remove using the appropriate restriction endonucleases, Sac I and Sal I. Then, by using the primers (forward, 5’ GTA GAG CTC A TGGATCTTGAAGGGGA CCGCAATGG AGGA GC 3’ and reverse, 5’ GTA GTC GAC AT C AGCTGCATTTT CTAA TTCAACTTCATTTCCTG 3’, restriction sites

underlined) and through polymerase chain reaction (PCR), the N-terminal ~1.9 kb section of the 3.8 kb long P-gp protein, encoding 1-642 amino acids was generated and ligated in-frame into open ends of GR-873. Therefore, the GR-873 protein at this intermediary stage consisted of the N-terminal of P-gp and the C-terminal portion of MRP1. Next, the remnant C-terminal 2.6 kb segment of MRP1 in the intermediary GR-873 is excised using the Sac II and Age I restriction enzymes. This detached C-terminal MRP1 fragment was replaced through ligation with a PCR-produced C-terminal ~1.9 kb fragment of P-gp encoding 643-1280 amino acids (stop codons removed), using the primers (Forward, 5' GTA CCG CGG GAA T CCAAAAGTGA AATTGA TGC CTTGGAAATGT C 3' and reverse, 5' GTA GTC GAC A T C AGCTGCATTTT CTAA TTCAACTTCATTTCCTG 3', restriction sites underlined). The final product is a recombinant 2- color P-gp protein, GR-642 in which the GFP protein is inserted at amino acid residue -642 connected to the Val-Asp and Pro-Arg linkers at the N-terminus and C-terminus respectively. The NBDs are predicted to make ligand-induced movements during catalytic activity, and hence their selection as sites for the attachment of the two fluorophores during genetic modification of the transporter. The whole process was repeated altering the GFP insertion sites on the NBD1 to produce the other five P-gp constructs namely; GR-647, GR-653, GR-662, GR-671, GR-678 as shown in the schematic diagram of the secondary structure of two-color P-gp in figure 3.1A. Table 3.1 summarizes the primers designed for the polymerization reactions of the P-gp gene. All regions of evolutionary importance the P-gp protein were cautiously avoided during the design of the two-color P-gp strategy. Figure 3.1B shows the tertiary structure of P-gp in the open and closed

conformations and FRET changes are expected to occur in the presence of ligands. All lyophilized primers were obtained from Europhins, Lancaster, PA.

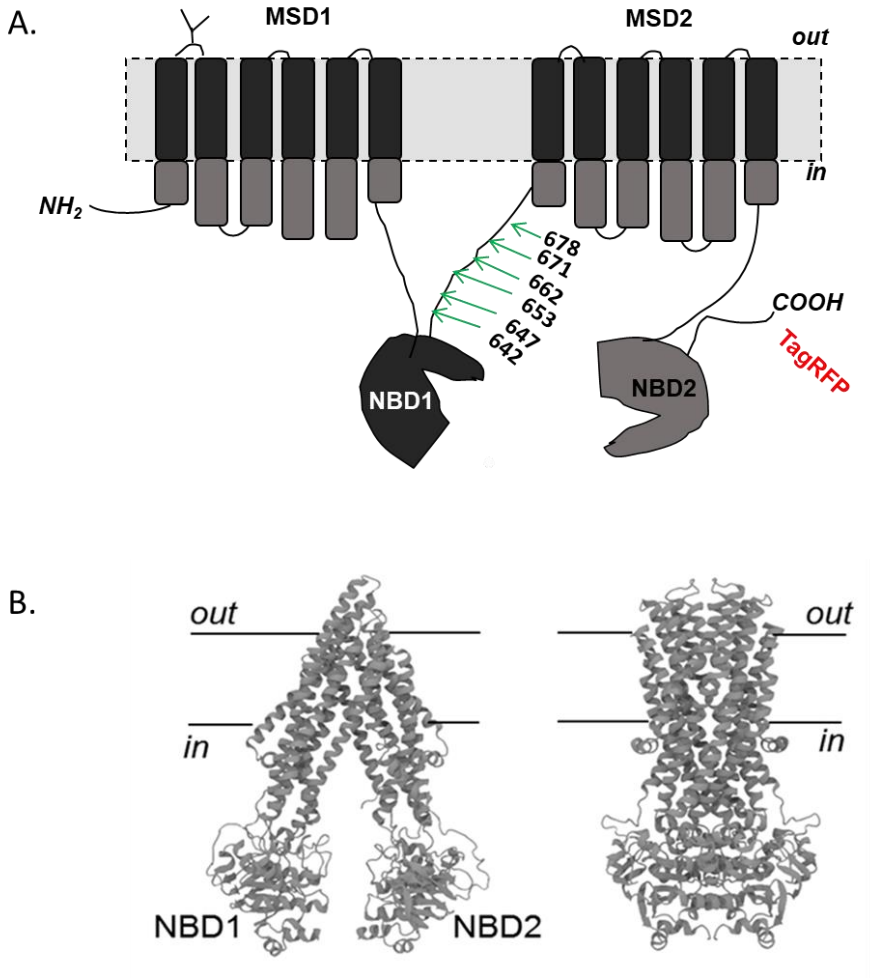

Figure 3.1. Schematic representations of the structure of P-gp. A. Schematic of the secondary structure of two-color P-gp showing the different GFP insertion sites at amino acid residues -647, -653, -662, -671, -678 which resulted in different constructs namely, GR-647, GR-653, GR-662, GR-671, GR-678. B. Tertiary structure of the P-gp depicted in the open (left) and closed (right) conformations of the NBDs. (PDB code:)

Preparation of stable cell lines

Transient transfection of the six two-color P-gp constructs into 293T cells was performed with jetPRIME (Polyplus-transfection SA, Illkrich, France) mammalian transfection reagent and following the manufacturers' protocol. The cells were allowed to grow for 24-hours before being rid of complete DMEM to prepare them for aminoglycoside antibiotic treatment. The removed complete DMEM was replaced with 400 µg/ml of geneticin- G418, for antibiotic selection of recombinant gene-expressing cells. Cultures were incubated for a fortnight prior to doubling the G418 concentration to 800 µg/ml. Flow activated cell sorting was performed to select cells expressing both GFP and RFP from non-expressing ones. After flow cytometry, the GFP and RFP expressing cells were maintained under 200 µg/ml geneticin.

Western blot analysis of two-color P-gp

293T cells were transfected with the different two-color P-gp plasmids in a 2:1 ration with jetPRIME transfection reagent. Halt Protease inhibitor (ThermoFisher Scientific, Waltham, MA) and RIPA buffer (ThermoFisher Scientific) were used in combination to prepare protein lysates of the cells. Protein concentration was determined using BCA protein assay (ThermoFisher scientific). After the protein assay, 20 µg of the protein lysates was used to perform SDS-PAGE electrophoresis before an hour-long membrane-blocking step was accomplished on 7.5% Mini-PROTEAN® TGX™ gels (BioRad, Hercules, CA) and transferred onto an Immobilon® PVDF membranes (EMD Millipore). Four degrees centigrade incubation of membranes was conducted with

primary antibodies, polyclonal anti-GFP or mouse monoclonal anti α-tubulin (Sigma Aldrich, St. Louis, MO) at dilutions of 1:5000 and 1:250 respectively. Membranes were incubated with horseradish peroxidase goat anti-mouse secondary antibody (IgG, ThermoFisher scientific) for one hour prior to detection of proteins with OMEGA Lum G using chemiluminescence substrate (PerkinElmer, Waltham, MA). Wild type pTC-P-gp (TransOmic Technologies Inc, Huntsville, AL) and non-transfected 293T cells were used as controls.

Membrane localization and doxorubicin transport activity

Firstly, 293T cells transfected with vectors containing different two-color P-gp plasmids using jetPRIME transfection reagent (Polyplus-transfection SA, Illkrich, France) were plated on cover glass in 25 mm 6-welll plates. The plated cells were then incubated at 370 C for 48-hours in humidified 5% CO2 incubator. After 2-days, images were taken using a confocal microscope equipped with a 63× oil-immersion objective (TILL Photonics GmbH, Gräfelfing, Germany. GFP was excited at 470 nm and emitted within the 496 nm-530 nm range, while RFP was excited at 561 nm with emission bands of 573-637 nm.

Two-color P-gp-expressing 293T cells were plated on poly-D-lysin-coated 6-well plates containing cover slips at 3 x 105 cells/well and incubated for 48-hours under similar conditions as described above. At the inception of drug treatment, complete DMEM was removed and replaced with a medium containing 10 µM Doxorubicin in 0.2% DMSO and incubated for 2-hours prior to imaging with the confocal microscope.

Doxorubicin was excited at 470 nm and emitted at 570-605 nm. GFP and RFP wavelengths were maintained as before.

Effect of verapamil on two-color Pgp-dependent doxorubicin transport

To ascertain if a known P-gp inhibitor will foil the efflux-transport of doxorubicin, 1 ml of 25 µM of verapamil was added to the 293T/two-color P-gp cells and removed after 30 minutes. DMEM medium containing another 25 µM of verapamil or DMSO were added to the 293T/two-color P-gp cells, in combination with 10 µM doxorubicin and incubated for 2 hours. The confocal microscope was used to observe the effect of verapamil on the ATP-dependent translocation of doxorubicin by the two-color P-gp biosensors. Experiments were performed concurrently with the doxorubicin-only treatment accumulation assay.

Preparation of membrane vesicles

Preparation of vesicular plasma membranes was performed using the method described previously by [25] with modification. Frozen two-color P-gp expressing cells dissolved in phosphate buffer saline were briefly thawed and dissolved in a hypotonic homogenizing buffer (250 mM sucrose, 50 mM Tris-HCl, 0.25 mM CaCl2, pH 7.4) containing 1x protease inhibitor tablets (supplemented with 1 mM EDTA, Santa Cruz Biotechnology, Santa Cruze, CA). To disrupt the plasma membranes, cells were subjected to 450 psi pressure in a nitrogen chamber on ice for 5 min, prior to centrifugation at speed and temperature of 500 x g and 40 C for 10 minutes (Sorvall

legend X1R centrifuge, ThermoFisher). The supernatant was pooled, and the cell pellets were re-dissolved in the 10 ml homogenizing buffer for a second round of 10-minute centrifugation. The collected supernatant was layered over high sucrose buffer (35% W/W sucrose, 10 mM Tris-HCl, and mM EDTA; pH 7.4) and ultra-centrifuged at 25000 rpm, 4 °C for 1 hour using a pre-cooled Beckman SW28 swinging bucket rotor in the Beckman Optima LE-80K ultracentrifuge (Beckman Coulter, Brea, CA). The plasma membrane portion which settled within the middle portion of the centrifuge tubes were carefully pipetted out and dissolved in low sucrose buffer (25 mM sucrose, 10 mM Tris-HCl, and mM EDTA; pH 7.4) for a second cycle of ultracentrifugation as before, only this time for 45 minutes. The plasma membrane pellets were salvaged and resuspended in 1 ml of Tris sucrose buffer (TSB) (250 mM sucrose, 50 mM Tris-HCl, pH 7.4), prior to a 4 0C, 20-minute ultracentrifugation at 55000 rpm in the Beckman TL-100 ultracentrifuge (Beckman Coulter, Brea, CA). A 27-gauge syringe was used to create membrane vesicles by passing the resulting pellets through it for about 20 cycles.

Fluorescence resonance energy transfer measurements

Membrane vesicle isolated from 293T cells prominently expressing the only functional two-color P-gp biosensor, GR-678 was used for fluorescence spectroscopy experiments. The Fluorimeter model FL3-11 (HORIBA Edison, New Jersey) was used to acquire all FRET measurements. First, two reactions were set up; the compound mix tube and the membrane vesicle tube. The compound mix reaction consisted of Tris sucrose buffer (TSB) (250 mM sucrose, 50 mM Tris-HCl, pH 7.4), 20 or 50 uM-compound under investigation and/or 4 mM/5 mM ATP/MgCl2. 20 µg of membrane vesicles and the

compound reaction were separately pre-incubated at 37 0C for 5- minutes prior to ligand-binding initiation. After pre-incubation, the compound reaction was mixed with the membrane vesicles and further incubated for 10 minutes at 37 0C to allow respective ligands to bind to the protein. Ligand-free condition in which no ligands, except TSB was included in the compound mix was prepared as control reaction and was also mixed with membrane vesicle. Since the two-color P-gp clones contained both GFP and RFP, a previously cloned GFP protein was used as the donor-only condition. The donor-only, prepared in the same way as the two-color vesicles, was collected into a 50 µL quartz cuvette, inserted in the FL3-11 model fluorometer and excited at 465 nm. Emission for the donor was monitored at 480nm to 650 nm using an integration time of 3s which yielded a specific intensity of the donor emission. Next, the cuvette was rinsed with buffer and the two-color P-gp ligand-free condition was loaded and measured for the GFP intensity. The intensity of the GFP in the ligand-free condition was normalized with the intensity of the GFP in the donor-only condition to generate a FRET efficiency for the apo condition of GR-678 using equation 1. The compound condition of two-color GR-678 was then measured while monitoring donor-quenching. The normalized donor (GFP) intensity of the ligand-free condition was subtracted from the normalized donor intensity of the ligand-induced condition to generate the percent (%) change in FRET the two-color biosensor.

$$(1 - I_{DA} / I_D) * 100 \qquad (1)$$

Where ID is donor intensity in the donor-only condition (counts per second, cps) and I DA is the donor intensity in the donor-acceptor or two-color condition.

Anti-cancer drug screening

A set of 50 anticancer library of compounds were screened using fluorescence spectroscopy as described above and the two-color GR-678 as the sole biosensor reporter. There were 50 compound conditions in this case with each compound repeated twice. As before, normalizing the apo condition FRET efficiency with the ligand-induced condition transfer efficiency results in the percent change in FRET efficiency. In each case of the duplicate FRET measurements, 20 µM of compounds and 20 µg of GR-678/293T membrane vesicles were used.

Results and discussion

P-glycoprotein ATP-dependently exports a broad spectrum of hydrophobic substrates against concentration gradient across plasma membranes. Consequently, predominant expression of P-gp is responsible for the acquisition of the MDR phenotype by a plethora of infectious diseases and tumor cells; a major obstacle in chemotherapy [7, 26] . Clinical MDR is characterized by the desensitization of cells to the effect of drugs due to energetic transport-efflux of these drugs out of cells by certain ABC transporter proteins, most prominently, P-gp [7]. A widely used anticancer agent and a notable substrate of P-gp, doxorubicin has recently been found to be more potent against hepatocellular carcinoma when used in combination with sorafenib [27]. Sorafenib was reported to significantly decrease the mRNA expression of P-gp [28]. The need to circumvent tumor MDR by withdrawal/discontinuation of culprit-anticancer agents or by combination-therapy with inhibitors, provide justification for identification of anticancer substrates of P-gp. The clinical importance of P-glycoprotein and the mandate by the FDA for profiling of drug interactions with P-gp have created opportunities for expansion in method developments targeted at novel P-gp ligand/substrate discovery.

Here, we present for the first time a recombinant two-color human P-gp biosensor which reports intramolecular FRET changes as a measure of structural changes in the transporter. This novel P-gp biosensor also identified six anti-cancer drugs which have direct interaction with the transporter, following a screening of 50 drug library of anticancer agents using steady state FRET. This P-gp biosensor model draws on the methodology and success of the two-color MRP1 biosensor our group recently engineered. The two-color MRP1 which demonstrates fluorescence sensitivity as a

function of conformational movements, was cloned by joining GFP and RFP proteins intra-sequence with the protein.

Expression and transport activity of two-color P-gp

Molecular cloning was employed to engineer six two-color human P-gp constructs. The constructs were genetically modified by sandwiching GFP protein in between two halves of the P-gp protein with TagRFP attached downstream of the C-terminal. To determine if the two-color P-gp proteins are immunologically active, we used anti-GFP antibodies to carry out immunoblot assay. Our results in figure 3.2 show that all six two-color P-gp constructs were expressed at ~210 kD size but only GR-678/293T showed an intense band. Combining the weighs of the ~170 kD permeability glycoprotein [3] with the ~27 kD weights each of GFP and RFP proteins, justifies the detection of the two-color P-gp via GFP at ~210 kD. The other five clones showed waning bands, suggesting an impairment in expression level of those two-color P-gp constructs. Regardless, the presence of faint or intense bands indicate the presence of the GFP cloned into the two-color P-gp constructs. The non-transfected parental 293T cells and the wild-type pPCT-Pgp/293T lanes were empty, an indication of the absence of GFP. The anti-α-tubulin antibody used detected the presence of α-tubulin, an endogenous housekeeping globular protein which validates the results of our immunoblot assay.

To determine if genetically modifying human P-gp by incorporating a fluorescent pair intra-sequence compromises the membrane localization and functionality of the P-gp, we transiently transfected 293T cells with the two-color P-gp plasmids. Using

confocal microscopy, we observed the plasma membrane trafficking of the two-color P-gp. Our results in figure 3.3 show that the localization of GR-643, GR-647, GR-652, GR-662, and GR-671 are smudged at the plasma membrane but GR-678 appear to traffic normally to the plasma membrane. This result is consistent with the blotting data from figure 3.2 which show GR-678 as the only properly expressed protein with an intense band. Our observations suggest that of the six dual-color P-gp recombinant clones, only GR-678 is precisely expressed and localized in the lipid-bilayer. The inserted GFP appear to be in undesired locations which do not support appropriate trafficking and/or maturation of the other constructs.

Doxorubicin accumulation assay was conducted on all six clones to investigate the functional activity of the biosensors. Doxorubicin is a commonly used chemotherapeutic drug for combating non-Hodgkin and Hodgkin lymphoma, acute lymphoblastic leukemia, breast cancer, ovarian carcinoma, bone carcinoma and a host of other malignancies [27]. The fluorescent doxorubicin doubles as a promiscuous substrate of P-gp and other ABC transporters and well-suited for testing transport activity of two-color P-gp. Our results in figure 3.4 showed doxorubicin was absent from 293T cell populations transfected with GR-678 but remained inside the nuclei of untransfected cells, after 2 hours of 10 µM doxorubicin treatment. However, there was hardly any two-color P-gp transfected cells detected in plasma membrane of the 293T cells supposed to expressing the other two-color constructs, nor was doxorubicin extruded out of the cells. These results suggest that GR-678 is a functional protein and shows no negative effects of molecular cloning. Our results also confirm the observation of impaired membrane

localization and concomitantly non-functionality of all the other recombinant proteins except GR-678.

Extensively characterized as an inhibitor of P-gp, verapamil has been shown to increase the area under the plasma drug concentration versus time curve (AUC) of doxorubicin when both drugs were administered to rodents [29, 30]. To unequivocally corroborate the functional activity of the two-color P-gp clones especially GR-678, we further explored the effect of 25 µM of verapamil on the doxorubicin efflux by the genetically modified transporters. We observed that in the presence of verapamil, two-color GR-678 failed to efflux doxorubicin as the drug remained in the nuclei of 293T cells expressing the two-color protein as shown in figure 3.5. This result is consistent with established report of inhibition of the extrusion of doxorubicin by verapamil [29] [31] and further enforces our notion that GR-678 is a normally functional transporter. Following the results of western blot, localization and functional experiments, only the purportedly functional GR-678 was selected as lead biosensor in all downstream FRET procedures.

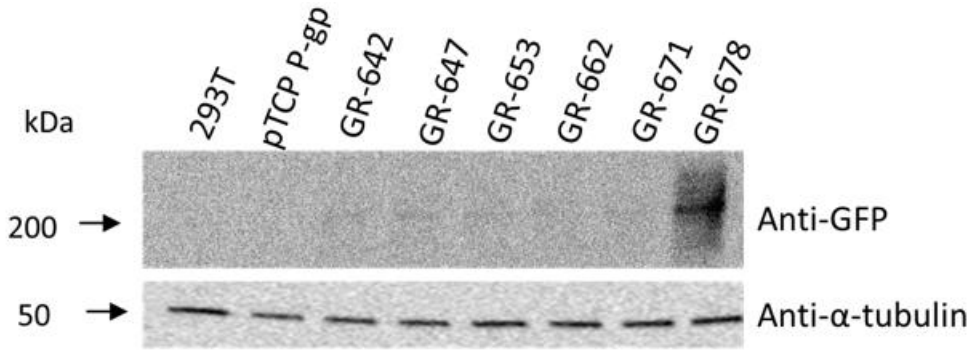

Figure 3.2. Western blot of two-color P-gp constructs. Ten **(**10) μg of whole cell lysates of non-transfected 293T, wild type 293T/pTCP-P-gp, and all six 293T/two-color P-gp were prepared. SDS-PAGE electrophoresis was performed after which antibody detection was done by rabbit polyclonal anti-GFP antibody (1:5000 dilution, overnight at 4 °C). The endogenous control, alpha tubulin was detected by mouse monoclonal anti-α-tubulin (1:8000 dilution, overnight at 4 °C).

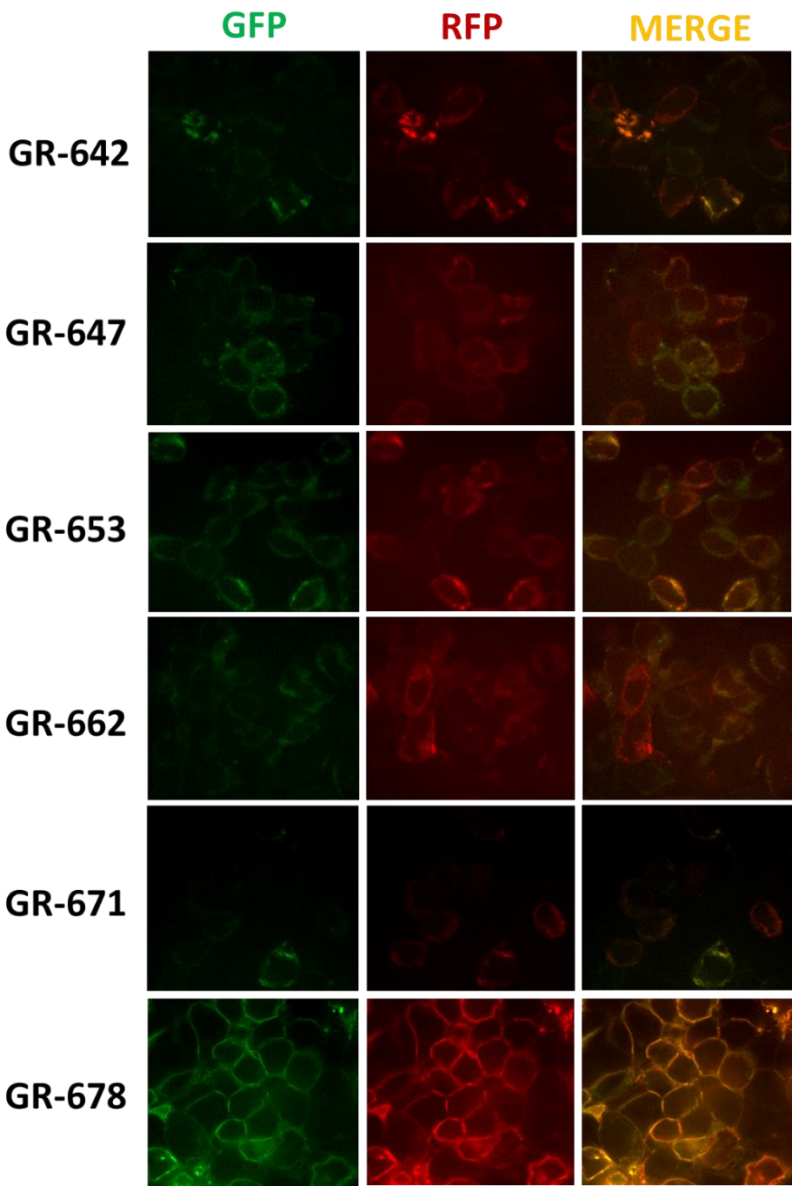

Figure 3.3. Localization of two-color P-gp in 293T cells. 293T cells were plated on cover glass and transfected with vectors containing different two-color P-gp constructs (GR-642, GR-647, GR-653, GR-662, GR-671 and GR-678). After 48- hours, images were taken with confocal microscope equipped with a 63× oil-immersion objective. GFP and tagRFP were excited at 470 nm and 561 nm, respectively. GFP and RFP emissions were achieved at 495-530 nm and 573-637 nm respectively.

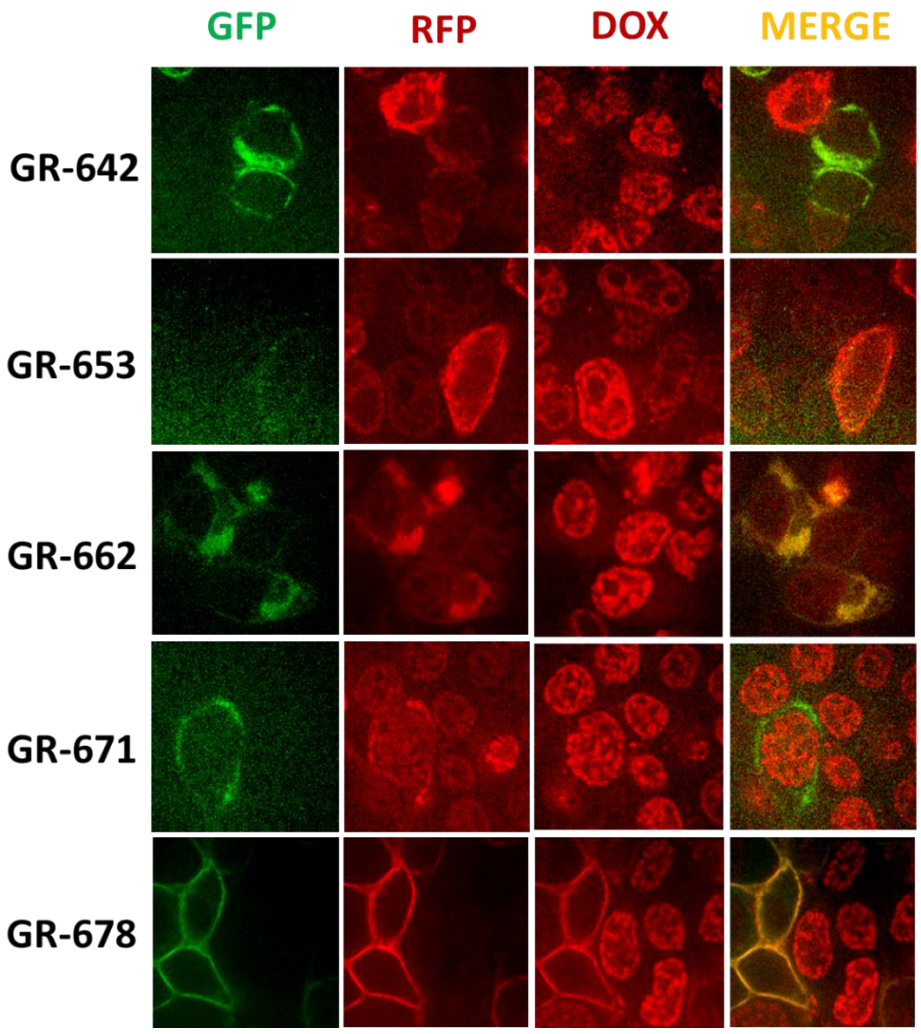

Figure 3.4. Doxorubicin transport activity by two-color P-gp biosensors. 293T ells were transiently transfected with the two-color plasmids, GR-642, GR-653, GR-662, GR-671 and GR-678 and incubated for 48 hours. At the inception of compound treatment, DMEM medium was pipetted out and replaced with 1 ml medium containing 10 µM doxorubicin for 2 hours prior to imaging with the confocal microscope.

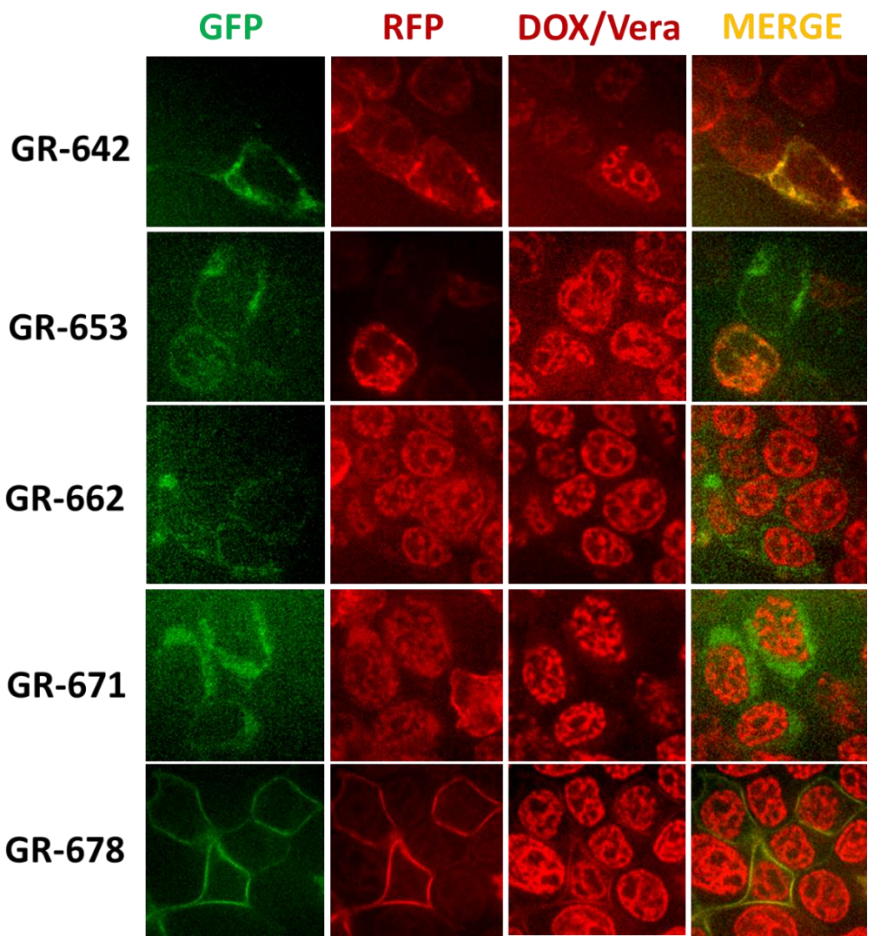

Figure 3.5. Effect of verapamil (vera) on doxorubicin efflux by two-color P-gp. To determine the effect of verapamil on doxorubicin transport by two-color P-gp, 293T cells were transfected with the two-color P-gp vectors and incubated for 48 hours. Next, the total transfection medium was removed and replaced with a medium consisting of 25 µM verapamil for 30 minutes. This medium was also pipetted out and discarded to be replaced by another medium made up of 25 µM verapamil or DMSO and 10 µM Doxorubicin and incubated again for 2 hours. The concentration of DMSO was kept at 0.2%. confocal microscope equipped with 63× objective was used to take images. GFP and Dox were excited at wavelength of 470 nm using Ar laser. RFP was excited at a wavelength of 561 nm. The emission band of 496-530 nm was used for GFP, 573-637 nm for RFP and 570-605 nm for Dox.

Two-color P-gp responds normally to dynamic FRET changes

FRET spectroscopy is a prominent technique for exploring structural movements of macromolecules which provide useful insights into structure-function mechanisms. We performed FRET spectroscopy to determine the ligand-induced structural dynamics of purified membrane vesicles of 293T/GR-678. Two-color P-pg, GR-678 was FRET-tested with ATP alone, etoposide alone, and sodium orthovanadate in the presence and absence of the nucleotide, ATP/ MgCl2. The DNA synthesis-targeting anticancer medication, etoposide, used to treat testicular cancer, lung cancer and neuroblastoma (ncbi.gov/etoposide 2004) is also a known P-gp substrate [32], It is expected that etoposide will induce proximity of the NBDs leading to increased percentage change in FRET efficiency relative to the ligand-free condition. FRET of the GFP donor was measured and normalized to the FRET of the ligand- free two-color P-gp. Our results show a ~1.5% increase in FRET efficiency for etoposide-induced two-color GR-678 compared with the ligand-free apo FRET. Upon the inclusion of ATP/$MgCl_2$, there was a further increase of ~1.5% change in the FRET efficiency of GR-678 representing a total of ~2.5% when normalized with the apo FRET. To verify the vanadate trapping reportage of the two-color GR-678, FRET was measured in the presence of sodium orthovanadate alone and etoposide/ATP/sodium orthovanadate. Our results show about ~1% increase in FRET of GR-678 in the presence of sodium orthovanadate alone while a high FRET change (~4%) was displayed in the presence of etoposide/ATP/sodium orthovanadate normalized with the apo FRET. These observations are consistent with the previously reported dynamic FRET response by P-gp [3] using P-gp mutants labelled with Alexa 488 (donor) and Atto 610 (acceptor).

It has been established that sodium orthovanadate or beryllium fluoride, when introduced into an ATP-catalyzed reaction, replaces inorganic phosphate to stabilize the ADP-bound hydrolytic stage [33, 34]. This phenomenon, referred to as vanadate-trapping, represses the ATPase catalysis and sustains the closed conformational state of the NBDs. This scenario is in tandem with our results shown in figure 6 as we observed the highest percent FRET change upon addition of ATP/sodium orthovanadate to the etoposide-induced GR-678 membrane vesicle reaction. JNJ which failed to demonstrate any signal in experiments from a previous study [35] by our group involving fluorescence spectroscopy, ligand transport and flow cytometry, was included as negative control. JNJ was unresponsive to dynamic FRET changes as shown in figure 3.6.

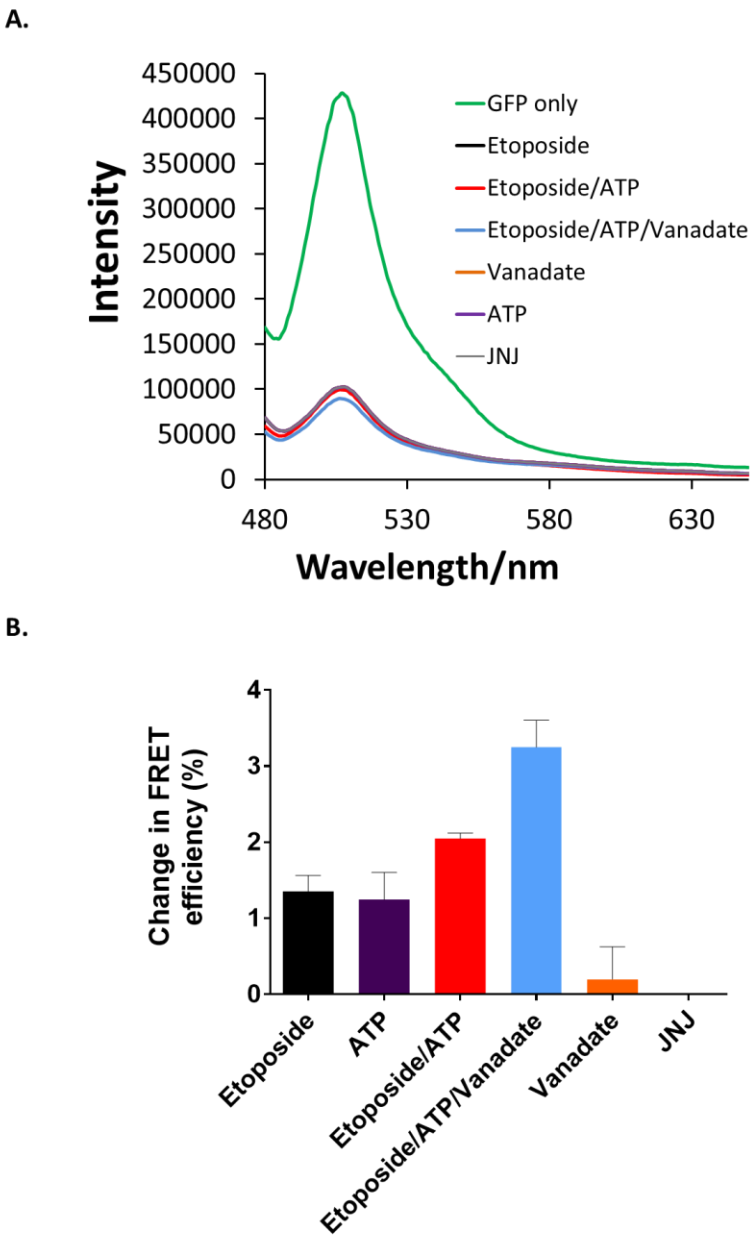

Figure 3.6. Normal FRET responses of two-color P-gp, GR-678. A. Spectral representation of the FRET responses of GR-678 in the presence of well-established ligands of P-gp. B. Histogram depiction of the ligand-induced FRET changes of GR-678 in the presence and absence of nucleotide, ATP/MgCl2. 20 µg of 273T cell-line membrane vesicles overexpressing two-color P-gp GR-678 were reacted with 20 µM etoposide, 4 mM ATP, 50 µM vanadate and 20 µM JNJ.

The % FRET efficiencies of ligand-induced conditions were normalized with the ligand-free condition to generate % FRET changes.

Two-color P-gp biosensor, GR-678 identifies six ligands in anticancer screening

P-gp mediated MDR is a major hindrance to therapy for various malignancies predominantly because chemotherapeutic drugs are frequently pumped out of tumor cells overexpressing the transporter. Here, using the two-color P-gp, GR-678 as the functional biosensor reporter, we screened 50 anticancer drugs from a pool of a clinically tested library. FRET efficiency from ligand-free GR-678 was subtracted from the drug-induced transfer efficiencies to obtain the percent FRET changes recorded for each drug as shown in figure 3.7A which represents data from one of two independent trials conducted. Six anticancer hit-drugs which displayed consistent percent FRET changes between the two independent screening experiments were identified as hits as shown in figure 3.7B. They are, the EGFR-inhibiting axitinib [36], the aurora kinase-inhibitor AT9283 [37], the survivin-targeting YM155, the Sirtuin 1-activating SRT1720 [38], the ZEB-1 gene-targeting mocetinostat and the B-cell lymphoma 2 (Bcl-2)-obstructing TW-37. Notably, all the hit drugs whose chemical structures are also presented in figure 3.8, are still at different stages of clinical trials. Interestingly, all the anti-malignancy hit-drugs displayed a higher FRET signal compared to the etoposide-induced (positive control) FRET change, indicating they have stronger interaction with the phosphor-glycoprotein transporter than does etoposide. Axitinib showed ~3%, AT9283 and mocetinostat showed ~4%, YM155 and SRT1720 showed about ~6 and TW showed the highest FRET change (~7%) compared to apo FRET. TW-37 is a small molecule inhibitor of the Bcl-2 family

of proteins. Interestingly, combination therapy with TW-37 and verapamil, a P-gp inhibitor has been reported to reverse paclitaxel resistance in esophageal carcinoma [39]. This, together with the observation that TW-37 is a ligand of P-gp from the present study may provide clues the drug needs to be a subject of investigation for precise interaction with the transporter protein. The hit drugs are at best ligands or potential modulators of P-gp and further investigation is recommended to ascertain their actual interactive indices with the transporter. Our group is currently developing a vesicular transport assay-based LC-MS/MS method to unambiguously confirm the six hit drugs as substrates or otherwise of P-gp.

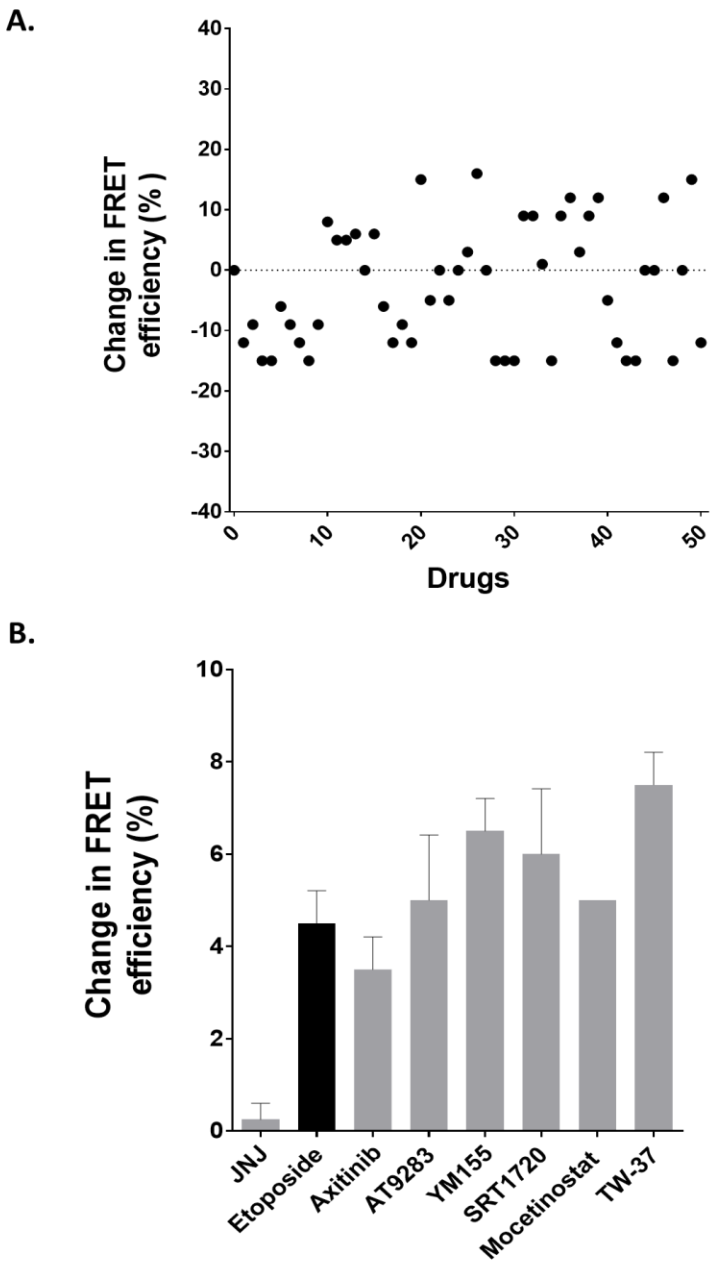

Figure 3.7 Screening of anticancer-library of drugs with two-color P-gp GR-678. 20 µg of isolated 293T/GR-678 membrane vesicles were added to 20 µM of each compound to initiate FRET signal reactions and incubated for 10 minutes at 370 C. The % FRET efficiencies calculated for the drugs were normalized with the transfer efficiency of the ligand-free apo FRET to obtain the percent changes in FRET for all drugs. A. Summarizes one independent screening experiment of the 50 anticancer compounds using two-color P-gp GR-678 through fluorescence

spectroscopy. B. Percent FRET changes of the six anticancer drug-hits identified by GR-678 using ensemble FRET spectroscopy. FRET changes of the six hits were higher than of the positive control, etoposide, a known substrate of P-gp. JNJ was included as a negative control anticancer drug as it showed consistent non-responsiveness to functional and FRET changes in previous experiments.

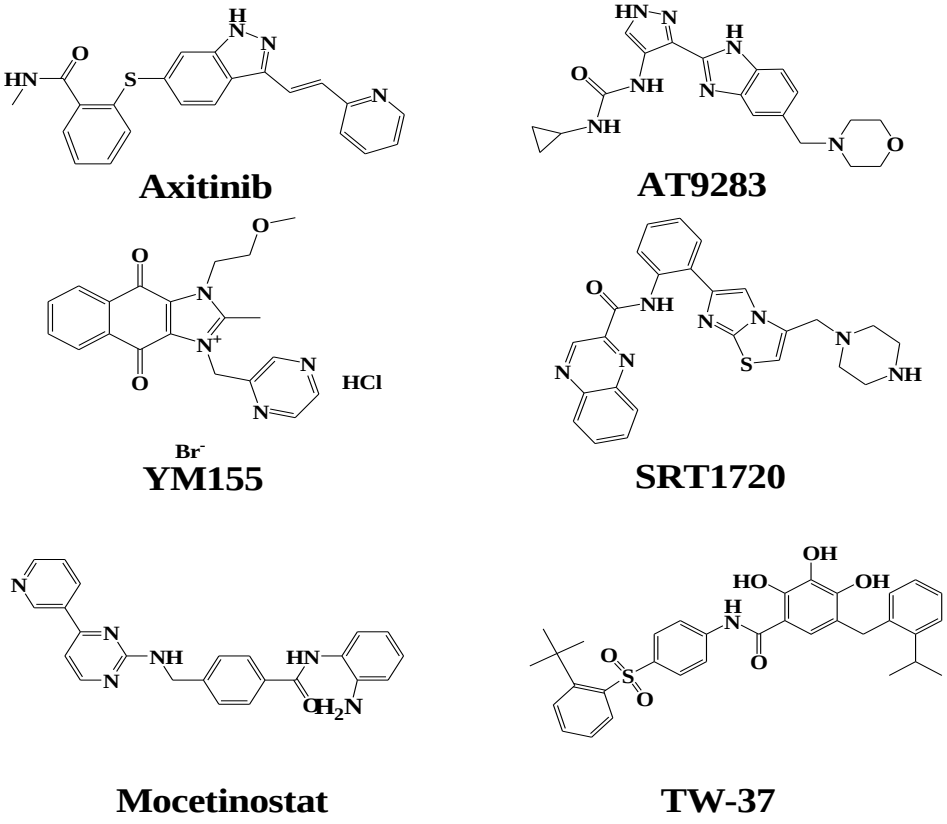

Figure 3.8. Chemical structures of the six chemotherapeutic drugs detected as hits. The hits were detected following steady state FRET screening of NIH clinically tested compounds. All drugs are currently under clinical trials. Axitinib targets.

Conclusion

Overall, we report for the first time the development of a two-color P-gp (GR-678) biosensor which does not only demonstrate intramolecular FRET capabilities as a function of structural changes in the transporter but also useful for identifying ligands of P-gp. We have optimized and improved the initial two-color MRP1 model by using membrane vesicles based steady state fluorescence. The two-color GR-678 P-gp biosensor could be a vital tool for high throughput screening of drugs which directly interact with the transporter using plate reader spectroscopy. Our two-color P-gp biosensor-based ensemble FRET assay provides an eminent alternative for research entities investigating compounds which interact directly with P-gp. Considering the affordability and accessibility of the fluorometer model H-11, our two-color P-gp ensemble FRET method offers a powerful and readily available substitute to more sophisticated FRET technologies in investigating the structure-function of P-gp. Research groups interested in developing biosensor models and bioengineering technologies should benefit from the two-color P-gp model presented here. Future expansion of our two-color model will include strategic site-directed mutagenesis to enhance FRET capability of the recombinant P-gp biosensor.

Table 3.1 Primer used to clone two-color P-gp constructs

Primer Names	Sequences (5'⟶3')
$Pgp_{1–642}$ forward	GTA GAG CTCA TGGATCTTGAAGGGGACCGCAATGGAGGA GC
$Pgp_{1–642}$ reverse	GTA GTC GACA T C AGCTGCATTTT CTAA TTCAACTTCATTTCCTG
$Pgp_{643–1280}$ forward	GTA CCG CGG GAATCCAAAAGTGA AATTGATGCCTTGGAAATGT C
$Pgp_{643–1280}$ reverse	GTA ACC GGT CTCTGGCGCTTTGTTCCAGCCTGGACACTG
$Pgp_{1–647}$ forward	GTA GAG CTCA TGGATCTTGAAGGGGACCGCAATGGAGGA GC
$Pgp_{1–647}$ reverse	GTA GTC GAC TT CACTT TTGGA TTCAT CAG CTGCATTTTCA
$Pgp_{648–1280}$ forward	GTA CCG CGG ATTGATGCC TTGGAAATGT CTTCAAATGA TTCAAG
M $Pgp_{648–1280}$ reverse	GTA ACC GGT CTCTGGCGCTTTGTTCCAGCCTGGACACTG
$Pgp_{1–653}$ forward	GTA GAG CTCA T GGATCTTGAAG G GGA CCGCAATGGAGGA GC
$Pgp_{1–653}$ reverse	GTA GTC GAC CATTTCCAAGGCATCAATTTCACTTTTGGATTCAT
$Pgp_{654–1280}$ forward	GTA CCG CGG T CTT CAAATGA TTCAAGAT CCA GT CTAATAA GAAA
$Pgp_{654–1280}$ reverse	GTA ACC GGT CTCTGGCGCTTTGTTCCAGCCTGGACACTG
$Pgp_{1–662}$ forward	GTA GAG CTCA TGGATCTTG AAGGGGACCGCAATGGAGGA GC
$Pgp_{1–662}$ reverse	GTA GTC GAC CATTTCCAA GGCATCAATTTCACTTTTGGATTCAT
$Pgp_{663–1280}$ forward	GTA CCG CGG T CTTCAAAT GA TTCAAGAT CCAGTCT AA TAA GAAA
$Pgp_{663–1280}$ reverse	GTA ACC GGT CTCTGGCG CTT TGTTCCAGCCTGGACACTG
$Pgp_{1–671}$ forward	GTA GAG CTCA TGGATCTTGAAGGGGACCGCAATGGAGGA GC
$Pgp_{1–671}$ reverse	GTA GTC GAC ACTCCTACGAGTTGATCTTTTTCTTATTAGACTGG
$Pgp_{672–1280}$ forward	GTA CCG CGG GTCC GTG GATCACAAGC CCAAGA C AGA AAGCTTAG
$Pgp_{672–1280}$ reverse	GTA ACC GGT CTCTG GCGCTTTGTTCCAGCCTGGACACTG
$Pgp_{1–678}$ forward	GTA GAG CTCA TGGATCTTGAAGGGGACCGCAATGGAGGA GC
$Pgp_{1–678}$ reverse	GTA GTC GAC T TGGGCTTGTGATCCACGGACACTCCTACGAGTTG
$Pgp_{679–1280}$ forward	GTA CCG CGG GACAGA AAGCTTAGTA CCAAAGAGGC TCTGGATGA

Pgp $_{679–1280}$ reverse	GTA ACC GGT CTCTGGCGCTTTGTTCCAGCCTGGACACTG
GFP-forward	GTA GTC GAC ATG GTG AGC AAG GGC GAG GAG CTG
GFP-reverse	CTA CCG CGG CTT GTA CAG CTC GTC CAT GCC GAG AG

References

1. Jones, P.M. and A.M. George, *The ABC transporter structure and mechanism: perspectives on recent research.* Cellular and Molecular Life Sciences, 2004. **61**(6): p. 682-699.
2. Rosenberg, M.F., et al., *Structure of the multidrug resistance P-glycoprotein to 2.5 nm resolution determined by electron microscopy and image analysis.* Journal of Biological Chemistry, 1997. **272**(16): p. 10685-10694.
3. Verhalen, B., et al., *Dynamic ligand-induced conformational rearrangements in P-glycoprotein as probed by fluorescence resonance energy transfer spectroscopy.* J Biol Chem, 2012. **287**(2): p. 1112-27.
4. Hodges, L.M., et al., *Very important pharmacogene summary: ABCB1 (MDR1, P-glycoprotein).* Pharmacogenetics and Genomics, 2011. **21**(3): p. 152-161.
5. Borst, P. and R.O. Elferink, *Mammalian ABC transporters in health and disease.* Annual Review of Biochemistry, 2002. **71**: p. 537-592.
6. Ambudkar, S.V., et al., *Biochemical, cellular, and pharmacological aspects of the multidrug transporter.* Annual Review of Pharmacology and Toxicology, 1999. **39**: p. 361-398.
7. Chang, G., *Multidrug resistance ABC transporters.* Febs Letters, 2003. **555**(1): p. 102-105.
8. Higgins, C.F., *Multiple molecular mechanisms for multidrug resistance transporters.* Nature, 2007. **446**(7137): p. 749-757.
9. Seigneuret, M. and A. Garnier-Suillerot, *A structural model for the open conformation of the mdr1 P-glycoprotein based on the MsbA crystal structure.* J Biol Chem, 2003. **278**(32): p. 30115-24.
10. Aller, S.G., *Structure of P-Glycoprotein Reveals a Molecular Basis for Poly-Specific Drug Binding.* Biophysical Journal, 2010. **98**(3): p. 755a-755a.
11. Iram, S.H., et al., *ATP-Binding Cassette Transporter Structure Changes Detected by Intramolecular Fluorescence Energy Transfer for High-Throughput Screening.* Mol Pharmacol, 2015. **88**(1): p. 84-94.
12. Fromm, M.F., *Importance of P-glycoprotein at blood-tissue barriers.* Trends in Pharmacological Sciences, 2004. **25**(8): p. 423-429.
13. Meijer, O.C., A.M. Karssen, and E.R. de Kloet, *Cell- and tissue-specific effects of corticosteroids in relation to glucocorticoid resistance: examples from the brain.* Journal of Endocrinology, 2003. **178**(1): p. 13-18.
14. Raviv, Y., A. Puri, and R. Blumenthal, *P-glycoprotein-overexpressing multidrug-resistant cells are resistant to infection by enveloped viruses that enter via the plasma membrane.* Faseb Journal, 2000. **14**(3): p. 511-515.
15. Schinkel, A.H., et al., *Disruption of the mouse mdr1a P-glycoprotein gene leads to a deficiency in the blood-brain barrier and to increased sensitivity to drugs.* Cell, 1994. **77**(4): p. 491-502.

16. Umbenhauer, D.R., et al., *Identification of a P-glycoprotein-deficient subpopulation in the CF-1 mouse strain using a restriction fragment length polymorphism.* Toxicol Appl Pharmacol, 1997. **146**(1): p. 88-94.
17. Binkhathlan, Z. and A. Lavasanifar, *P-glycoprotein inhibition as a therapeutic approach for overcoming multidrug resistance in cancer: current status and future perspectives.* Curr Cancer Drug Targets, 2013. **13**(3): p. 326-46.
18. Kuo, M.T., *Redox regulation of multidrug resistance in cancer chemotherapy: molecular mechanisms and therapeutic opportunities.* Antioxid Redox Signal, 2009. **11**(1): p. 99-133.
19. Thomas, H. and H.M. Coley, *Overcoming multidrug resistance in cancer: an update on the clinical strategy of inhibiting p-glycoprotein.* Cancer Control, 2003. **10**(2): p. 159-65.
20. Loscher, W. and H. Potschka, *Role of multidrug transporters in pharmacoresistance to antiepileptic drugs.* Journal of Pharmacology and Experimental Therapeutics, 2002. **301**(1): p. 7-14.
21. Hermann, D.M., et al., *Role of drug efflux carriers in the healthy and diseased brain.* Ann Neurol, 2006. **60**(5): p. 489-98.
22. Zhou, S., L.Y. Lim, and B. Chowbay, *Herbal modulation of P-glycoprotein.* Drug Metab Rev, 2004. **36**(1): p. 57-104.
23. Chan, H.S., et al., *P-glycoprotein expression as a predictor of the outcome of therapy for neuroblastoma.* N Engl J Med, 1991. **325**(23): p. 1608-14.
24. Sokolowska, J., et al., *Immunohistochemical detection of P-glycoprotein in various subtypes of canine lymphomas.* Pol J Vet Sci, 2015. **18**(1): p. 123-30.
25. Tan, K.W., et al., *Identification of novel dietary phytochemicals inhibiting the efflux transporter breast cancer resistance protein (BCRP/ABCG2).* Food Chem, 2013. **138**(4): p. 2267-74.
26. Clarke, R., F. Leonessa, and B. Trock, *Multidrug resistance/P-glycoprotein and breast cancer: review and meta-analysis.* Semin Oncol, 2005. **32**(6 Suppl 7): p. S9-15.
27. Kauffman, M.K., et al., *Fluorescence-Based Assays for Measuring Doxorubicin in Biological Systems.* React Oxyg Species (Apex), 2016. **2**(6): p. 432-439.
28. Hoffmann, K., et al., *Sorafenib modulates the gene expression of multi-drug resistance mediating ATP-binding cassette proteins in experimental hepatocellular carcinoma.* Anticancer Res, 2010. **30**(11): p. 4503-8.
29. Bansal, T., et al., *Effect of P-glycoprotein inhibitor, verapamil, on oral bioavailability and pharmacokinetics of irinotecan in rats.* Eur J Pharm Sci, 2009. **36**(4-5): p. 580-90.
30. Perez-Tomas, R., *Multidrug resistance: Retrospect and prospects in anti-cancer drug treatment.* Current Medicinal Chemistry, 2006. **13**(16): p. 1859-1876.
31. Choi, J.S. and X. Li, *The effect of verapamil on the pharmacokinetics of paclitaxel in rats.* Eur J Pharm Sci, 2005. **24**(1): p. 95-100.
32. Luo, F.R., et al., *Intestinal transport of irinotecan in Caco-2 cells and MDCK II cells overexpressing efflux transporters Pgp, cMOAT, and MRP1.* Drug Metab Dispos, 2002. **30**(7): p. 763-70.

33. Urbatsch, I.L., et al., *P-glycoprotein is stably inhibited by vanadate-induced trapping of nucleotide at a single catalytic site.* J Biol Chem, 1995. **270**(33): p. 19383-90.
34. Sankaran, B., S. Bhagat, and A.E. Senior, *Inhibition of P-glycoprotein ATPase activity by beryllium fluoride.* Biochemistry, 1997. **36**(22): p. 6847-53.
35. Peterson, B.G., et al., *High-content screening of clinically tested anticancer drugs identifies novel inhibitors of human MRP1 (ABCC1).* Pharmacol Res, 2017. **119**: p. 313-326.
36. Rixe, O., et al., *Axitinib treatment in patients with cytokine-refractory metastatic renal-cell cancer: a phase II study.* Lancet Oncol, 2007. **8**(11): p. 975-84.
37. Foran, J.M., et al., *Phase I and pharmacodynamic trial of AT9283, an aurora kinase inhibitor, in patients with refractory leukemia.* Journal of Clinical Oncology, 2008. **26**(15).
38. Mitchell, S.J., et al., *The SIRT1 Activator SRT1720 Extends Lifespan and Improves Health of Mice Fed a Standard Diet.* Cell Reports, 2014. **6**(5): p. 836-843.
39. Shi, X., et al., *Targeting the Bcl-2 family and P-glycoprotein reverses paclitaxel resistance in human esophageal carcinoma cell line.* Biomed Pharmacother, 2017. **90**: p. 897-905.
40. https://pubchem.ncbi.nlm.nih.gov/compound/etoposide#section=Top accessed 09/01/2018.

CHAPTER 4

RELEVANT CONTRIBUTIONS

Scope

This chapter catalogues relevant contributions which the current project made to the general goals of our research group. These are side projects which impact other scholarly activities in our research group. The projects described in this section are categorized into three. One of the projects relates to discovery of twelve clinically tested anticancer drugs from a high throughput screening using high-content imaging. The second project relates to determination of the effects of vitamin D analogues on MRP1 transcript. The third project concerns the discovery of eighteen inhibitors of MRP1 which were identified predominantly using doxorubicin as a fluorescent substrate probe. Firstly, we expound the use of two-color multidrug resistance associated protein-1 (MRP1) engineered in our lab to show that MRP1 inhibitor hits discovered by our lab directly interact with the transporter. The fluorescence resonance energy transfer technique was used to evaluate the interaction of the twelve hits with the two-color recombinant biosensor. Next, we show how reverse transcriptase-quantity polymerase chain reaction (qPCR or RT-PCR) was used to determine the effect of vitamin D analogues, calcitriol and calcipotriol on the mRNA of MRP1. The qPCR experiments were carried out to support or contradict the data obtained from western blot in which the effects of the calcitriol and calcipotriol on the MRP1 protein were investigated. In the third and final project, eighteen MRP1 inhibitor hits following high content screening with doxorubicin of anticancer library of compounds. These hits had been further evaluated as MRP1 inhibitors with flow cytometry, doxorubicin accumulation assay via confocal microscopy and shown reversal

of cytotoxicity. We designed a project to determine the effects of the eighteen-test compound-hits on the mRNA of MRP1. We also assessed the interactivity of the drug hits with MRP1 by using the purified membrane vesicles expressing GR-888 biosensor, engineered in the current project in a fluorescent spectroscopy approach.

Two-color MRP1 biosensor-based FRET detects direct interaction of twelve MRP1 inhibitors with the transporter.

Introduction

Recently, our research group developed a high content method for identification of novel inhibitors of multidrug resistance associated protein-1 (MRP1). The high content method discovered twelve inhibitor hits of MRP1 following screening of clinically tested anticancer library of drugs. The initial high throughput screening which found the hits used calcein green as the fluorescent MRP1 substrate reporter. Interestingly, of the twelve potent inhibitors, two (cyclosporin A and rapamycin) are well-established inhibitors of MRP1 and ten are novel; tipifarnib, AZD1208, deforolimus, everolimus, temsirolimus, HS-173, YM201636, ESI-09, TAK-733, and CX-6258 [1]. Next, the hits were validated as true MRP1 inhibitors using several different functional assays.

First, doxorubicin accumulation assay was performed in the presence of the inhibitor-hits to determine if the hit-drugs would obstruct the efflux-extrusion of doxorubicin by MRP1 using HEK cells overexpressing GFP-MRP1, a 1-color recombinant MRP1 engineered by our group. Using confocal microscopy for imaging, the assay proved the inhibitor hits impeded the normal function of MRP1 by ensuring the accumulation of doxorubicin in the nuclei of the cells. The potency of the small molecules as inhibitor-hits of MRP1 was further confirmed by flow cytometry, vesicular transport using radiolabeled (E217βG and LTC4) of MRP1 as reporter. In both assays, the twelve hits showed as potent inhibitors of the transporter under investigation, MRP1.

While reviewers found the study well-researched with appropriate techniques and assays to report our findings, they cited one concern. All assays reported showed the twelve hits are true hits of MRP1 but failed to show the drugs had direct interaction the transporter. On the other hand, it is established that in all the three major types of inhibition, competitive, noncompetitive, and uncompetitive, one thing is mutual. Competitive inhibition occurs when the inhibitor shares a similar chemical structure with the substrate and competes for the same active site with the substrate. In this case the inhibitor binds only to the free enzyme (figure 1). In noncompetitive inhibition, the inhibitor does not resemble the substrate structurally and binds to both the enzyme and the enzyme-substrate complex. However, the inhibitor in uncompetitive inhibition only binds to the enzyme-substrate complex and does not share structural similarities with the substrate (Figure 4.1)[2]. In all three instances of enzyme-inhibition, the common theme is that the inhibitor must directly bind to the enzyme to be able to enact its inhibitory efficacy on it. This may have been the rationale behind the request to demonstrate that the twelve MRP1 inhibitor-hits directly interacts with the transporter. ABC transporters are ATPases (enzymes which hydrolyze ATP) and they thrive on catalytic hydrolysis to perform their efflux functions [3-5]. It is expected that ABC transporters submit to the general rule of direct interaction of inhibitors with enzymes.

In the present project, we designed a strategy to address the reviewers' comments. The two-color MRP1 biosensor engineered by our group and coupled with fluorescence spectroscopy displays dynamic FRET changes in the presence of ligands of the reporter. This is an indication that the two-color biosensor is useful for detection of direct interaction with MRP1. To address the concern posed by reviewers, we used the one of

the FRET sensitive two-color MRP1 biosensors engineered by our research group to evaluate the interaction of the twelve hits with MRP1.

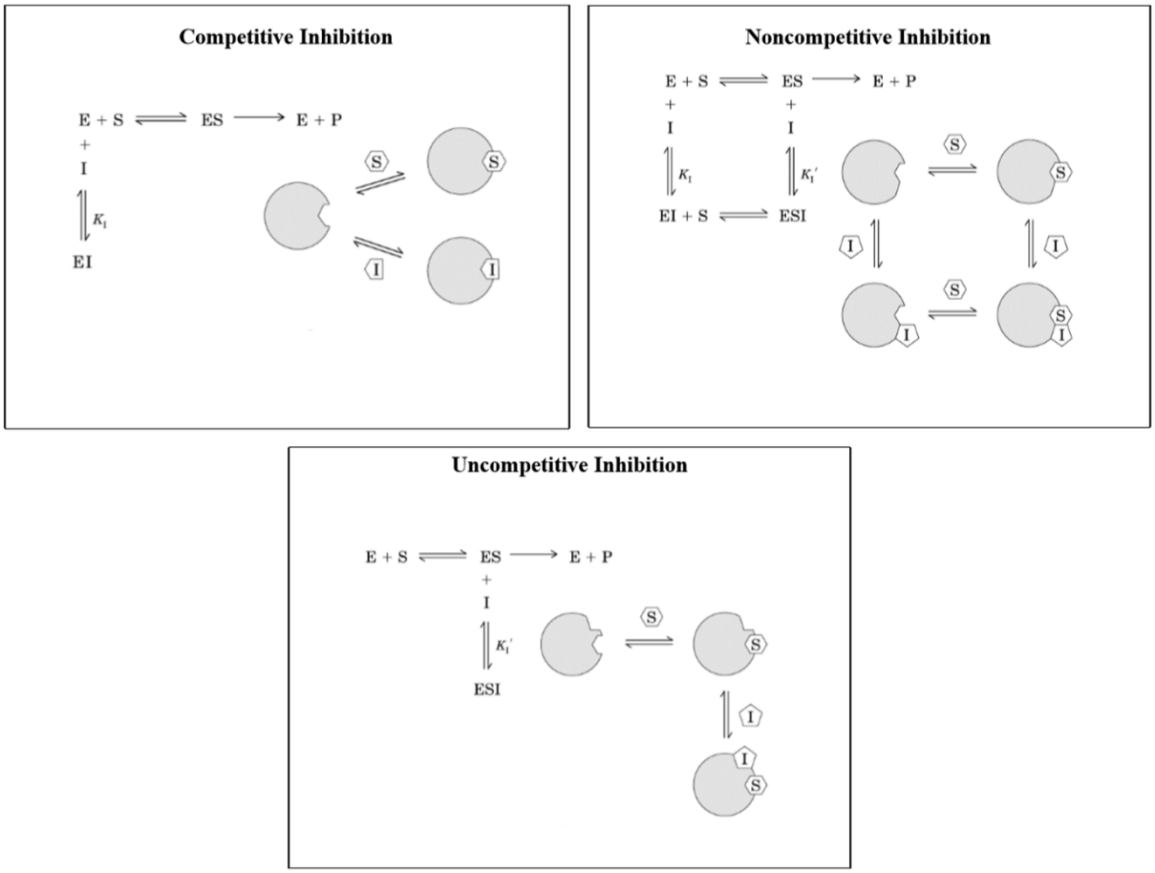

Figure 4.1. Schematic diagram of the types of enzymatic inhibition.

In competitive inhibition, the inhibitor shares similar structural characteristics with the substrate and competes with the substrate for the same active site. In non-competitive inhibition, the inhibitor is structurally dissimilar from the substrate and binds to the enzyme at a site different from where the substrate binds. Like non-competitive inhibitor, in uncompetitive inhibition, the inhibitor doesn't resemble the substrate but here, the inhibitor binds only to the enzyme-substrate complex [10].

Methodology: Steady state fluorescence spectroscopy

Previously, a two-color MRP1 biosensor had been genetically engineered in our lab by fusing a green fluorescent protein (GFP) and a red fluorescent protein (RFP) to the transporter. This genetically modified two-color MRP1 reported ligand-induced steady-state fluorescence resonance energy transfer (FRET) change [6]. Membrane vesicles of GFP-MRP1 (donor control containing only GFP without RFP) and two-color MRP1 (acceptor) were purified from human embryonic kidney (HEK-293) cells stably expressing either proteins. Steady-state fluorimetry was employed for ligand-free (apo) and ligand-induced FRET analysis using experimental conditions described by [7] with modification. Membrane vesicles (10 µg) in Tris sucrose buffer (250 mM Tris, 50 mM sucrose, pH 7.4) was prepared and pre-incubated for 10 minutes at 370 C. Membrane vesicles were then incubated with 10 µM of test compounds for 10 minutes at 370 C in a water bath prior to FRET measurements. Ensemble fluorescence spectroscopy was carried out in a 50 µL quartz glass cuvette using the Fluorimeter model FL3-11 (HORIBA Edison, New Jersey). GFP excitation was observed at 480 nm and RFP, at 530 nm. Emission for both GFP and RFP with integration time of 3 seconds was recorded at 480-650 nm. One emission scan of the donor only (GFP-MRP1 sample) was first collected while monitoring average donor emission peak. Another emission scan was collected in the apo condition (ligand-free two-color MRP1); donor quenching was monitored, and the average donor emission peak was recorded. The test compound conditions were similarly scanned, and donor quenching monitored. Each emission scan was collected at an interval of 5 nm every 3 seconds for a total of 10 minutes. Two independent experiments were performed in technical triplicates.

Results and Discussion

The relative fluorescence of the donor in the presence and absence of the acceptor was used to analyze data. The ratio of the average donor emission peak intensity (in counts per second, cps) in the donor-acceptor sample (two-color MRP1) to the average donor emission peak intensity in the donor only control (GFP-MRP1)) was subtracted from one to obtain the transfer efficiency of apo and compound-induced conditions. Transfer efficiencies of compound-induced samples were normalized with that of the apo condition to obtain the percent change in FRET. The standard deviation of triplicates was calculated for each test compound condition and the results, presented as mean ± SEM.

FRET spectroscopy was performed to investigate test compound-induced changes in FRET efficiency of MRP1. The concept of donor quenching in FRET analysis, as reported by Lakowicz in 1999 [8] is an established method for calculating the transfer efficiency of an ensemble. The ratio of average donor intensity (cps) in the two-color MRP1 (apo or test compound induced) samples to donor intensity in the GFP-MRP1 sample deducted from unity represents the transfer efficiency of the specific two-color MRP1. Percent change in FRET efficiency was calculated by subtracting the transfer efficiency of apo condition from transfer efficiency of test compound conditions. MK-571, a widely known MRP1 inhibitor showed an 8% increase in FRET efficiency relative to the apo condition. JNJ, which in previous functional assays conducted by our group failed to show inhibitory activities against MRP1 from doxorubicin efflux, showed no change in FRET efficiency. All test compounds showed increase in FRET efficiency in comparison to the apo condition. Tipifarnib showed the smallest FRET change (2.4%) and Deforolimus, the largest FRET change (9.67%) (Figure 4.2).

All twelve test compounds demonstrate varying degrees of compound-induced intramolecular FRET changes in two-color MRP1 through fluorescent spectroscopy, suggesting they all directly interact with the MRP1. A known MRP1 inhibitor, MK-571 used as a positive control showed similar trend of FRET change as the test compounds confirms the finding they are candidate-inhibitors of MRP1. Having failed previous inhibitor test assay, negative control JNJ showed no change in FRET efficiency, indicating the validity of the steady state FRET assay.

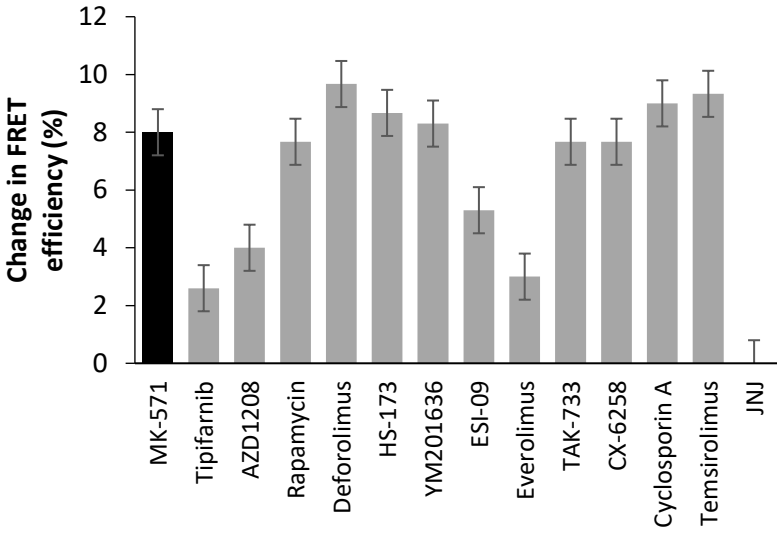

Figure 4.2. Compound induced conformational changes in MRP1. Membrane vesicles were prepared from stable HEK293/GFP-MRP1 and HEK293/two-color MRP1 cells. Membrane vesicles (10 µg) were incubated with 10 µM of each test compound for 20 minutes at 37 °C prior fluorescence spectroscopy using Fluorimeter model FL3-11. GFP excitation was accomplished at 480 nm and RFP was excited at 530 nm. Emission for both GFP and RFP with integration time of 3 seconds was recorded at 480-650 nm. GFP excitation was observed at 480 nm and RFP, at 530 nm. Emission for both GFP and RFP was collected at 480-650 nm with 3-seconds integration time. Data is represented from two independent experiments in triplicates. MK571 and JNJ-26854165 were used as positive and negative controls, respectively. To calculate the change in

FRET efficiency for test compound conditions, the basal apo FTRET efficiency was subtracted from the compound-induced FRET efficiencies and results are presented as Mean ± SEM [1].

The effects of calcitriol and calcipotriol on mRNA levels of MRP1

Introduction

Our research group previously cloned a two-color MRP1 which reports changes in intramolecular FRET as a function of structural conformations of the protein. The recombinant protein also identified eight potential substrate hits of MRP1 during a high throughput screening of National Institute of Health library of drugs [6]. The compounds included antioxidants such as EGCG and hyperoxide, vitamin D analogue, calcitriol and calcipotriol, anti-inflammatory mesalamine, antibiotic, meropenem, antiparasitic nitazoxanide and antipsychotic droperidol. The results from the wide screening was not conclusive about the substrate or inhibitor status of the eight hit compounds. The compounds were at best considered ligands or potential modulators of MRP1. This left room for further characterization of the hit drugs for their specific interactive index with MRP1. To do this, functional assays were performed to determine if the hit drugs inhibited MRP1 efflux of doxorubicin and calcein in H69AR/MRP1 and HEK/MRP1 cell lines. The results showed that of the eight, only the vitamin D analogues, calcitriol and calcipotriol demonstrated inhibitory activity towards MRP1 [9] (Tan et al, 2018). Vesicular transport assay using tritium-labelled substrate of MRP1 confirmed the strong inhibition of MRP1 by calcitriol and calcipotriol. Following the new find that these vitamin D metabolites are strong inhibitors of MRP1, we sought to understand the effect of these drugs on the mRNA and protein expression of MRP1. The rationale for this research is that an inhibitor of MRP1 which also depresses the expression of the MRP1 transcript could be a more potent inhibitor than one which increases the expression significantly. The methods which follow, were designed and executed in response to

reviewers who raised the query about the effect of calcitriol and calcipotriol on MRP1 mRNA and protein expression. Only data from the mRNA expression experiments are shown here as it has direct correlation with the broader perspective covered by the current project.

Methodology: RNA Isolation and real-time RT-PCR analysis

Approximately 10^6 cultured MRP1-over-expressing HEK and AR cells treated with either DMSO, 1 µM or 10 µM calcitriol, or 1 µM or 10 µM calipotriol were pelleted by centrifugation and stored for RNA isolation. Cultured parental HEK and H69 were included in experiments as MRP1-non-expressing negative controls. Total RNA was isolated from the cells using the Ambion TRIzol plus RNA purification kit (Thermo Fisher Scientific, USA). To rid the freshly prepared total RNA of possible DNA contamination, DNase1 enzyme treatment was performed using the Turbo DNA-free kit (Life technologies, U.S.A.). The concentration and integrity of RNA was determined using the 260/280 ratios generated by a Nano-drop U.V. spectrophotometer. cDNA synthesis was done with the recombinant M-MuLV-based ProtoScript II First strand cDNA synthesis kit (New England Biolabs Inc., MA, U.S.A.) using 1µg of the total RNA as starting material. Gene-specific primers were designed using the Primer3 software via Pubmed and synthesized by Europhins U.S.A. Table 1 shows the list of primers sequences and their corresponding amplicon lengths. Numbers inserted in parenthesis in columns three and four of table 1 represent region in gene template where primers anneal to. The syber green dye-based Luna universal qPCR master mix (New England Biolabs Inc., MA, U.S.A.) was used to perform quantitative PCR analysis. Total reaction-mix of 20 µL was prepared consisting of 2 µL of cDNA (20 ng/ µL), 10 µL of Luna universal qPCR master mix (New England Biolabs Inc., MA, U.S.A.), 1 µL of primer mix and made up to maximum volume with 7 µL of Nuclease-free water. The Quantstudio3 Real-time system (Thermo Fisher Scientific) was used for the qPCR analysis. The three-step PCR conditions used are as follows chronologically: 950 C denaturation for 1.2 minute,

45 cycles of (annealing at 600 C for 20 seconds, extension at 720 C for 30s), and denaturation for 10 seconds. This was followed by melting curve stage from 600 C to 950 C for 20 seconds while scanning for fluorescence. Relative quantitation was performed using the 2 -ΔΔCt method and data was normalized against housekeeping genes, β-actin and ubiquitin conjugating enzyme (UbCE) of respective samples. The relative messenger RNA (mRNA) expression level was calculated as a percentage of the both reference genes. After qPCR, 0.9% agarose gel electrophoresis was used to verify lengths of amplicons.

Results and Discussion

The effect of calcitriol and calcipotriol at concentrations of 1 µM and 10 µM on the MRP1 transcript in H69AR/MRP1 and HEK/MRP1 cells were evaluated through RT-PCR. The average cycle threshold (Ct) values of target protein, MRP1 after qPCR were normalized with those of endogenous controls ubiquitin conjugating enzyme and β-actin. 1 µM of calcitriol and calcipotriol did not significantly affect the transcription of MRP1 either in HEK/MRP1 or H69AR/MRP1 cell lines. The results showed however, that in HEK/MRP1 cells at 10 µM, calcitriol slightly increased the relative expression of MRP1 transcript by 1.5-fold, while 10 µM calcipotriol displayed the same expression fold as the DMSO control reaction. In H69AR/MRP1 cells however, the transcript expression of MRP1 in the presence of calcitriol dwindled significantly by 0.5-fold while calcipotriol had a 1.6-fold expression on mRNA of the protein (figure 3). DMSO showed no effect on the mRNA of MRP1 or on the endogenous controls in both HEK and AR cells. The parental H69 and HEK cells showed the least amount of mRNA expression which is consistent with normal MRP1 expression of cells which have not been prior induced to overexpress the protein. The two metabolites of vitamin D, calcitriol and calcipotriol also did not have any effect on the expression of the mRNA of the housekeeping genes, ubiquitin conjugating enzyme and beta-actin. Our results suggest that calcipotriol does not significantly influence the mRNA expression of MRP1, whereas calcitriol significantly reduced the expression of the MRP1 transcript only in AR/MRP1 cells. This observation could be because of cell specific effect and may not be considered that calcipotriol generally causes a decline in MRP1 expression. These results of qPCR

experiments are consistent with the western blotting quantification data (not shown in the present document).

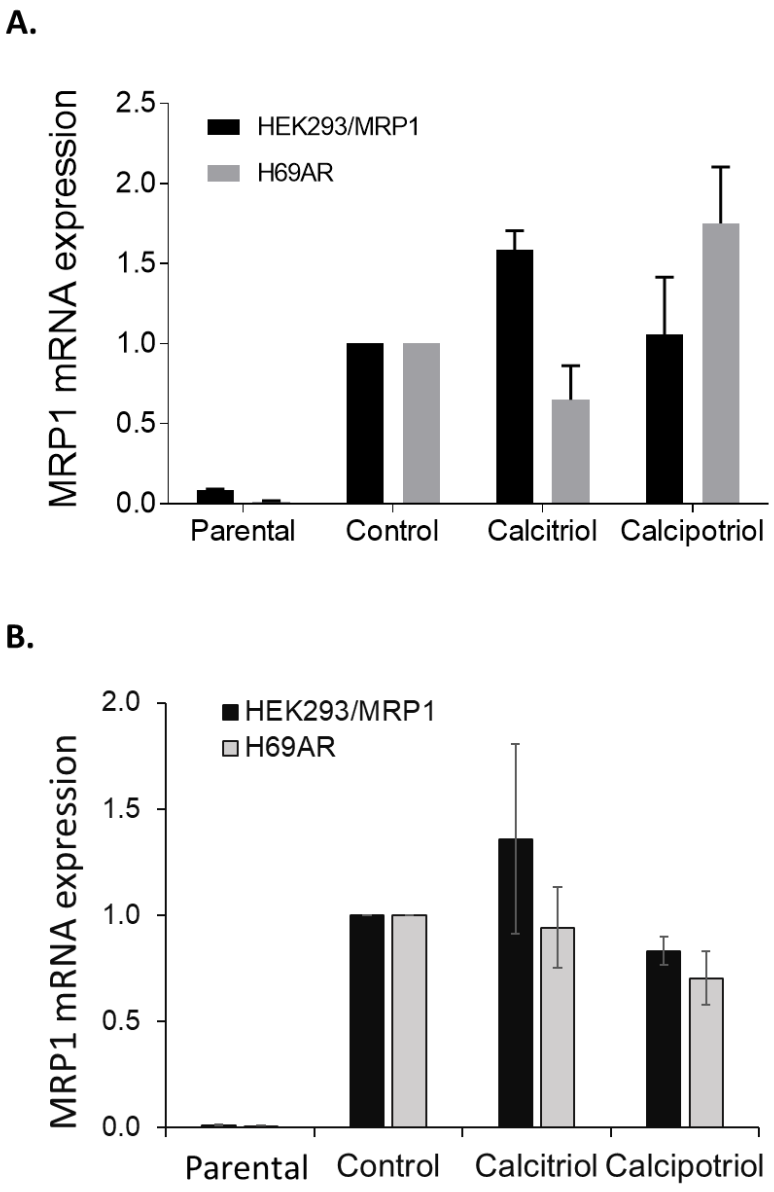

Figure 4.3 Relative expression of MRP1 mRNA in the presence of calcitriol and calcipotriol. **A.** HEK and H69AR cells were treated with 10 µM of calcitriol and calcipotriol. Calcitriol significantly reduces the mRNA expression of MRP1 in H69AR cells but has no effect on HEK

cells. Calcipotriol on the other hand has no significant influence on the MRP1 transcript. **B**. HEK and H69AR cells were treated with 1µM of calcitriol and calcipotriol. At 1µM, none of the drugs had any significant effect on the MRP1 transcript. All cycle threshold values were normalized to those of the housekeeping genes used as endogenous controls. The test compounds results were normalized with the DMSO results [9].

Table 4.1 Primer sequences and amplicon lengths

Gene	Genbank number	Forward primer	Reverse primer	Amplicon length
MRP1	NM_004996.3	AGGACACGTCGGAACAAGTC (915-934)	GGAAGTAGGGCCCAAAGGTC (1151-1132)	237
β-Actin	NM_001101	CATGTACGTTGCTATCCAGGC (393-413)	CTCCTTAATGTCACGCACGAT (642-622)	250
Ubiquitin CE	NM_001282161.1	ATGCGGGACTTCAAGAGGAG (273-292)	AAAATGACCGCGTTCCACAC (360-341)	88

Detection of direct interaction of the eighteen doxorubicin hits with MRP1

Introduction

Following a mass screening of clinically tested anticancer compounds using high content microscope, eighteen drugs were discovered as preliminary inhibitor-hits of MRP1. These compound-hits were confirmed as true using quantitative approaches, the flow cytometry and other qualitative means, confocal microscopy. ABC transporters like MRP1 are ATPases which utilize ATP hydrolysis to transport a host of structurally divergent substrates. Apart from substrates which interact with ABC proteins including MRP1, compounds which inhibit their function must also associate with the protein one way or another. Being ATPases, MRP1 acts like enzymes and as inhibitors must interact with the enzymes they impede, inhibitors of MRP1 must operate in a similar fashion. Discovery of the eighteen compounds as inhibitors of MRP1 using a myriad of well-established functional assays does not complete the story of the study. It was imperative to prove that the eighteen compounds directly interact with MRP1. To validate that the eighteen compounds directly interact with MRP1, we designed a membrane vesicle-based fluorescent spectroscopy screen of the drug hits using two-color GR-888, developed in the present study, as the probe.

Methods

The methods used to accomplish the evaluation of the interaction of the eighteen compound hits with MRP1 are outlined in (25) without any modifications. Isolated two-color GR-888-expressing membrane vesicles were prepared and reacted with test compounds at 37^0 C FRET measurements using the fluorometer. FRET was measured in the presence and absence of test drugs and the difference of FRET efficiency between these two conditions was calculated as percent FRET efficiency change. Each trial was repeated three times and the triplicate results were combined as reporter as mean ± SEM

Results and discussion

Fluorescent spectroscopy was used to evaluate the direct interaction between the eighteen inhibitors discovered with MRP1. In the presence of an inhibitor, movement of the NBDs on which are located the intramolecularly inserted fluorescent-pair, GFP and RFP. The dynamism of the NBDs is detected as a fluorescent signal and interpreted as FRET efficiency which is subtracted from the basal FRET condition to generate values of FRET efficiency change. Two-color GR-888 displayed different degrees of percent FRET efficiency changes in the presence of the eighteen doxorubicin hits as shown in figure 4.4. Our results suggest that all eighteen compounds directly interact with MRP1 with altering degrees of strength. Notably, eleven of the drugs show higher percent FRET efficiency changes (~7-9%) compared with the FRET change of MK-571 (~5%), a known MRP1 inhibitor used here as a positive control. JNJ, which usually shows no signal in previous functional assays, displayed almost no FRET change, validating our results.

We have developed a two-color ABC transporter biosensor based-FRET technique which constitutes a standard routine protocol in the detection of direct interaction of inhibitors and substrates with ABC proteins. Our method developed can be mirrored by researchers interested in understanding the mechanism of interaction between diverse types of proteins particularly receptor proteins and their ligands. Fundamental questions of receptor-ligand associations could be answered by incorporating our FRET-based approach.

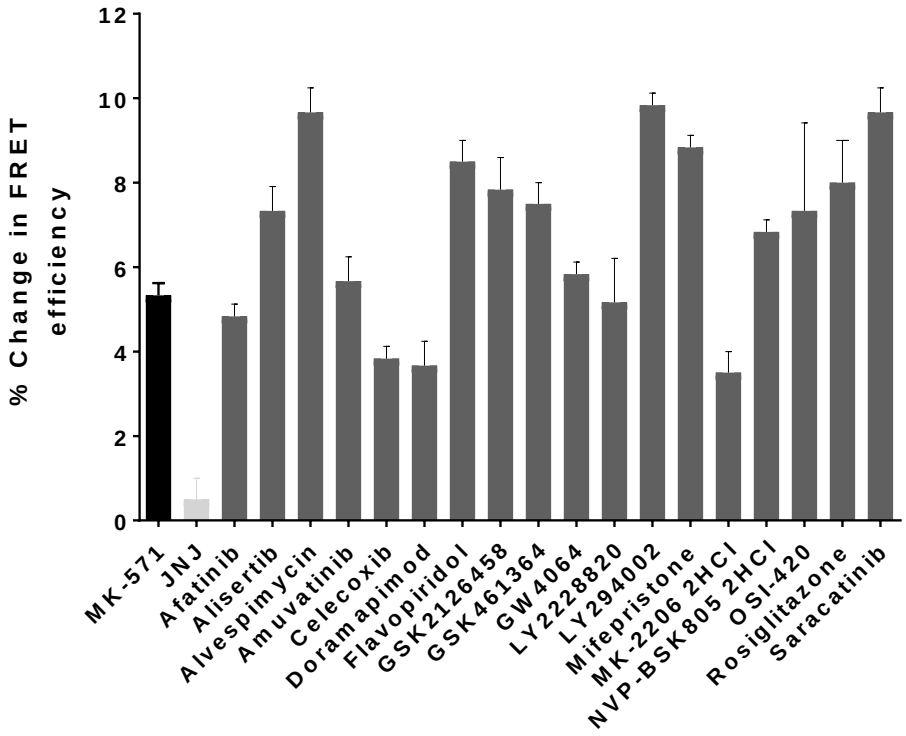

Figure 4.4. FRET analysis of eighteen anticancer compounds. 20 µM of each compound was added to 10 µg of two-color MRP1 GR-888 expressing HEK membrane vesicles and incubated at 37^0C. GFP emission and quenching was translated to FRET efficiency. Excitation and emission for GFP were 465 nm and 480-530 nm respectively.

Effect of eighteen doxorubicin inhibitor–hits on MRP1 transcript

Introduction

The eighteen compounds identified through a variety of functional assays as inhibitors of MRP1 were further evaluated for their effects on the transcription of the MRP1 gene. Determination of how a drug influences mRNA expression requires the use of quantitative PCR. The rationale for performing qPCR is that a MRP1 inhibitor which additionally impedes the expression of MRP1 mRNA is more desired as a potent inhibitor than drugs which inhibit only function of MRP1 but not its expression.

Method

Methods used for conducting qPCR including primer design, RNA isolation, cDNA synthesis are the same as described previously. HEK cells overexpressing MRP1 were treated with 1 μM of each drug and lysates were prepared which were divided into two for RT-PCR and western blot purposes.

Results and discussion

Our results show that only 5 of the eighteen drugs at 1 μM significantly increased MRP1 mRNA expression by 2-fold or more. The ability of these five drugs to prominently improve the mRNA expression of MRP1 could work against their inhibitory properties. These results need to be substantiated with further experiments. The rest of the drugs did not significantly affect mRNA expression as they showed slightly above or below 1-fold.

Notably, Sarcatinib showed a 0.5-fold decrease of mRNA expression of MRP1. These results are consistent with western blotting data (not shown here) which evaluated the effect of the same drugs on the protein expression of MRP1. Our results suggest that Sarcatinib may be the most potent inhibitor overall due to its ability to not only affect the protein function but also dwindle the transcript of MRP1 gene. Further downstream tests may be necessary to confirm these findings.

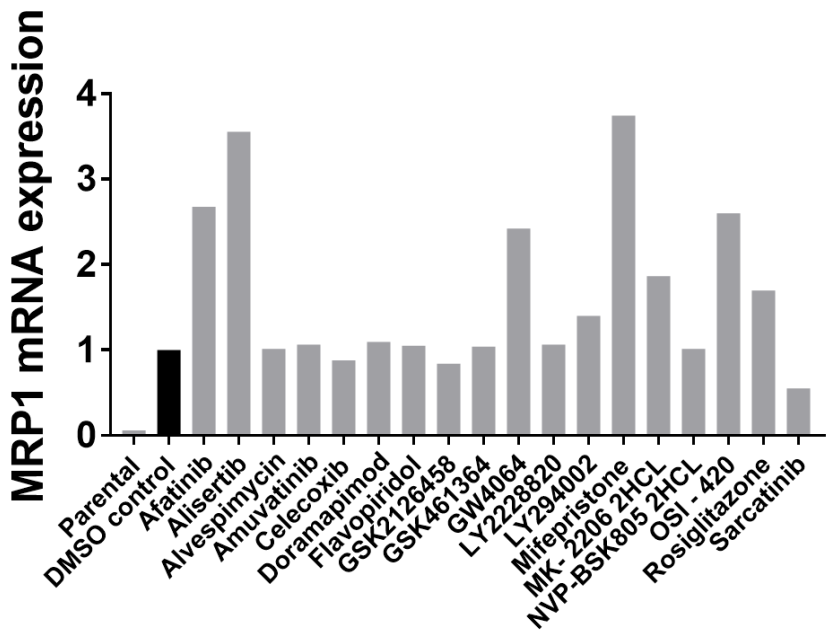

Figure 4.5 effect of test compounds on the mRNA transcript of MRP1.

References

1. Peterson, B.G., et al., *High-content screening of clinically tested anticancer drugs identifies novel inhibitors of human MRP1 (ABCC1).* Pharmacol Res, 2017. **119**: p. 313-326.
2. Safaa Mohammed M. Alsanosi Craig, S., Sandosh Padmanabhan, *Handbook of Pharmacogenomics and Stratified Medicine*. 2014: Glasgow, United Kingdom.
3. Schneider, E. and S. Hunke, *ATP-binding-cassette (ABC) transport systems: functional and structural aspects of the ATP-hydrolyzing subunits/domains.* FEMS microbiology reviews, 1998. **22**(1): p. 1-20.
4. Altenberg, G.A., *The engine of ABC proteins.* News Physiol Sci, 2003. **18**: p. 191-5.
5. Cole, S.P. and R.G. Deeley, *Multidrug resistance mediated by the ATP-binding cassette transporter protein MRP.* Bioessays, 1998. **20**(11): p. 931-940.
6. Iram, S.H., et al., *ATP-Binding Cassette Transporter Structure Changes Detected by Intramolecular Fluorescence Energy Transfer for High-Throughput Screening.* Mol Pharmacol, 2015. **88**(1): p. 84-94.
7. Verhalen, B., et al., *Dynamic ligand-induced conformational rearrangements in P-glycoprotein as probed by fluorescence resonance energy transfer spectroscopy.* J Biol Chem, 2012. **287**(2): p. 1112-27.
8. Lakowicz, J.R., *Energy transfer in Principles of FluorescenceSpectroscopy*. 2nd ed. 1999, Plenum, New York.
9. Tan, K.W., et al., *Calcitriol and Calcipotriol Modulate Transport Activity of ABC Transporters and Exhibit Selective Cytotoxicity in MRP1-overexpressing Cells.* Drug Metab Dispos, 2018.
10. http://www.csun.edu/~hcchm001/5enzyme.pdf

CHAPTER 5

FINAL DISCUSSIONS

MRP1 and P-gp are two of the most important ABC transporters which play a significant role in the disposition and efflux-translocation of a variety of compounds and therapeutic agents in an ATP-dependent hydrolysis, while mediating tissue defense of sanctuary sites such as the blood-testis barrier, as shown through mice studies [1-5]. The prominent expression of MRP1, P-gp along with BCRP in leukemias, breast cancer and other tumors confers multidrug resistance (MDR) to anticancer agents, leading to poor patient outcomes during chemotherapy [1, 6]. Therefore, profiling of the interaction of these important transporters with pharmacological agents is imperative but the absence of a high-throughput assay for the identification of substrates of these ABC proteins remains an impediment to extensive drug screening. In our previous study, we developed a two-color MRP1 biosensor which reports intramolecular FRET efficiency as a measure of conformational changes in the presence of E217βG and other ligands. This recombinant reporter (GR-873) also identified eight compounds including the antibiotic nitazoxanide and the flavonoid EGCG, through a high throughput screening of a library of clinically tested drugs using Fluorescence lifetime technology.

In the present study, to enhance the sensitivity of the 2-color-FRET model and expand it to other ABC transporters, we cloned a set of six two-color MRP1 and P-gp proteins by altering the locations of the GFP on the transporters. The strategic goal of the study was to investigate which of the two-color constructs through steady state FRET, would exhibit better FRET sensitivity than GR-873. We employed the most FRET-sensitive two-color biosensor in fluorescence spectroscopy to identify novel modulators/ligands of

MRP1 and P-gp. Here, we report that two-color MRP1(GR-881)- and to some extent, GR-888 and GR-905 and two-color P-gp GR-678, is more FRET sensitivity than GR-873 and hold promise for high throughput screening and identification of novel substrates of the two most important ABC transporter proteins.

Molecular cloning is a robust technique which has over the years, enhanced investigation of several biological processes and has led to an immense understanding of the genetic basis of several diseases [7]. However, genetically modifying membrane proteins could compromise their functionality and proper localization in the plasma membrane. In the present study, using molecular cloning, we engineered the 27 kD GFP and the similarly 27 kDa TagRFP into the MPR1 and P-gp proteins and verified some of the recombinant proteins properly localize in the plasma membrane. We have shown that one P-gp and four MRP1 and constructs localize in the plasma membrane which contradict earlier suggestions of intracellular localization of MRP1 [8]. Doxorubicin, a common chemotherapeutic drug with a broad-spectrum efficacy against solid tumors such as small cell lung cancer, leukemias and breast cancer [9, 10] is also a fluorescent substrate of MRP1. Our engineered two-color MRP1 biosensors (except GR-859) and two-color P-gp, GR-678, evacuate doxorubicin, suggesting these clones are as functional as the wild-type transporters. Our data essentially supports a widely reported phenomenon that clinical MDR mediating ABC efflux pumps such as MRP1, P-gp and BCRP extrude doxorubicin out of the cell, diminishing the intracellular concentration of the drug [11-13]. Furthermore, two-color P-gp GR-678 mediated export of doxorubicin was inhibited verapamil, a well-known P-gp inhibitor, confirming the functionality and utility of our engineered clone.

The utilization of Fluorescence resonance energy transfer (FRET) in understanding the structure and mechanism of biomolecules and bioprocesses has gained prominence over the years [14-19]. Generally, the relationship between FRET efficiency and the distance between the two fluorescent protein pair is characterized by a sigmoidal curve [20]. This curve is steepest at its midpoint ~0.5 or 50% and provides insights that a reporter which functions within the 40-60% region is anticipated to exhibit large ligand-induced FRET changes [21]. This phenomenon forms the bedrock of the present study to find a new two-color biosensor from the set of four with an apo FRET efficiency closer to or slightly above ~50%. The two-color MRP1 (GR-873) from our previous study showed a ligand-free FRET of ~17% [11] using the cell-based epifluorescence microscopy assay. However, two-color MRP1 biosensor GR-881 and two-color P-gp, GR-678 with basal FRETs of ~63% and ~70% respectively, close to our desired range were anticipated to demonstrate larger and more consistent compound-dependent FRET change than GR-873 in downstream experiments. These clones were consequently chosen as lead biosensors for subsequent FRET testing. We speculate that the use of membrane vesicles, other than live cells, provided a purer matrix which significantly compensated for the sub-sensitivity of the fluorometer and consequently better FRET signal was shown in the present study. Interestingly, for MRP1, we observed that the more proximal the inserted GFP in the NBD1 is to the TagRFP in the NBD2 position, the higher the ligand-free transfer efficiency of the two-color proteins. Our data is consistent with the already known notion of sigmoidal relationship between inter-fluorophore distance and FRET efficiency [21]. We, however do not rule out the fact that FRET efficiency is not only influenced by

positional dynamics of the protein pair but also by their orientational fluorophore dynamics [14].

Estradiol-D-17β-Glucuronide (E217βG), a conjugated metabolite of the endogenous estradiol, is a widely known substrate of MRP1 [22-24]. E217βG-alone induced a stronger FRET signal in two-color MRP1, GR-881 and GR-888 and etoposide-induced FRET change in GR-678 was appreciable; these indicate we have developed a more powerful tool than GR-873 [11], useful for identifying substrates of MRP1. Vanadate trapping is a process where sodium orthovanadate prolongs ATP-hydrolytic signal in the ADP condition [25], a phenomenon which was confirmed in a-2012 FRET study of P-gp mutants [26]. The highest FRET change was displayed upon inclusion of E217βG + ATP + vanadate to two-color MRP1 or etoposide + ATP + vanadate while vadadate-alone barely showed any FRET signal. These observations are consistent with the vanadate trapping model earlier reported. Our data does not only indicate that the two-color MRP1 biosensors portray vanadate-locking of ATP but also suggest that the recombinant biosensors also demonstrate normal FRET responses to known ligands.

To further validate the two-color ABC transporter model, MRP1 GR-881 two-color P-gp GR-678 were selected as lead biosensors and used for steady-state FRET screening of 40 to 50 anticancer drugs. In the MRP1 screening, ten drugs were identified based on their reproducible display of FRET changes consistent with or higher than FRET changes of the positive control EGCG, were determined as hits and ligands of MRP1. Notably, none of the 10-compound hits were discovered as hits from a recent study by our group, which identified 12 calcein green-probed inhibitors of MRP1 from a high throughput screening of the same anticancer drug-pool using high content high and

confirmed by vesicular transport and flow cytometry among tools [27]. We propose that these 10-hits could be ligands or possibly potential substrates of MRP1. The insulin receptor inhibitor, Linsitinib is the only drug of the ten still under clinical trials. In a recent study of the effect of anticancer agents including linsinitib, rapamycin and JNJ-38877605, linsinitib did not inhibit cell proliferation [28]. It is however unclear if MRP1 mediated MDR was partly responsible for this observation and further tests are therefore warranted. On the other hand, the P-gp screening of 50-anticancer agents yielded 6-drug hits. Interestingly two drugs, TW-37 and Axitinib were found as common hits from the MRP1 and P-gp screenings. This suggests an earlier notion that some ABC transporters particularly MRP1, BCRP and P-gp share common ligands, substrates and inhibitors.

The two-color MRP1 (GR-881) and P-gp (GR-678) are improvement of the original two-color MRP1 GR-873 are better suited for profiling of pharmacological interactions with the transporters. GR-881 identified 10 out of 40 drugs as hits while P-gp detected 6 out of 50 drugs as hits. These represent 25% and 12% respective FRET sensitivities of the recombinant biosensors. Considering that the earlier two-color biosensor (GR-873) detected 8 out of 446 drugs screened with fluorescence lifetime plate reader, representing just 1.8% detectability, we think the ABC biosensors developed under this current project are more powerful and reliable tools for drug profiling to identify substrates.

Conclusion

Overall, we have engineered and validated two-color biosensors GR-881 (MRP1) and GR-678 (P-gp), which reports improved intermolecular FRET changes as a function of structural changes in response to interactions with substrates or ligands. GR-881 biosensor has further identified ten of forty and GR-678 biosensor, six out of fifty clinically tested anticancer agents as potential ligands of the respective transporters. These biosensors and hold promise for use in high throughput screening for detection of drug-ABC transporter interactions and identification of substrates of the proteins.

By using isolated membrane vesicles and a steady state fluorimeter-based approach, we have not only improved the initial two-color MRP1 model but also made it an economical and a more accessible tool for profiling of direct interaction of ligands with MRP1. The original two-color MRP1 GR-873 biosensor was coupled with epifluorescence microscopy and fluorescence lifetime plate reader in cell-based assays. Here we have harnessed the purity and less complexity of membrane vesicle matrix coupled with the appreciable sensitivity of the steady state fluorometer to economize the two-color model without compromising quality.

Based on the FDA mandate to test all therapeutic drugs bound for clinical trials to be tested for their interaction with P-gp, there are several approaches being incorporated for such testing in most pharmaceutical industries. Most approaches use the vectoral, monolayer transport assay using the human epithelial colorectal adenocarcinoma (Caco-

2) or the Madin-Darby Canine Kidney (MDCK) cell lines. These approaches are laborious and time-consuming. We anticipate that our two-color ABC transporter coupled steady state FRET will find great alterative the pharmaceutical industries interested in characterizing substrates of P-gp and MRP1.

Researchers studying biosensors of ABC proteins and other biological processes will benefit from our two-color FRET model by incorporating our strategy. LC-MS/MS method for eight compounds has been development with promising results with pure molecules. Future projects will focus on development a vesicular transport coupled LC-MS/MS assay to verify the substrate-status of the hits. We also plan to develop a two-color MRP1 fluorescent plate reader-based high throughput screening assay to identify more novel substrates of MRP1.

Future direction

Vesicular transport-coupled LC-MS/MS method development for identification of substrates of ABC transporters

Following the discovery of eight potential substrate-hits for MRP1 from our previous study, 10-hits of MRP1 from the present study and 6 P-gp ligands also from the present study, it was imperative to confirm the true status of the interaction of these hits with their transporters. All drugs discovered are at best potential modulators of their transporters without a strong claim that they are substrates. We planned out to develop a standard protocol which combines transport and an analytical technique to analyze the transported drugs. After unsuccessful trials with high performance liquid chromatography (HPLC) mainly due to coelution of analytes with ATP, we resorted to LC-MS/MS as the analytical tool. The HPLC-coupled ultraviolet light (UV) analysis could not detect the signal in the presence of drugs or was not sensitive enough. The diagram in figure 5.1 represents a calibration curve generated from measurement of pure E217βG. First, we placed our attention on the 8 MRP1 hits from our previous study [11]. We developed LC-MS/MS methods for the 8 compounds which showed desired signal peaks at the expected elution times. We achieved good standard calibration curves following analysis of the 8-drugs in their pure states. Figure 2 shows calibration curves for pure EGCG and calcipotriol as well as graph of peak area and elution times.

In the future, there are two anticipated tracks for this project. First is the use of membrane vesicle-based transport assay followed by analysis of the transported drugs using the established LC-MS/MS methods. The alternative technique is a cell-based transport assay prior to analysis with LC-MS/MS method. These approaches will be useful to determine the actual mode of interaction of drug-hits discovered in our lab with ABC transporters, MRP1 and P-gp and others under study. The future perspectives could also shed more light on the mechanisms of interactions. These are potentially powerful tools to unequivocally determine substrates of the ABC transporters under investigation.

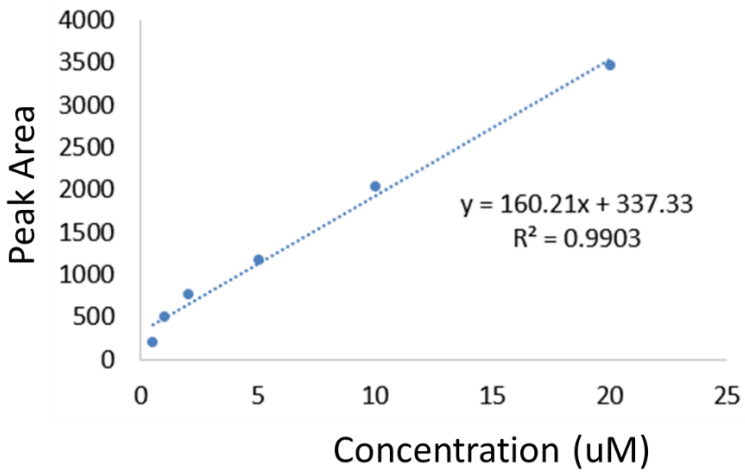

Figure 5.1 Data showing the standard calibration curve of different E217βG using HPLC. Mobile phases of 80:20 ethanol and water were used as mobile solvents and wavelength of 246 nm was used to detect test compound, E217βG.

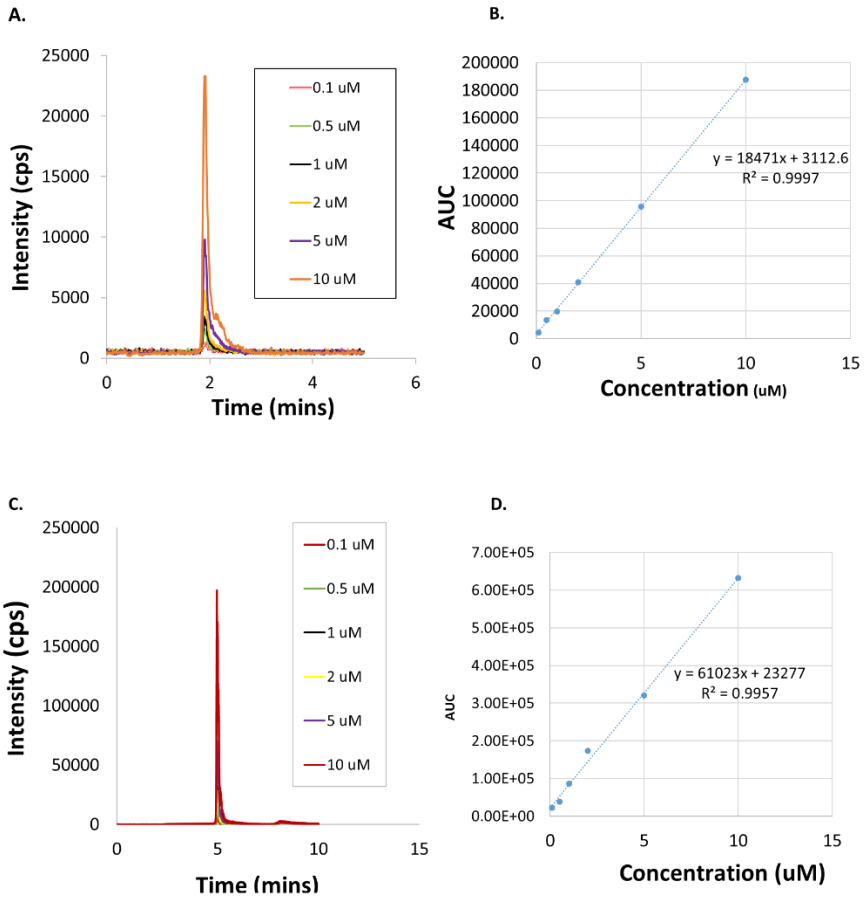

Figure 5.2 LC-MS/MS analysis of standards and calibration of pure calcipotriol and EGCG. Method development for compounds to detect potential substrates of MRP1 following vesicular transport assay and LC-MS/MS analysis. A. Peak height versus elution time of pure calcipotriol at different concentrations. B. Standard calibration curves of pure calcipotriol. Mobile phase A: 0.1% Ammonium hydroxide, Mobile phase B: 100% methanol for calcipotriol in a buffer medium of 80:20 methanol/NH4OH. Parent molecular ion mass of 411 in multiple reaction

monitoring (MRM) transitions of 395.3 and 343.2 for product ions upon fragmentation. Electrospray ionization was employed with negative polarity. Flow rate used was 1.0 ml/min. C. EGCG peak height against elution time at variable concentrations. D. Calibration curves EGCG standard concentrations. For EGCG, the following LC-MS/MS experimental conditions were employed: Mobile phase A: water/0.1% formic acid, mobile phase B: 100% Acetonitrile/0.1% formic acid at a flow rate of 0.6 ml/min. Negative ionization was used with single reaction monitoring parameter masses of 457 to 169 product ion for EGCG. 80:20 of mobile phase A and B was used infusion buffer.

References

1. Chen, Z.S. and A.K. Tiwari, *Multidrug resistance proteins (MRPs/ABCCs) in cancer chemotherapy and genetic diseases.* Febs j, 2011. **278**(18): p. 3226-45.
2. Cole, S.P., et al., *Overexpression of a transporter gene in a multidrug-resistant human lung cancer cell line.* Science, 1992. **258**(5088): p. 1650-4.
3. Leslie, E.M., R.G. Deeley, and S.P. Cole, *Multidrug resistance proteins: role of P-glycoprotein, MRP1, MRP2, and BCRP (ABCG2) in tissue defense.* Toxicol Appl Pharmacol, 2005. **204**(3): p. 216-37.
4. Wijnholds, J., et al., *Increased sensitivity to anticancer drugs and decreased inflammatory response in mice lacking the multidrug resistance-associated protein.* Nat Med, 1997. **3**(11): p. 1275-9.
5. Wijnholds, J., et al., *Multidrug resistance protein 1 protects the oropharyngeal mucosal layer and the testicular tubules against drug-induced damage.* The Journal of experimental medicine, 1998. **188**(5): p. 797-808.
6. Deeley, R.G. and S.P. Cole, *Substrate recognition and transport by multidrug resistance protein 1 (ABCC1).* FEBS Lett, 2006. **580**(4): p. 1103-11.
7. Schamhart, D.H.J. and A.C.C. Westerhof, *Strategies for gene cloning.* Urological Research, 1999. **27**(2): p. 83-96.
8. Rajagopal, A., et al., *In vivo analysis of human multidrug resistance protein 1 (MRP1) activity using transient expression of fluorescently tagged MRP1.* Cancer Res, 2002. **62**(2): p. 391-6.
9. Carvalho, C., et al., *Doxorubicin: the good, the bad and the ugly effect.* Curr Med Chem, 2009. **16**(25): p. 3267-85.
10. Szebeni, J., et al., *Liposomal doxorubicin: the good, the bad and the not-so-ugly.* J Drug Target, 2016. **24**(9): p. 765-767.
11. Iram, S.H., et al., *ATP-Binding Cassette Transporter Structure Changes Detected by Intramolecular Fluorescence Energy Transfer for High-Throughput Screening.* Mol Pharmacol, 2015. **88**(1): p. 84-94.
12. Iram, S.H. and S.P. Cole, *Differential functional rescue of Lys(513) and Lys(516) processing mutants of MRP1 (ABCC1) by chemical chaperones reveals different domain-domain interactions of the transporter.* Biochim Biophys Acta, 2014. **1838**(3): p. 756-65.
13. Aller, S.G., et al., *Structure of P-glycoprotein reveals a molecular basis for poly-specific drug binding.* Science, 2009. **323**(5922): p. 1718-22.
14. Wozniak, A.K., et al., *Single-molecule FRET measures bends and kinks in DNA.* Proceedings of the National Academy of Sciences of the United States of America, 2008. **105**(47): p. 18337-18342.
15. Ha, T., et al., *Probing the interaction between two single molecules: Fluorescence resonance energy transfer between a single donor and a single acceptor.* Proceedings of the National Academy of Sciences of the United States of America, 1996. **93**(13): p. 6264-6268.

16. Rasnik, I., et al., *DNA-binding orientation and domain conformation of the E-coli Rep helicase monomer bound to a partial duplex junction: Single-molecule studies of fluorescently labeled enzymes.* Journal of Molecular Biology, 2004. **336**(2): p. 395-408.
17. Andrecka, J., et al., *Single-molecule tracking of mRNA exiting from RNA polymerase II.* Proceedings of the National Academy of Sciences of the United States of America, 2008. **105**(1): p. 135-140.
18. Mekler, V., et al., *Structural organization of bacterial RNA polymerase holoenzyme and the RNA polymerase-promoter open complex.* Cell, 2002. **108**(5): p. 599-614.
19. Rothwell, P.J., et al., *Multiparameter single-molecule fluorescence spectroscopy reveals heterogeneity of HIV-1 reverse transcriptase: primer/template complexes.* Proceedings of the National Academy of Sciences of the United States of America, 2003. **100**(4): p. 1655-1660.
20. Lam, A.J., et al., *Improving FRET dynamic range with bright green and red fluorescent proteins.* Nature Methods, 2012. **9**(10): p. 1005-+.
21. Lam, A.J., et al., *Improving FRET Dynamic Range with Bright Green and Red Fluorescent Proteins.* Biophysical Journal, 2013. **104**(2): p. 683a-683a.
22. Beedholm-Ebsen, R., et al., *Identification of multidrug resistance protein 1 (MRP1/ABCC1) as a molecular gate for cellular export of cobalamin.* Blood, 2010. **115**(8): p. 1632-9.
23. Leier, I., et al., *ATP-dependent glutathione disulphide transport mediated by the MRP gene-encoded conjugate export pump.* Biochem J, 1996. **314 (Pt 2)**: p. 433-7.
24. Jedlitschky, G., et al., *Transport of glutathione, glucuronate, and sulfate conjugates by the MRP gene-encoded conjugate export pump.* Cancer research, 1996. **56**(5): p. 988-94.
25. Senior, A.E., M.K. al-Shawi, and I.L. Urbatsch, *The catalytic cycle of P-glycoprotein.* FEBS Lett, 1995. **377**(3): p. 285-9.
26. Verhalen, B., et al., *Dynamic ligand-induced conformational rearrangements in P-glycoprotein as probed by fluorescence resonance energy transfer spectroscopy.* J Biol Chem, 2012. **287**(2): p. 1112-27.
27. Peterson, B.G., et al., *High-content screening of clinically tested anticancer drugs identifies novel inhibitors of human MRP1 (ABCC1).* Pharmacol Res, 2017. **119**: p. 313-326.
28. Li, W., et al., *Effectiveness of inhibitor rapamycin, saracatinib, linsitinib and JNJ-38877605 against human prostate cancer cells.* Int J Clin Exp Med, 2015. **8**(4): p. 6563-7.

Appendix A

List of the 50 anticancer drugs FRET-screened with GR-881 and GR-678	
ABT-263 (Navitoclax)	Entinostat (MS-275 SNDX-275)
Afatinib (BIBW2992)	SB 431542
PD0325901	SU11274
Trichostatin A (TSA)	KU-55933
BMS-599626 (AC480)	LY294002
AUY922 (NVP-AUY922)	XL147
Brivanib (BMS-540215)	Saracatinib (AZD0530)
PF-04217903	Dovitinib (TKI-258)
BI 2536	Lenalidomide (Revlimid)
TW-37	Sunitinib Malate (Sutent)
Mocetinostat (MGCD0103)	Elesclomol
SRT1720	GDC-0941
YM155	MK-2206 2HCl
MLN8237 (Alisertib)	Linsitinib (OSI-906)
AT9283	GDC-0879
Andarine (GTX-007)	Triciribine (Triciribine phosphate)
AZD6244 (Selumetinib)	Axitinib
CI-1040 (PD184352)	Cediranib (AZD2171)
Motesanib Diphosphate (AMG-706)	Lapatinib Ditosylate (Tykerb)
Tandutinib (MLN518)	STF-62247

ABT-888 (Veliparib)	Nutlin-3
Bosutinib (SKI-606)	SB 216763
Imatinib Mesylate	Refametinib (RDEA119 Bay 86-9766)
Sorafenib (Nexavar)	Rucaparib (AG-014699 PF-01367338)
VX-680 (MK-0457 Tozasertib)	JNJ-38877605